INDIRECT DARK MATTER DETECTION

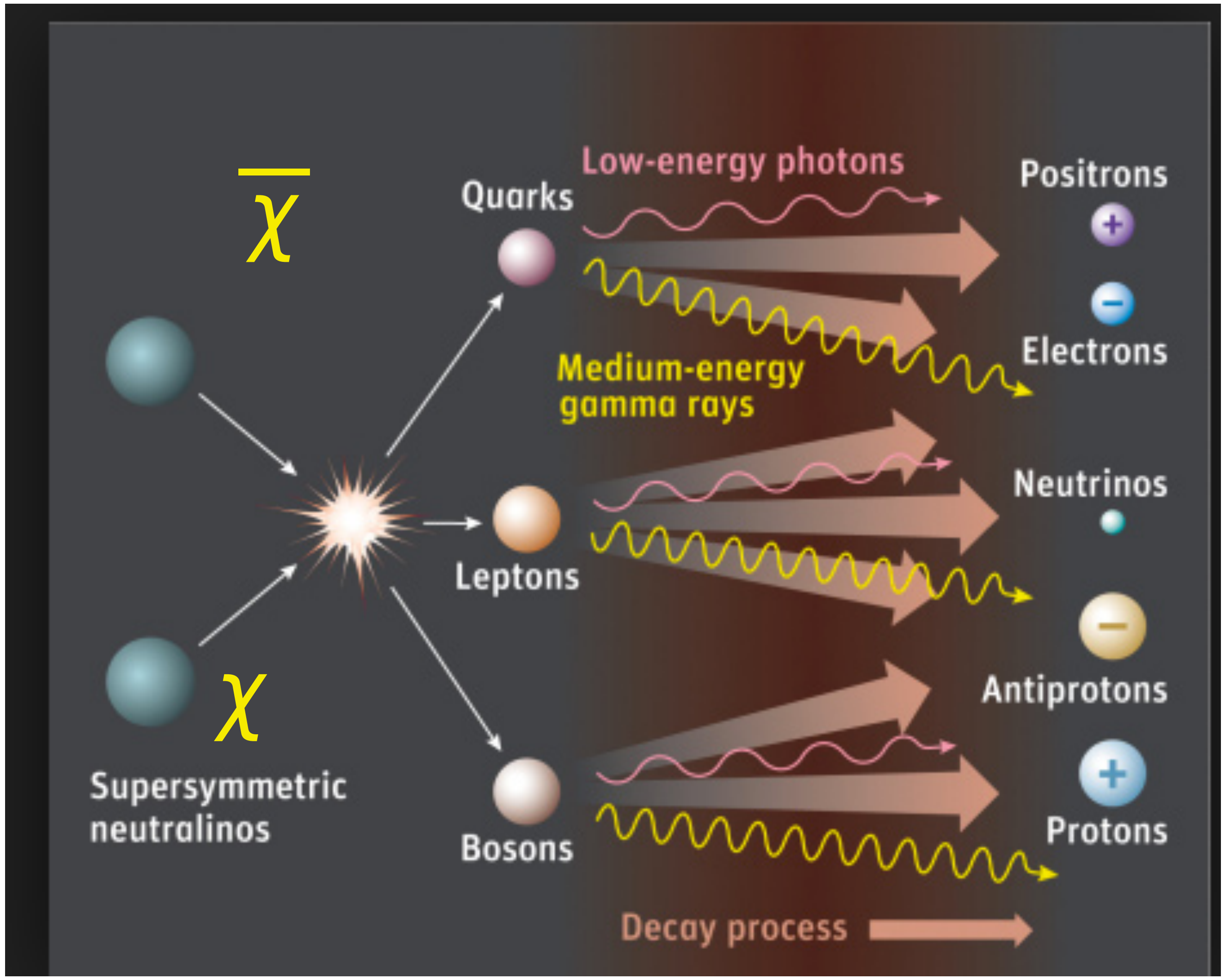

http://www.mpi-hd.mpg.de/lin/research_DM.en.html

Ivone Freire Mota Albuquerque
IFUSP

Invisibles School - Durham - July 2013

Lecture 2

Neutrinos + Gammas

1. Neutrino telescopes and results on DM searches
2. Gamma, e^- e^+ telescopes and results on DM searches

Hints on DM?

3. Neutrino / Gamma correlated signals

4. FermiLAT bubble and line signal

IceCube Detector

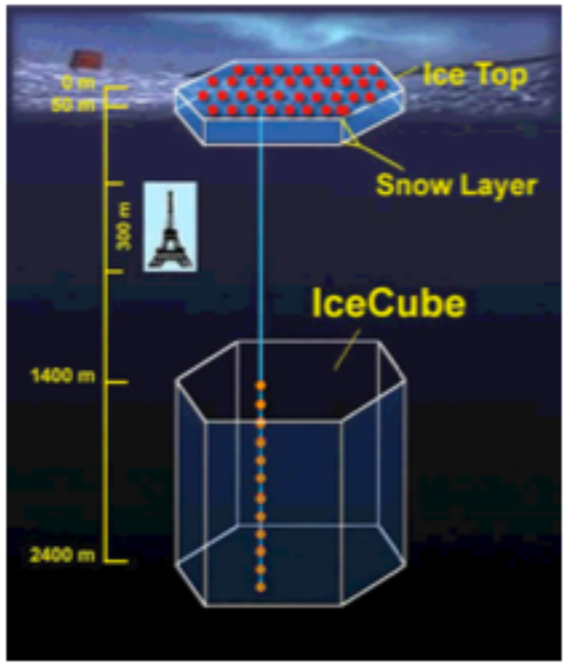

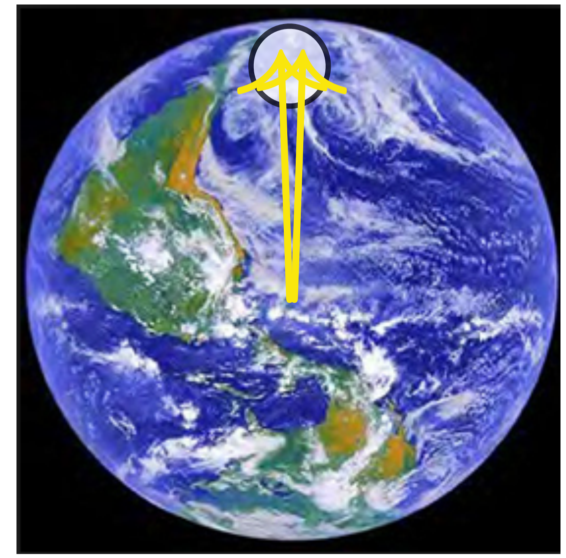

Earth as target

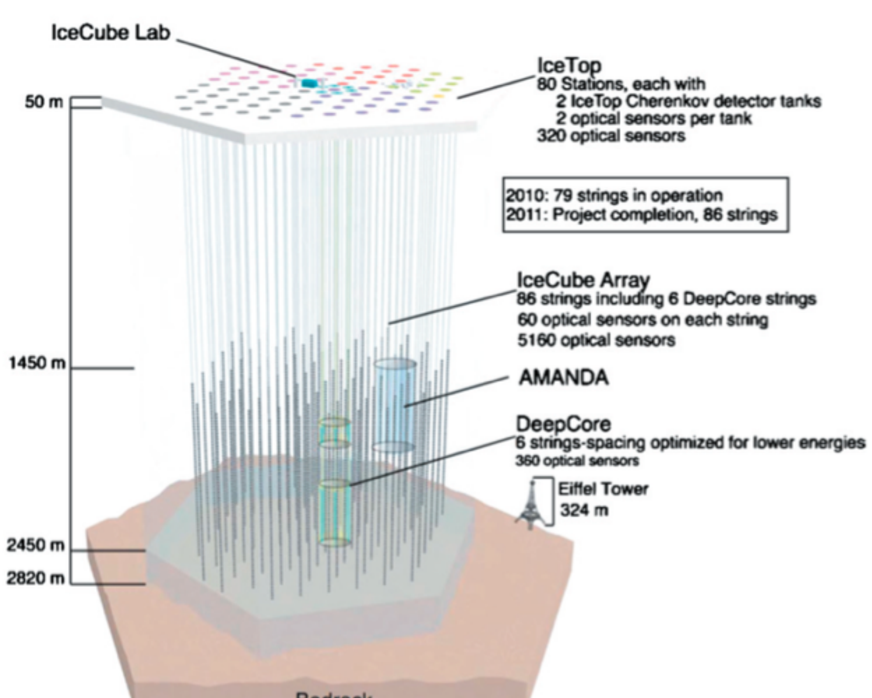

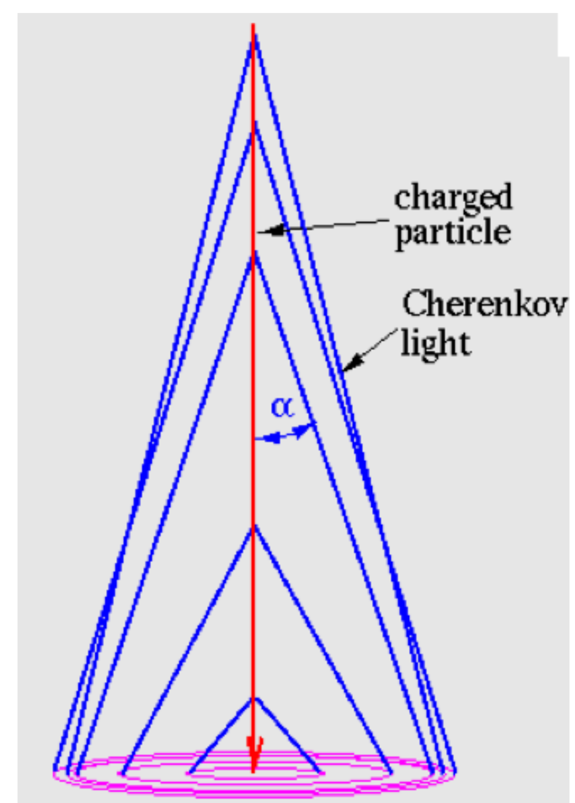

125(17) m between strings (optical modules)
DeepCore: densely instrumented
(7/10 m DOM 2 DOM)

IceCube Detector

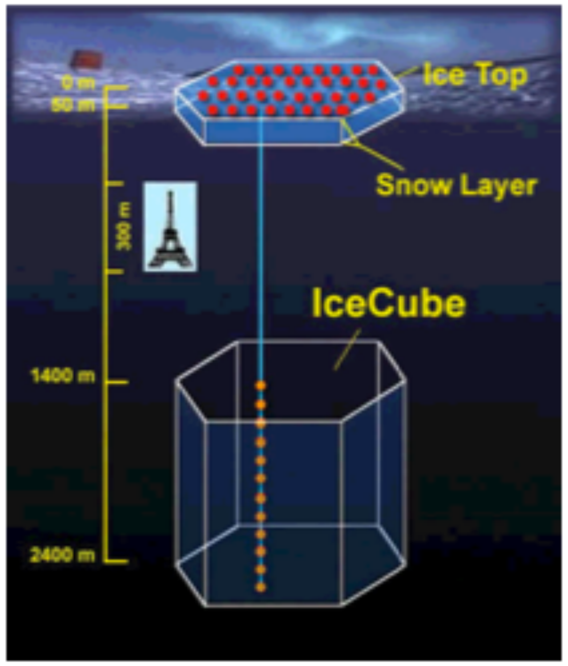

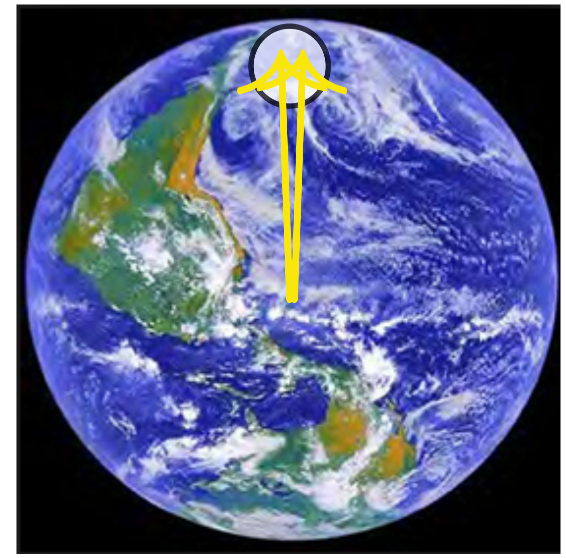

Earth as target

IA, G. Smoot
PRD **64** (2001)

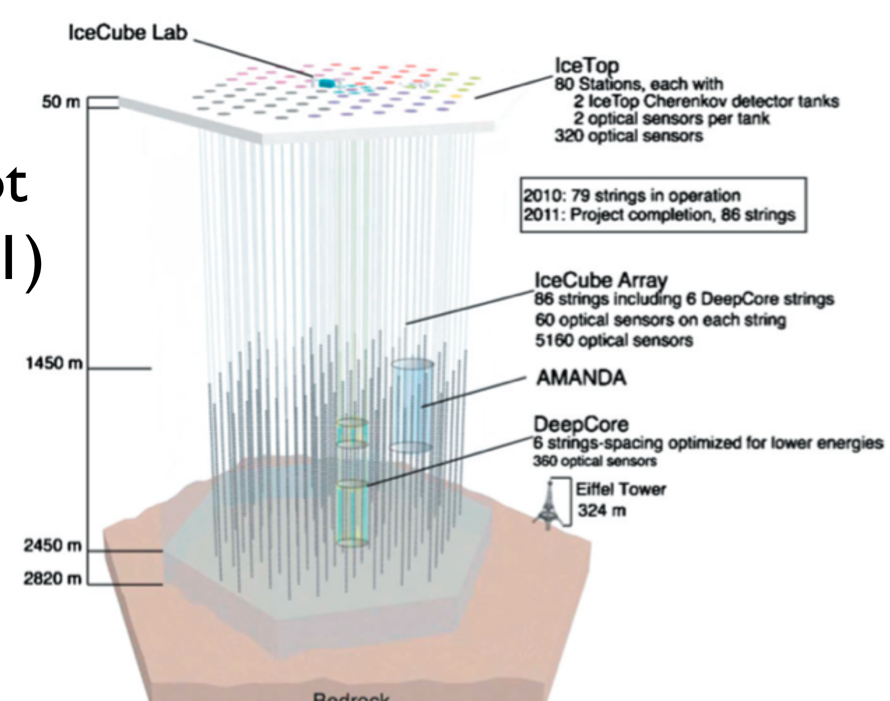

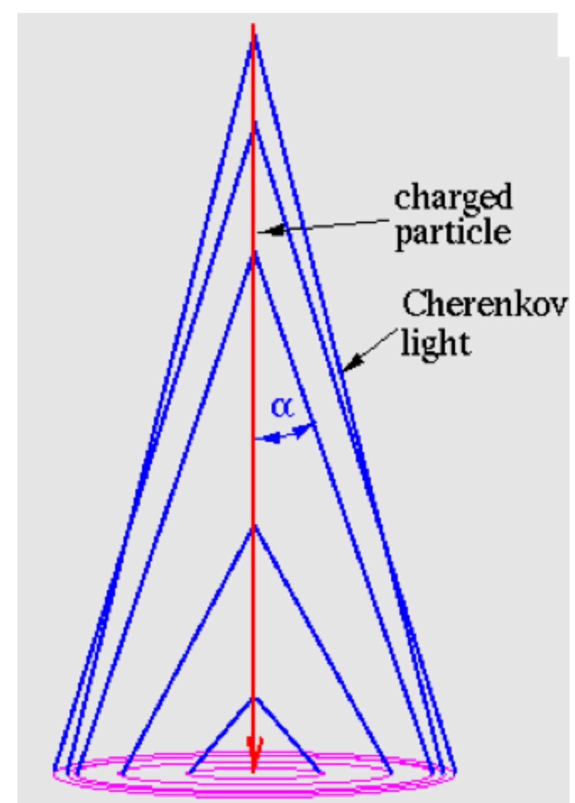

125(17) m between strings (optical modules)
DeepCore: densely instrumented
(7/10 m DOM 2 DOM)

IceCube Detector

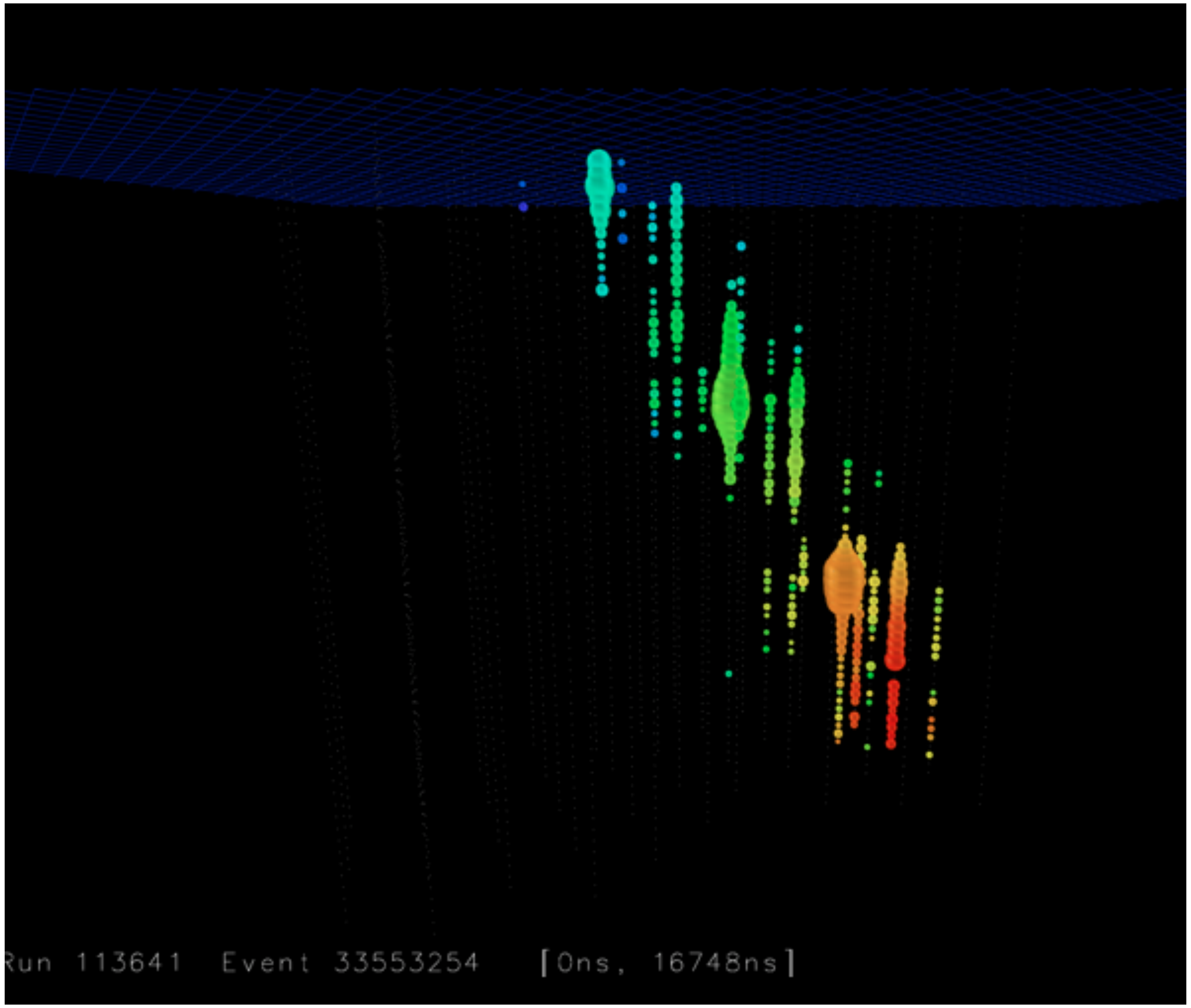

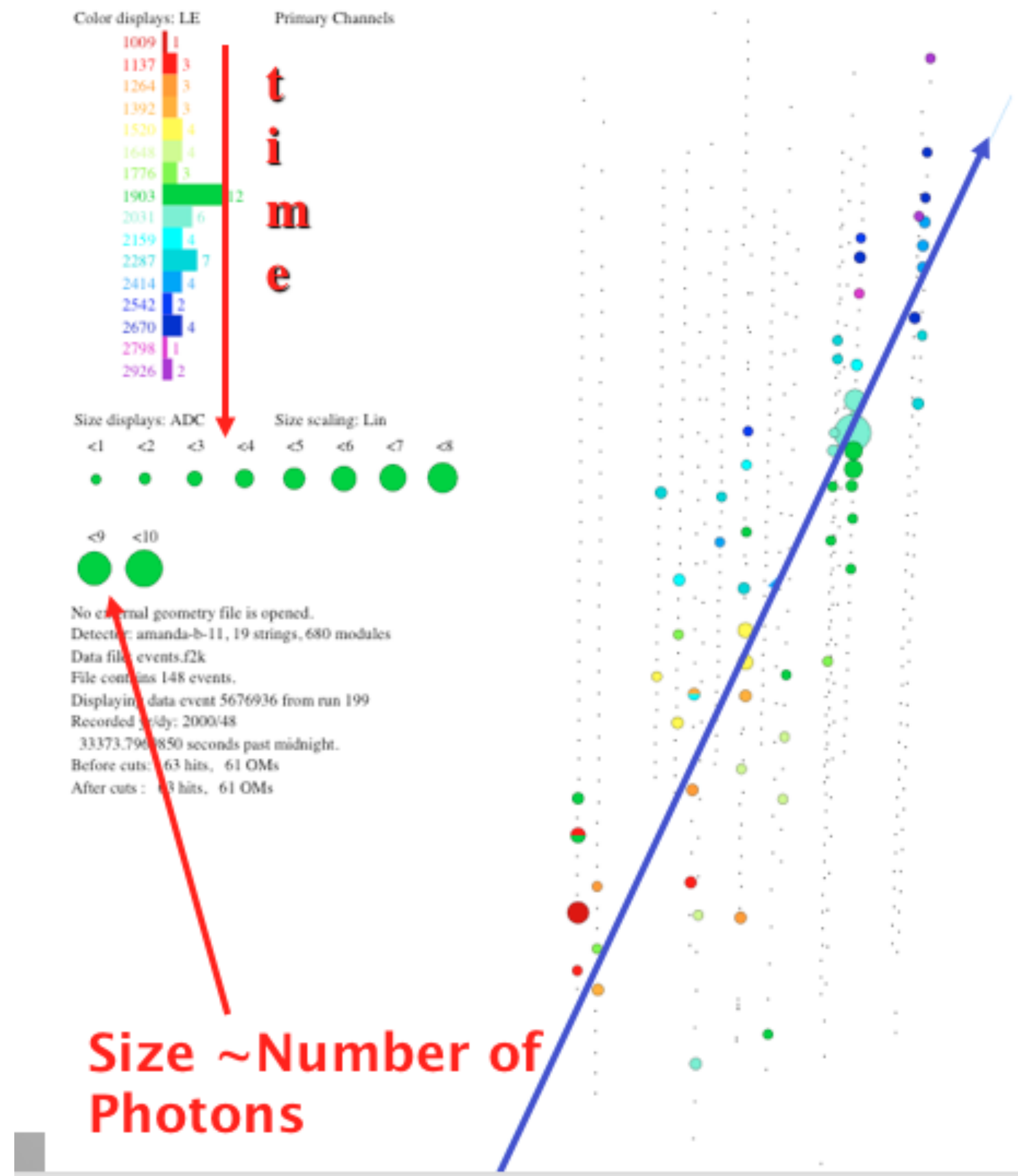

- Energy Threshold: ~150 GeV

→ depends on string spacing => Deep Core => below 100 GeV (10 GeV)

Neutrino Telescopes

Baikal NT200

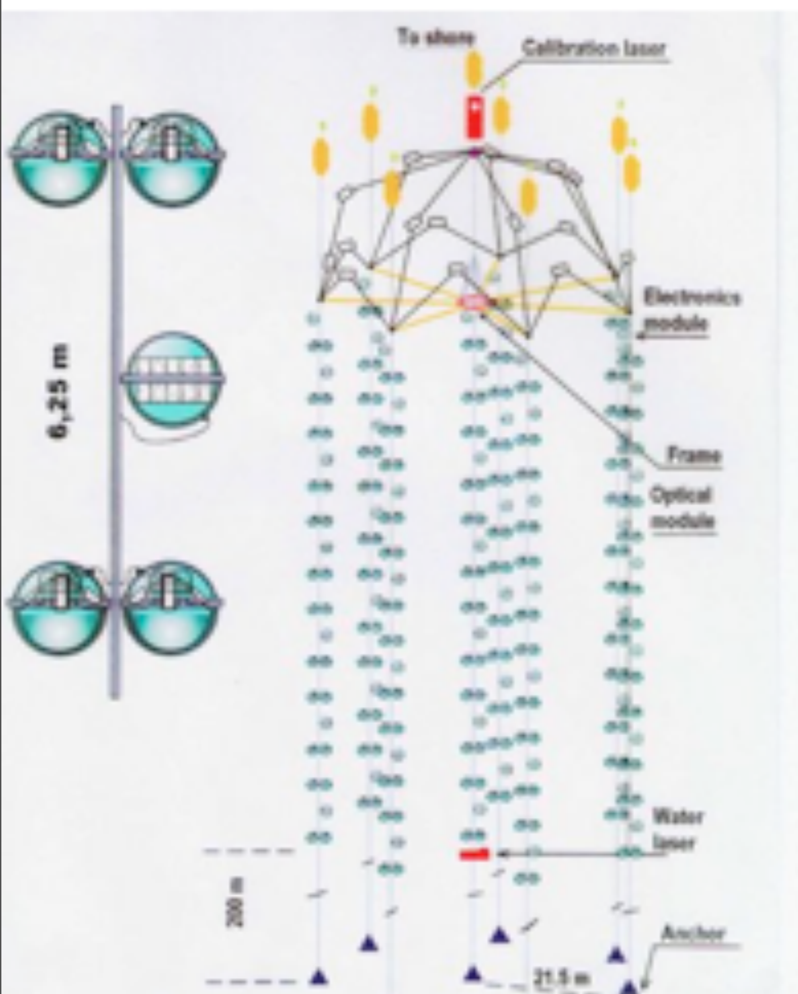

Lake Baikal - Russia (1993)
2005 NT200+
Height x diam = 210m x 200m

Antares

Mediterranean Sea (2008)
2005 NT200+
200m x 350m

Nestor

Pylos Greece (2003)
2005 NT200+
~300mx32m

Antares Detector

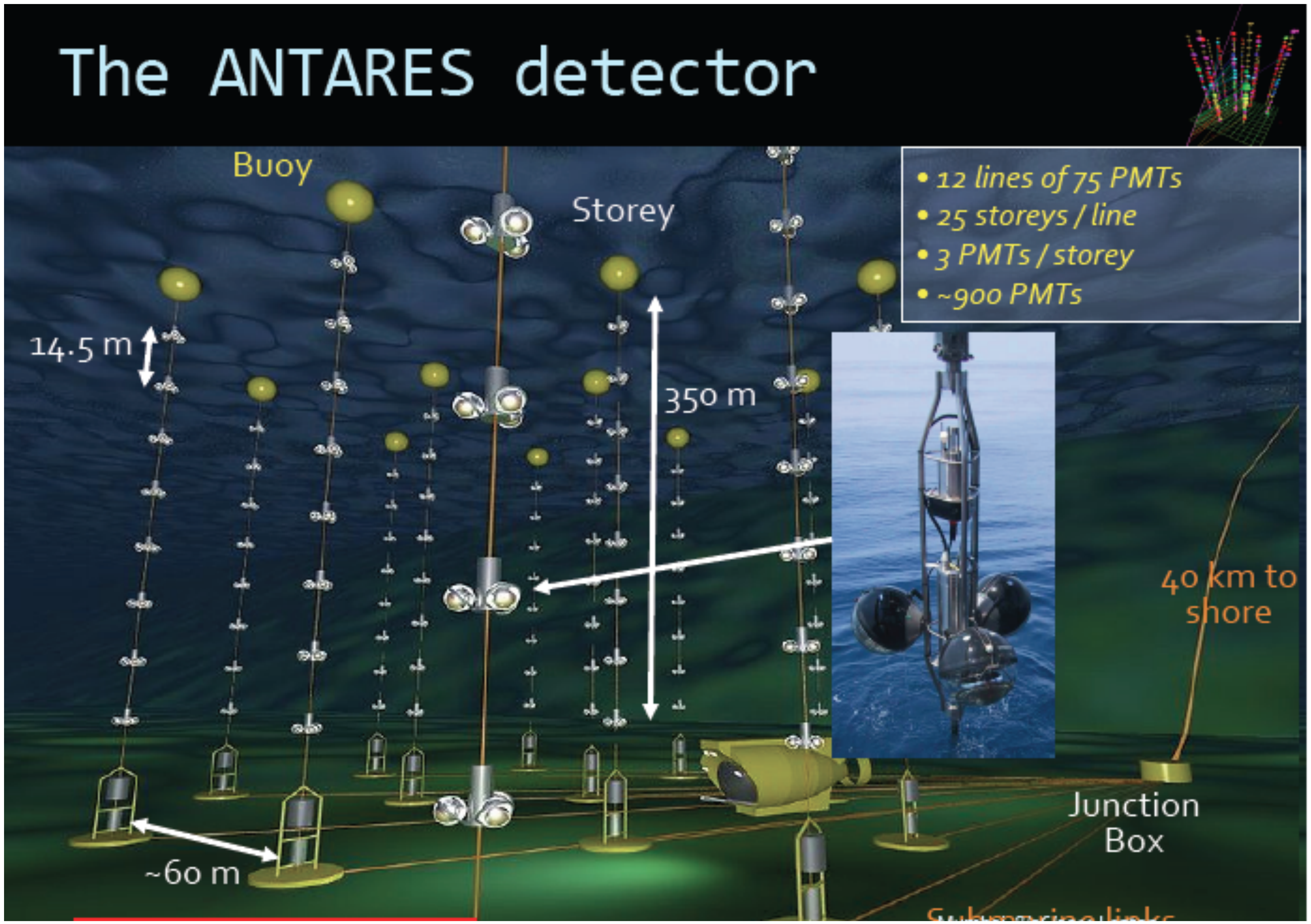

Antares Detector

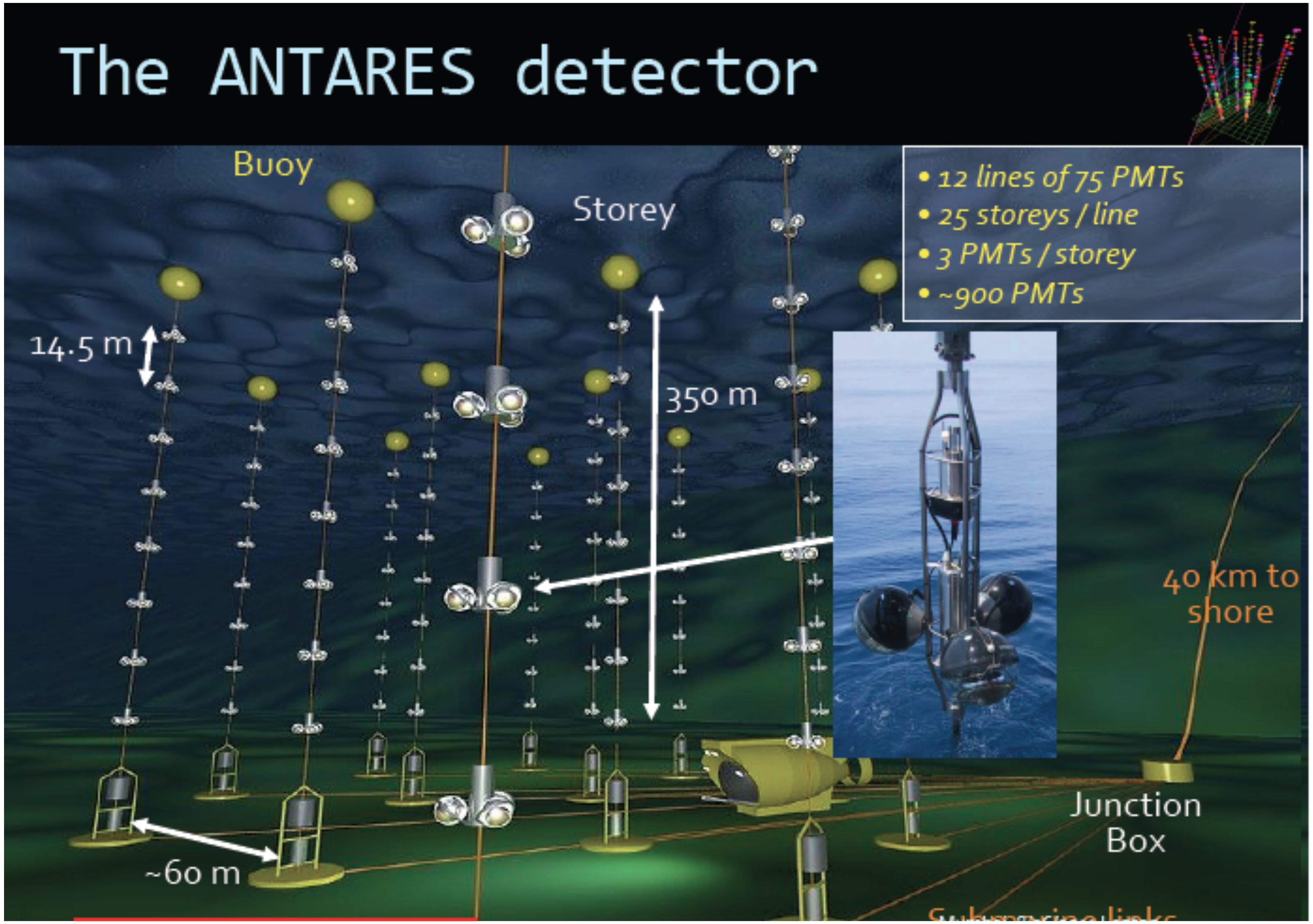

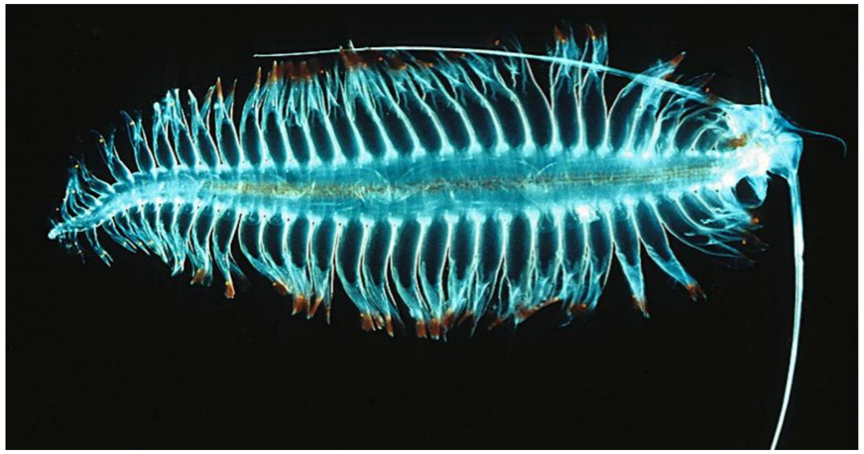

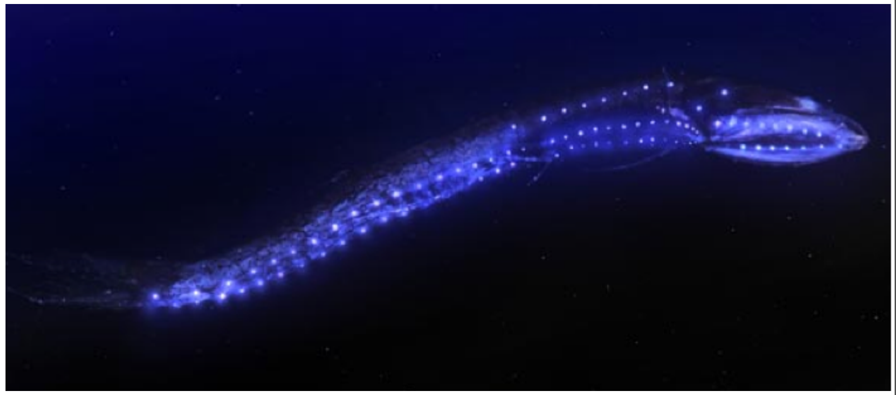

Field of View

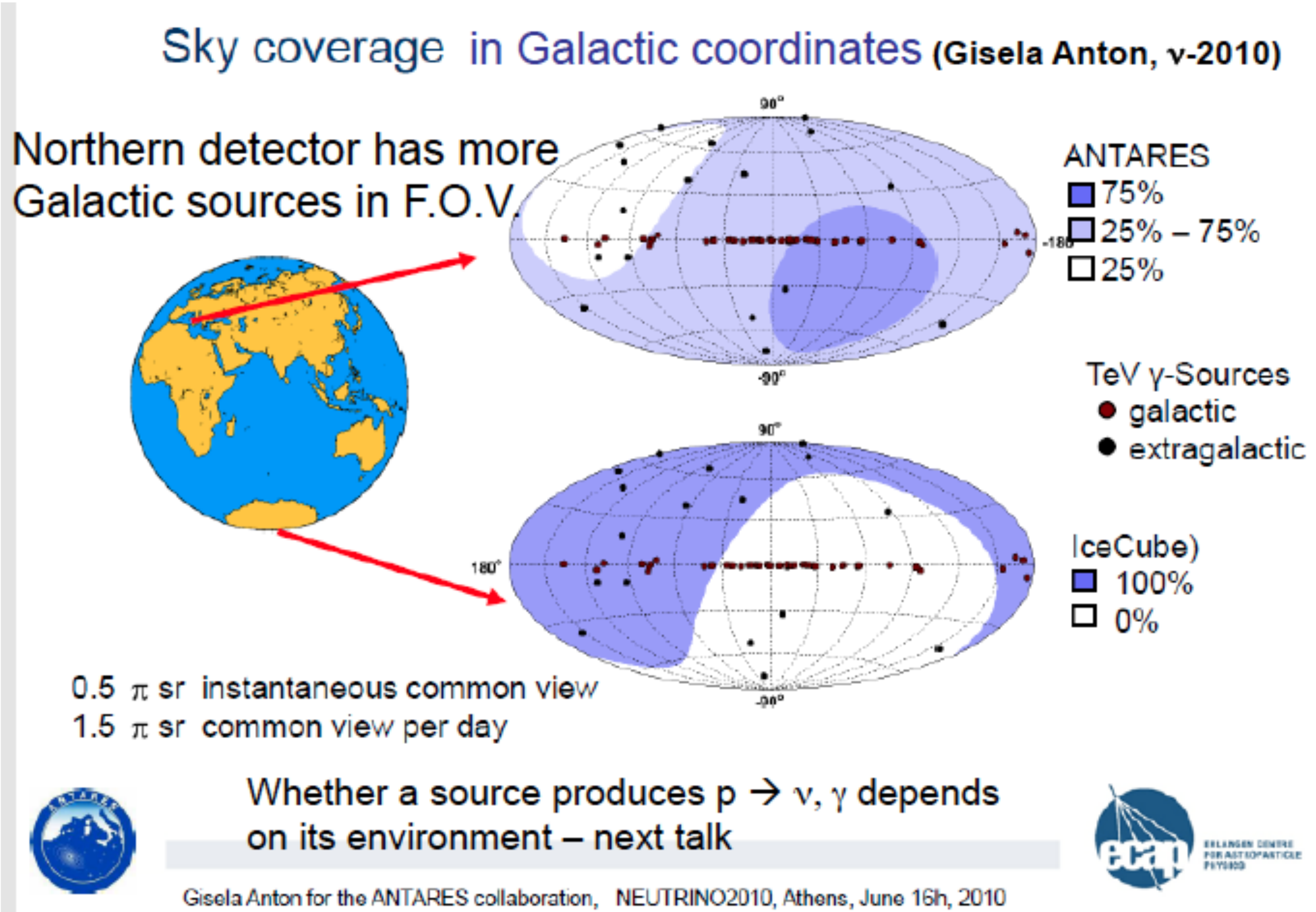

Future Telescopes

The next generation
multi-km^3
neutrino telescope

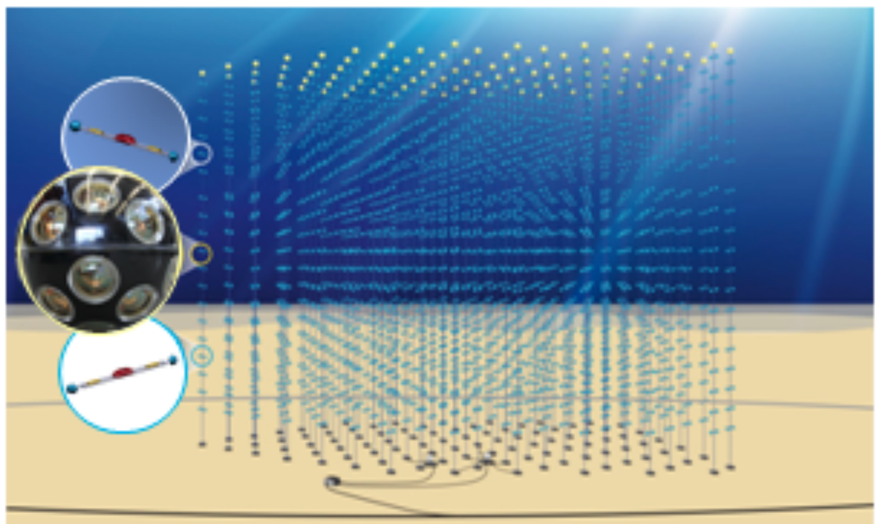

Mediterranean Sea
ANTARES+NESTOR
(european collaboration)

PINGU

Denser Infill Array in
IceCube
Extension to lower energy neutrinos
1 GeV threshold
neutrino oscillations

IceCube Search for WIMPs

$$\chi + \overline{\chi} \to \mathbf{W^+ W^-}$$
$$\to \tau^+ \tau^- \quad (\mathbf{below\ m_W = 80.4\,GeV})$$
$$\to \mathbf{b\,\overline{b}}$$

- IceCube detector (79 strings)
- Deep Core => E_{thr} = 20 GeV
- 317 live days of data

IceCube Coll. - Aartsen et al.
PRL **110** (2013)

IceCube Search for WIMPs

$$\begin{aligned}\chi + \overline{\chi} &\rightarrow \mathbf{W^+ W^-} \\ &\rightarrow \tau^+ \tau^- \quad (\mathbf{below\ m_W\ =\ 80.4\,GeV}) \\ &\rightarrow \mathbf{b\,\overline{b}}\end{aligned}$$

- IceCube detector (79 strings)
- Deep Core => E_{thr} = 20 GeV
- 317 live days of data

IceCube Coll. - Aartsen et al.
PRL **110** (2013)

Simulated signal: Wimpsim and DarkSusy

→ assumes capture and annihilation rates are in equilibrium

IceCube Search for WIMPs

$$\chi + \overline{\chi} \rightarrow \mathbf{W^+ W^-}$$
$$\rightarrow \tau^+ \tau^- \quad (\mathbf{below\ m_W = 80.4\,GeV})$$
$$\rightarrow \mathbf{b\,\overline{b}}$$

- IceCube detector (79 strings)
- Deep Core => E_{thr} = 20 GeV
- 317 live days of data

IceCube Coll. - Aartsen et al.
PRL **110** (2013)

Simulated signal: Wimpsim and DarkSusy

→ assumes capture and annihilation rates are in equilibrium

- Expected background: atmospheric ν and μ

→ simulated with Corsika (D. Heck et al., FZKA Report No. 6019, 1998)

→ follows well (M. Honda et al., Phys. Rev. D 75, 2007)

IceCube Results

WH winter high energy events

WL winter low energy events

SL summer low energy events

Low energy: μ tracks starting in DeepCore

Summer: μ tracks starting in DeepCore having IC as atm μ veto

below the horizon

above the horizon

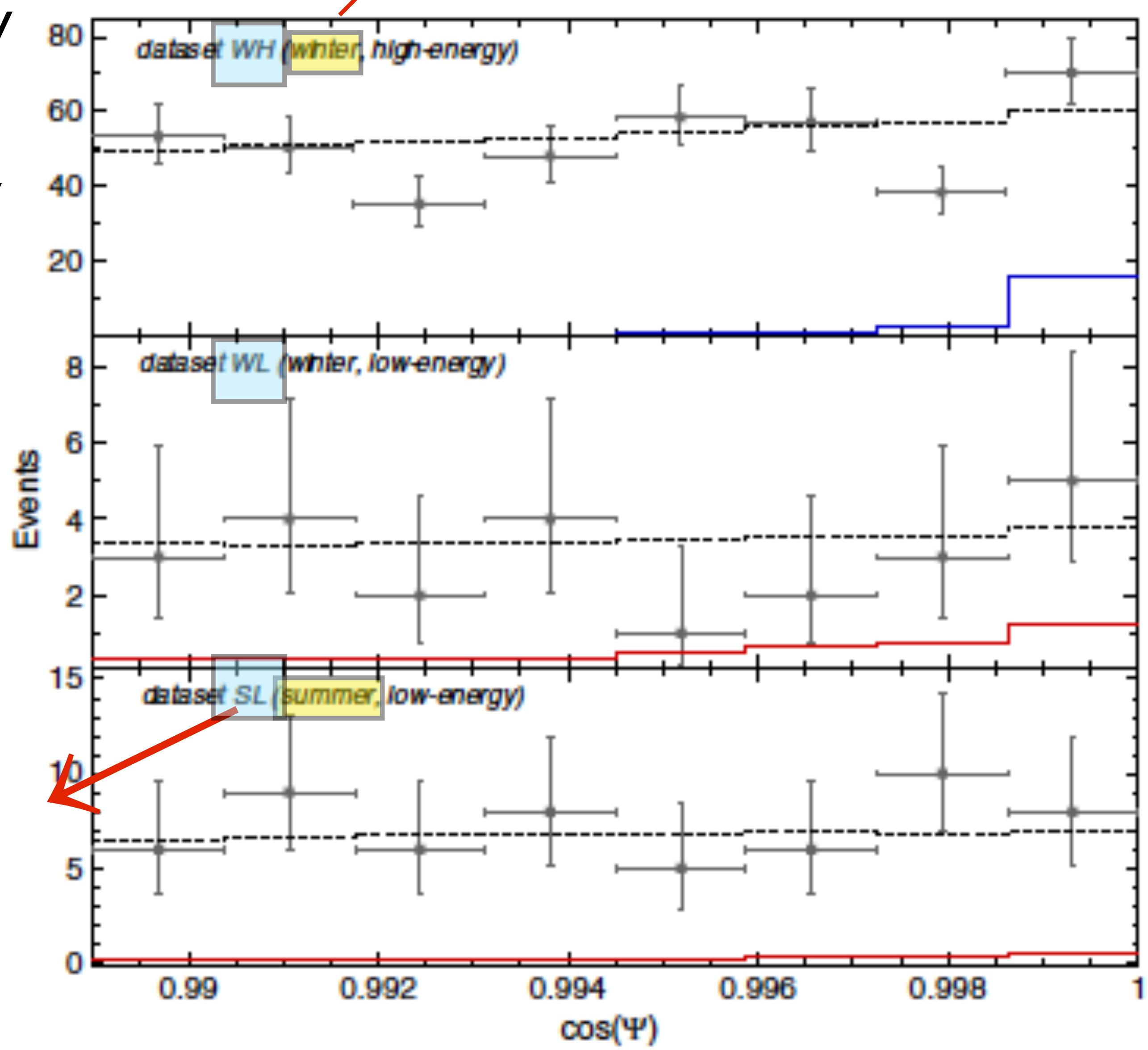

(angle between event reconstructed track and Sun direction)

$m_\chi = 1\,\mathrm{TeV}$

----- expected backgrd

—— simulated events

$m_\chi = 50\,\mathrm{GeV}$

IceCube Results

TABLE I. Results from the combination of the three independent data sets. The upper 90% limits on the number of signal events μ_s^{90}, the WIMP annihilation rate in the Sun Γ_A, the muon flux Φ_μ and neutrino flux Φ_ν, and the WIMP-proton scattering cross sections (spin independent, $\sigma_{\mathrm{SI},p}$; spin dependent, $\sigma_{\mathrm{SD},p}$) at the 90% confidence level, including systematic errors. The sensitivity $\bar{\Phi}_\mu$ (see the text) is shown for comparison.

m_χ (GeV/c^2)	Channel	μ_s^{90}	Γ_A (s^{-1})	$\bar{\Phi}_\mu$ (km^{-2}y^{-1})	Φ_μ (km^{-2}y^{-1})	Φ_ν (km^{-2}y^{-1})	$\sigma_{\mathrm{SI},p}$ (cm^2)	$\sigma_{\mathrm{SD},p}$ (cm^2)
20	$\tau^+\tau^-$	162	2.46×10^{25}	5.26×10^4	9.27×10^4	2.35×10^{15}	1.08×10^{-40}	1.29×10^{-38}
35	$\tau^+\tau^-$	70.2	1.03×10^{24}	1.03×10^4	1.21×10^4	1.02×10^{14}	6.59×10^{-42}	1.28×10^{-39}
35	$b\bar{b}$	128	1.99×10^{26}	5.63×10^4	1.04×10^5	6.29×10^{15}	1.28×10^{-39}	2.49×10^{-37}
50	$\tau^+\tau^-$	19.6	1.20×10^{23}	4.82×10^3	2.84×10^3	1.17×10^{13}	1.03×10^{-42}	2.70×10^{-40}
50	$b\bar{b}$	55.2	1.75×10^{25}	2.06×10^4	1.80×10^4	5.64×10^{14}	1.51×10^{-40}	3.96×10^{-38}
100	W^+W^-	16.8	3.35×10^{22}	1.49×10^3	1.19×10^3	1.23×10^{12}	6.01×10^{-43}	2.68×10^{-40}
100	$b\bar{b}$	28.9	1.82×10^{24}	7.57×10^3	5.91×10^3	6.34×10^{13}	3.30×10^{-41}	1.47×10^{-38}
250	W^+W^-	29.9	2.85×10^{21}	3.04×10^2	4.15×10^2	9.72×10^{10}	1.67×10^{-43}	1.34×10^{-40}
250	$b\bar{b}$	19.8	1.27×10^{23}	1.85×10^3	1.45×10^3	4.59×10^{12}	7.37×10^{-42}	5.90×10^{-39}
500	W^+W^-	25.2	8.57×10^{20}	1.46×10^2	2.23×10^2	2.61×10^{10}	1.45×10^{-43}	1.57×10^{-40}
500	$b\bar{b}$	30.6	4.12×10^{22}	8.53×10^2	1.02×10^3	1.52×10^{12}	6.98×10^{-42}	7.56×10^{-39}
1000	W^+W^-	23.4	6.13×10^{20}	1.19×10^2	1.85×10^2	1.62×10^{10}	3.46×10^{-43}	4.48×10^{-40}
1000	$b\bar{b}$	30.4	1.39×10^{22}	4.33×10^2	5.99×10^2	5.23×10^{11}	7.75×10^{-42}	1.00×10^{-38}
3000	W^+W^-	22.2	7.79×10^{20}	1.09×10^2	1.66×10^2	1.65×10^{10}	3.44×10^{-42}	5.02×10^{-39}
3000	$b\bar{b}$	26.1	4.88×10^{21}	2.52×10^2	3.47×10^2	1.89×10^{11}	2.17×10^{-41}	3.16×10^{-38}
5000	W^+W^-	22.8	8.79×10^{20}	1.01×10^2	1.58×10^2	1.77×10^{10}	1.06×10^{-41}	1.59×10^{-38}
5000	$b\bar{b}$	26.4	6.50×10^{20}	2.21×10^2	3.26×10^2	1.63×10^{11}	4.89×10^{-41}	7.29×10^{-38}

Consistent with expected background

IceCube Coll. - Aartsen et al. - PRL **110** (2013)

Limits on Neutralino DM

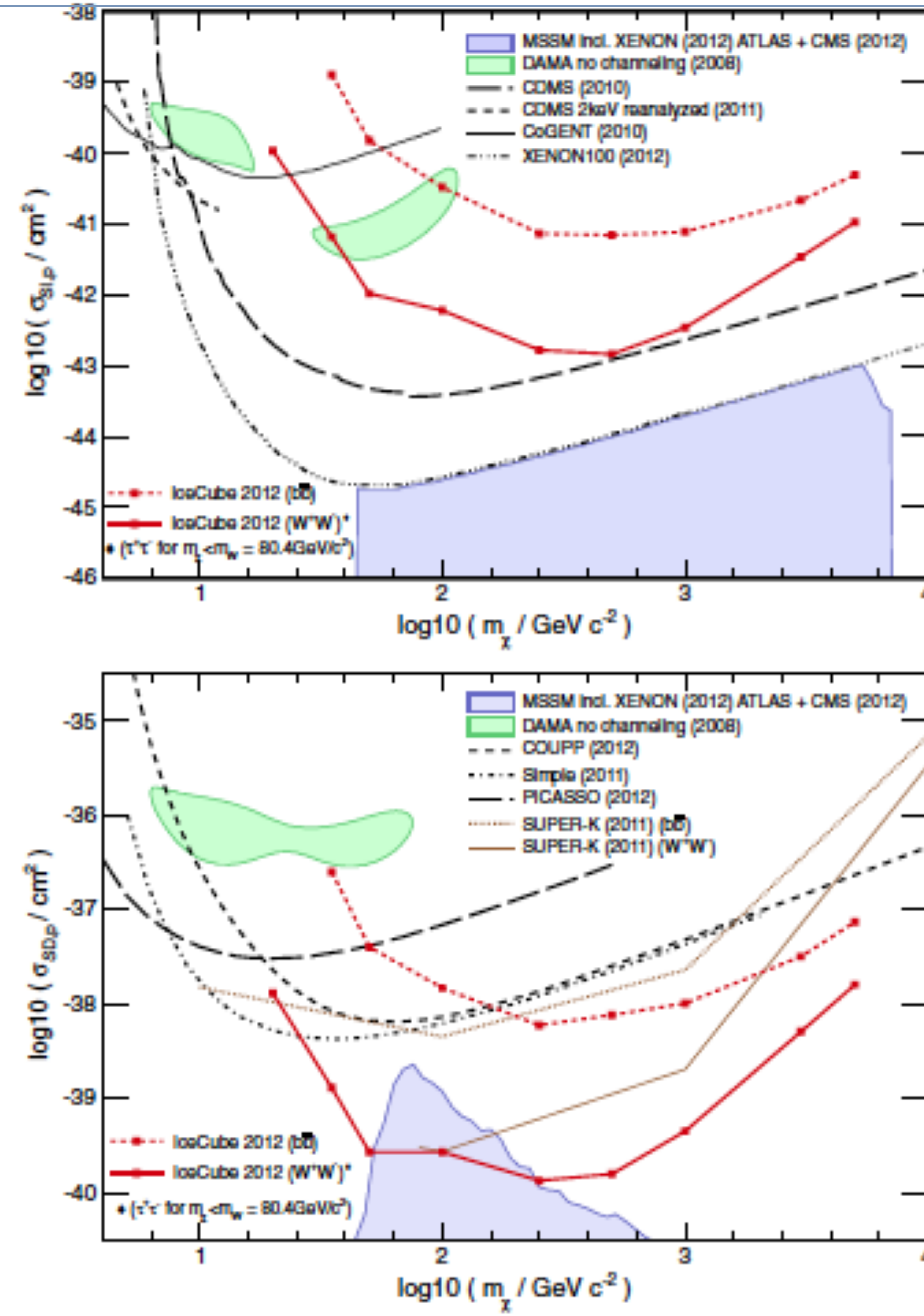

90% CL

IceCube Coll. - Aartsen et al.
PRL **110** (2013)

Limits on Neutralino DM

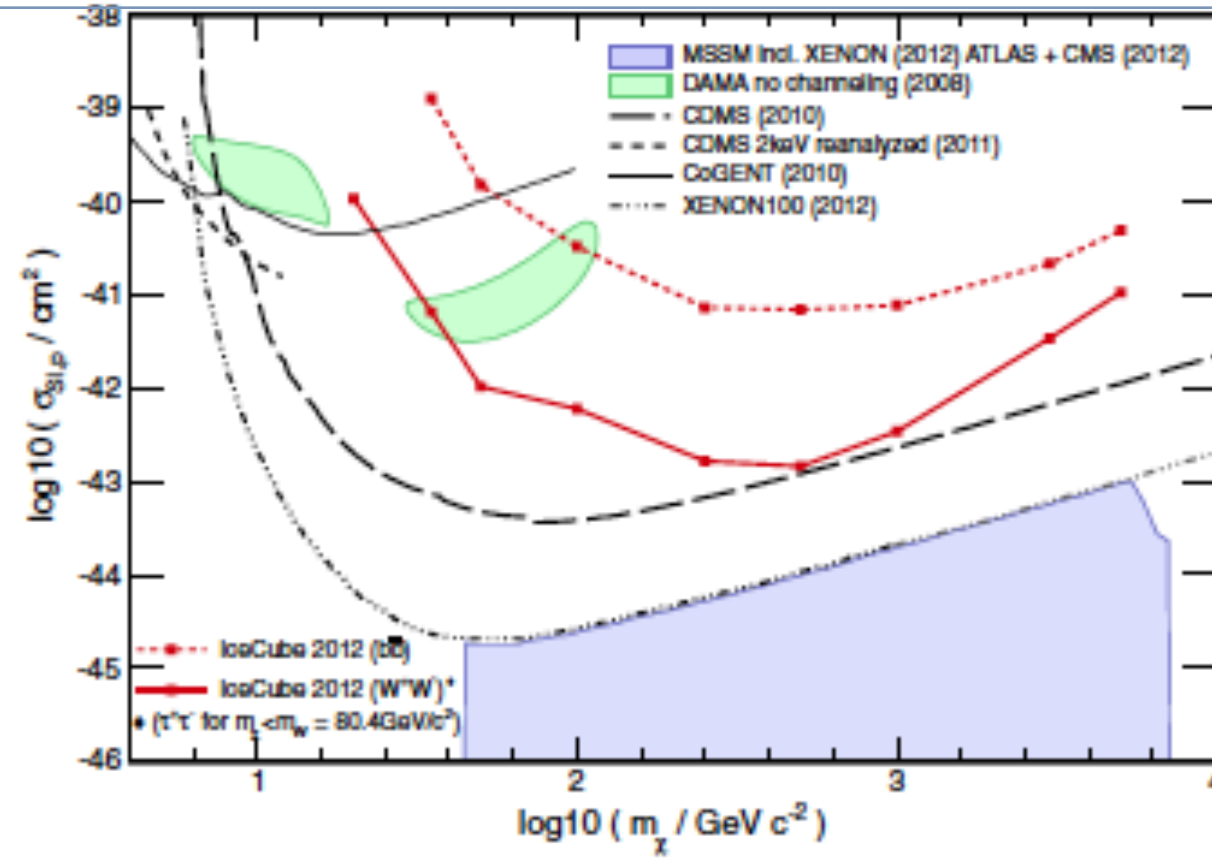

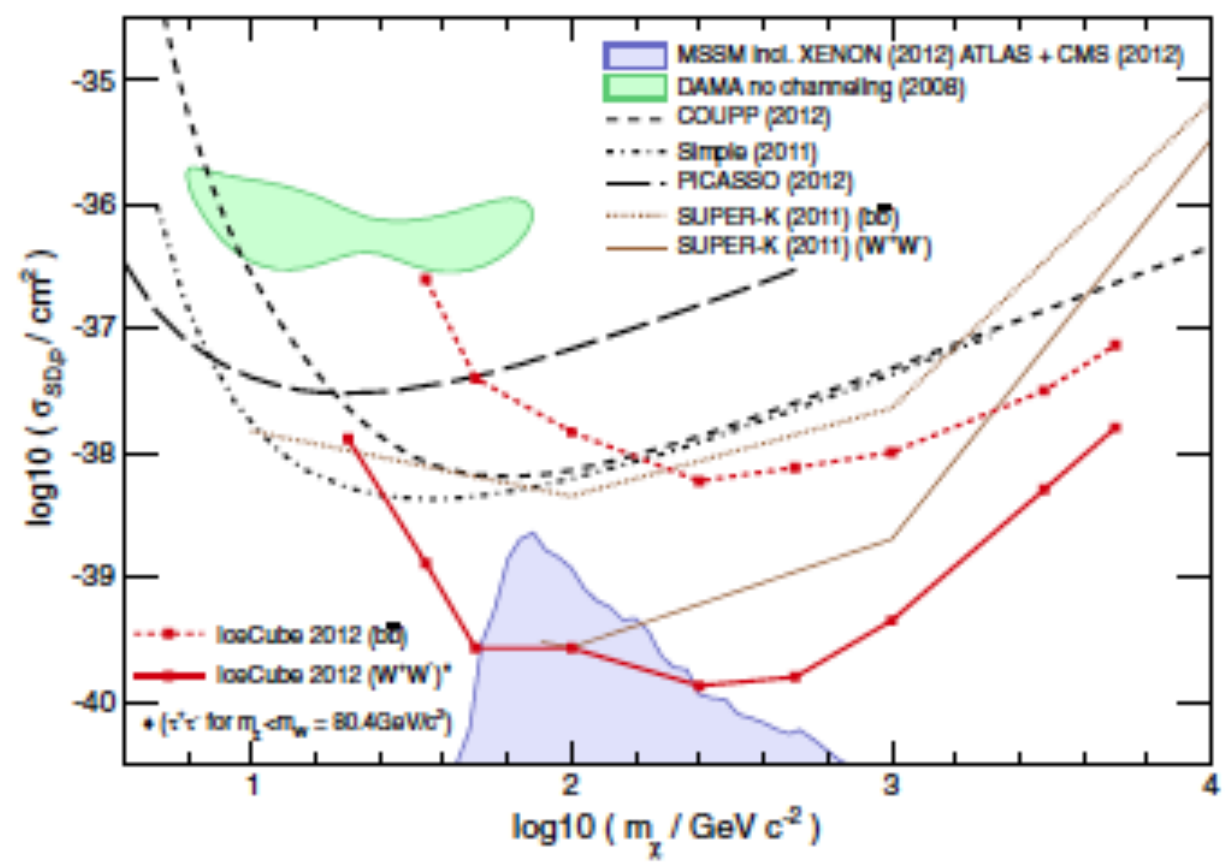

90% CL

So far this is the most stringent limit

IceCube Coll. - Aartsen et al. PRL **110** (2013)

Combined AMANDA-II + IceCube Data

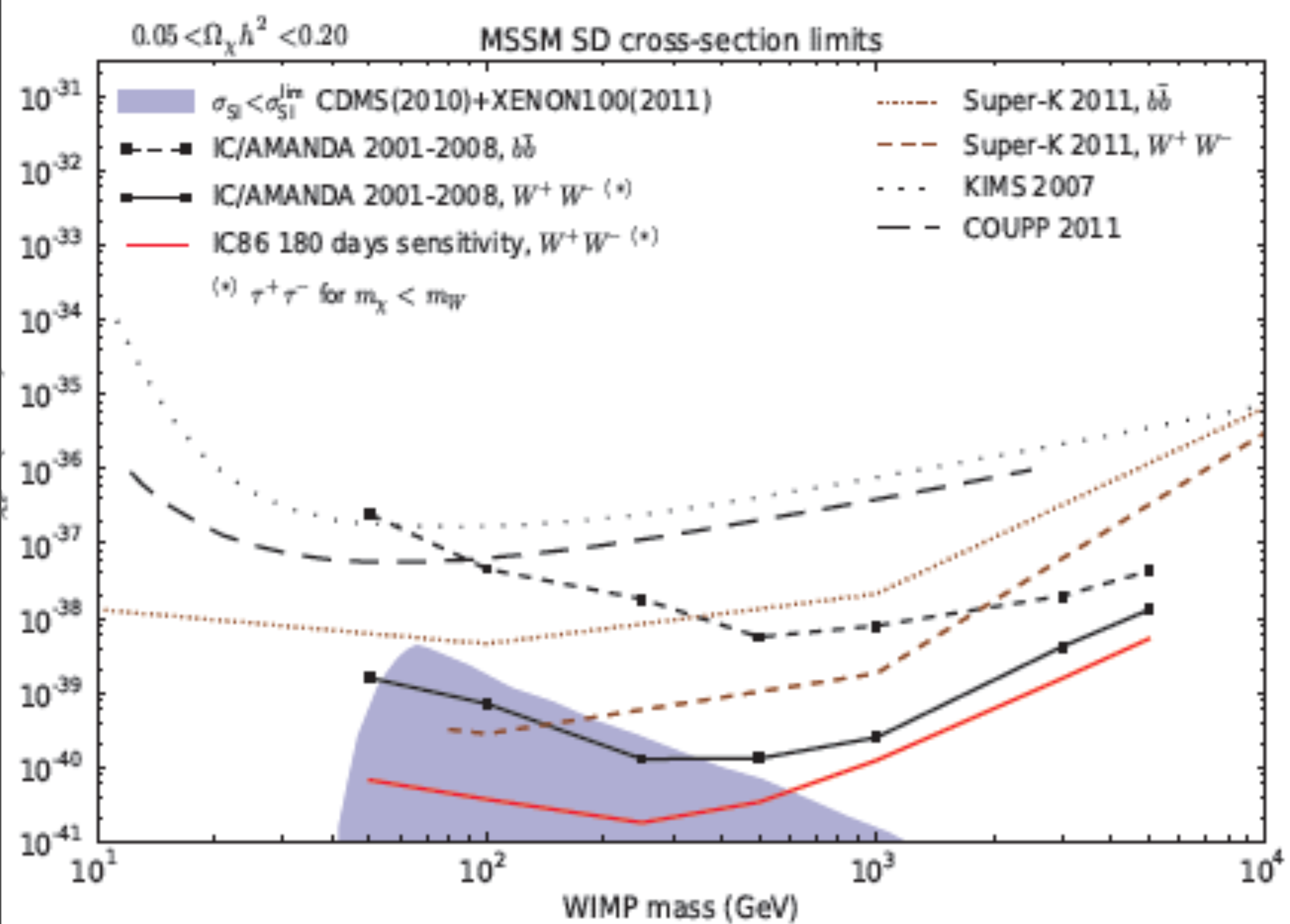

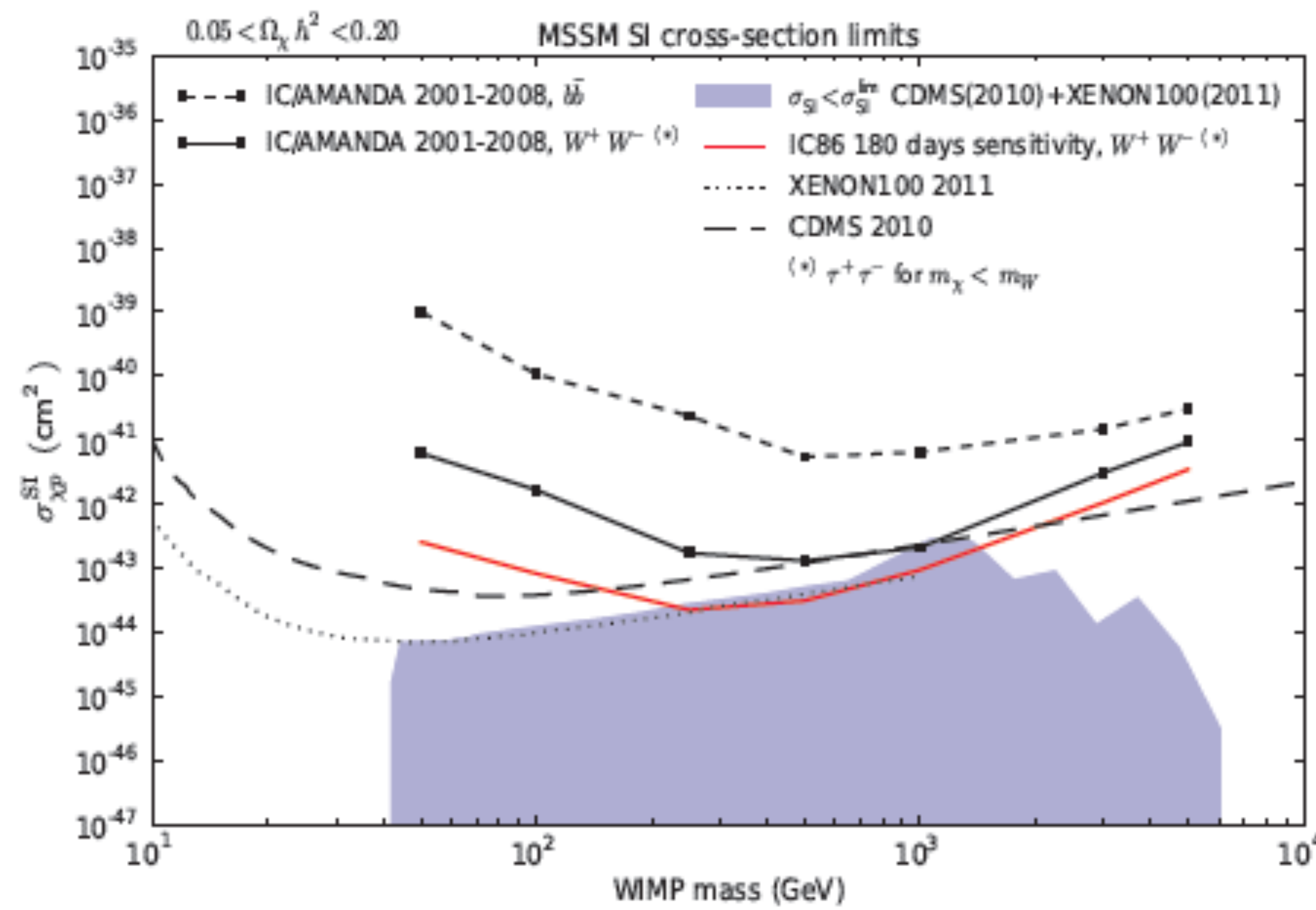

IceCube - 22 strings

Total live time 1065 days

IceCube Coll. - Abbasi et al. PRD **85** (2012)

Indirect and Direct Detection

Complementarity among indirect and direct detection

INDIRECT

spin-dependent

low velocity (easier to capture)

DIRECT

spin-independent

high velocity (easier to detect)

Indirect and Direct Detection

Complementarity among indirect and direct detection

INDIRECT	DIRECT
spin-dependent	spin-independent
low velocity (easier to capture)	high velocity (easier to detect)

Note: CDMS has natural Ge and Si
~8% ^{73}Ge(spin 9/2) and ~5% ^{29}Si(spin 1/2)

Indirect and Direct Detection

Complementarity among indirect and direct detection

INDIRECT	**DIRECT**
spin-dependent	spin-independent
low velocity (easier to capture)	high velocity (easier to detect)

Note: CDMS has natural Ge and Si
~8% ^{73}Ge(spin 9/2) and ~5% ^{29}Si(spin 1/2)

different sensitivities to structures in DM halo

Indirect and Direct Detection

Complementarity among indirect and direct detection

INDIRECT

spin-dependent

low velocity (easier to capture)

DIRECT

spin-independent

high velocity (easier to detect)

Note: CDMS has natural Ge and Si
~8% ^{73}Ge(spin 9/2) and ~5% ^{29}Si(spin 1/2)

different sensitivities to structures in DM halo

clumps (voids) might enhance (lower) annihilation
and
lower chances of direct detection

IceCube Search for LKP

UED: KK photon $\gamma^{(1)}$ as LKP

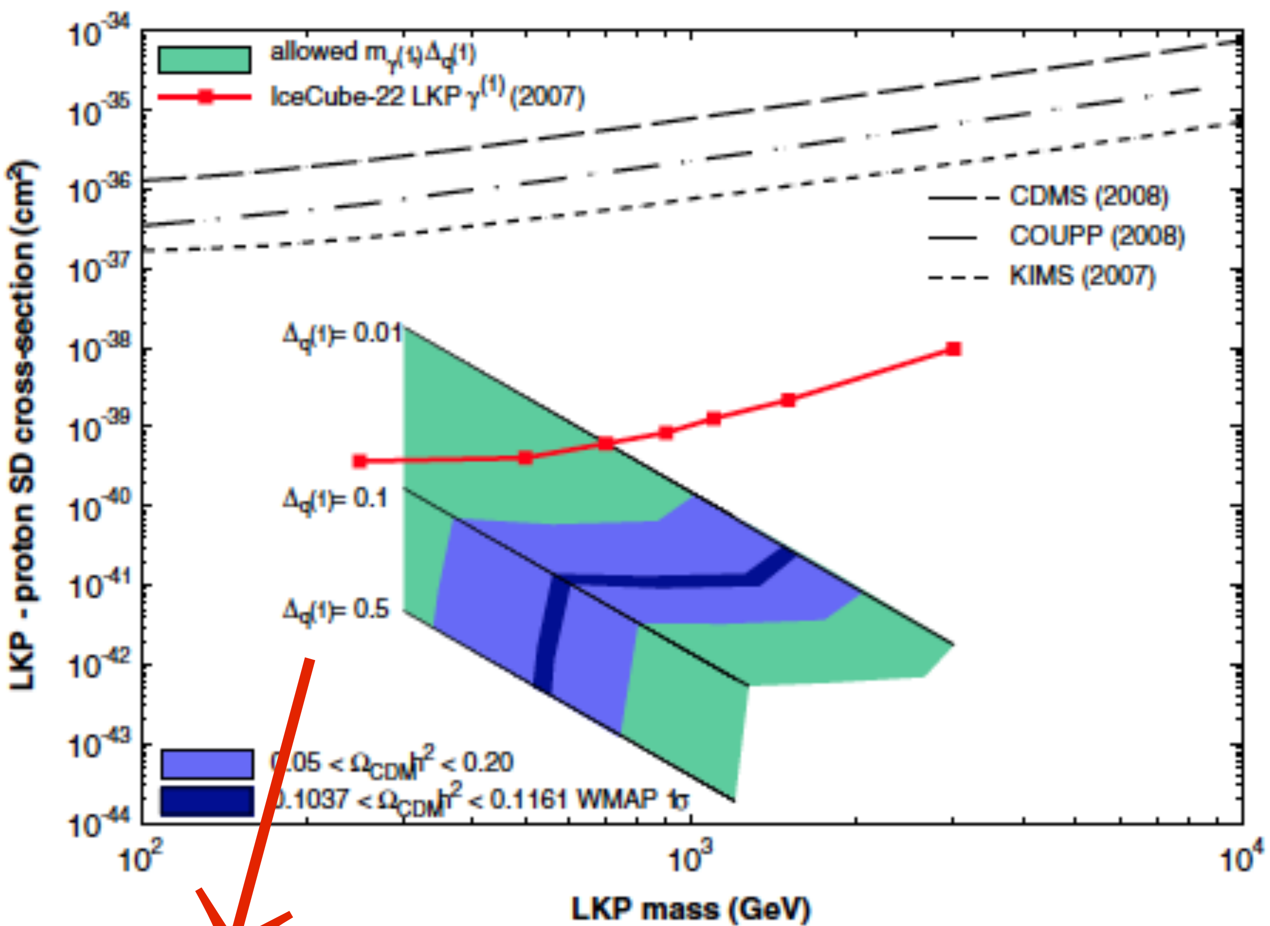

mass splitting to 1st excitation

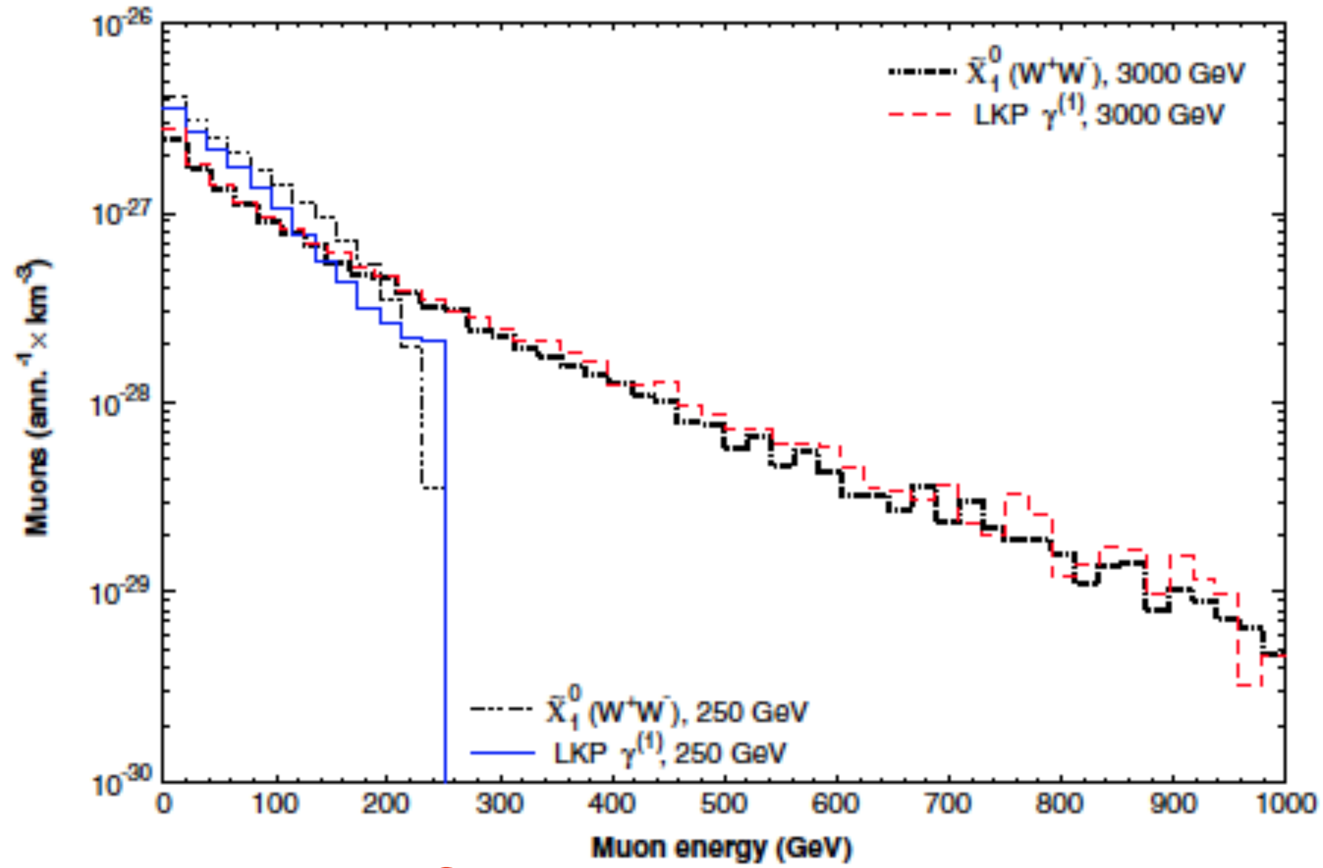

γ(1) and χ muon spectrum at detector

Channel	Branching ratio	
	$\Delta_{q^{(1)}} = 0$	$\Delta_{q^{(1)}} = 0.14$
(e^+e^-), $(\mu^+\mu^-)$, $\tau^+\tau^-$	0.20	0.23
$(u\bar{u})$, $c\bar{c}$, $t\bar{t}$	0.11	0.077
$(d\bar{d})$, $(s\bar{s})$, $b\bar{s}$	0.007	0.005
$\nu_e\bar{\nu}_e$, $\nu_\mu\bar{\nu}_\mu$, $\nu_\tau\bar{\nu}_\tau$	0.012	0.014
$(\Phi, \Phi^*)^\dagger$	0.023	0.027

IceCube Coll. - Abbasi et al. PRD **81** (2010)

γ from DM

[redacted]

1)

$$\chi\overline{\chi} \rightarrow \mathbf{H}\,\overline{\mathbf{H}}$$

$$\mathbf{H} \rightarrow \cdots \rightarrow \mathbf{x}\,\pi^{\mathbf{0}} \rightarrow \gamma\gamma$$

$$\frac{dN_\gamma}{dE} \text{ is symmetric around } E = \frac{m_{\pi^0}}{2} \text{ (in log scale)}$$

2) Secondary photons from radiative processes

→ energy loss processes for e^+ / e^- : inverse Compton or synchroton emission

smooth energy spectrum

γ from DM

Can we get light out of DM?

1)

$$\chi\bar{\chi} \rightarrow \mathbf{H}\,\overline{\mathbf{H}}$$

$$\mathbf{H} \rightarrow \cdots \rightarrow \mathbf{x}\,\pi^{\mathbf{0}} \rightarrow \gamma\gamma$$

$$\frac{dN_\gamma}{dE} \text{ is symmetric around } E = \frac{m_{\pi^0}}{2} \text{ (in log scale)}$$

2) Secondary photons from radiative processes

→ energy loss processes for e^+ / e^- : inverse Compton or synchroton emission

smooth energy spectrum

γ from DM

Can we get light out of DM?

1)

$$\chi\bar{\chi} \rightarrow \mathbf{H}\,\overline{\mathbf{H}}$$

$$\mathbf{H} \rightarrow \cdots \rightarrow \mathbf{x}\,\pi^{\mathbf{0}} \rightarrow \gamma\gamma$$

$$\frac{dN_\gamma}{dE} \text{ is symmetric around } E = \frac{m_{\pi^0}}{2} \text{ (in log scale)}$$

2) Secondary photons from radiative processes

→ energy loss processes for e^+ / e^- : inverse Compton or synchroton emission

smooth energy spectrum

e+ / e- diffusion
+ energy loss

Secondary Photons

- Inverse Compton emission:

$$\mathbf{e^{\pm} + \gamma \rightarrow e^{\pm} + \gamma^{*}}$$

Secondary from DM annihilation or decay

Interstellar radiation field

Up-scattered photon

$$\mathbf{E_{\gamma^*} = \frac{4}{3}\left(\frac{E_e}{m_e}\right)^2 E_\gamma}$$

Secondary Photons

- Inverse Compton emission:

$$\mathbf{e^{\pm} + \gamma \rightarrow e^{\pm} + \gamma^{*}}$$

Secondary from DM annihilation or decay

Interstellar radiation field

Up-scattered photon

$$\mathbf{E_{\gamma^*} = \frac{4}{3}\left(\frac{E_e}{m_e}\right)^2 E_\gamma}$$

→ interstellar field radiation: CMB $(\mathbf{E_\gamma \sim 2.6 \times 10^{-4}\,eV})$

dust $(\mathbf{E_\gamma \sim 10^{-2}\,eV})$

stars $(\mathbf{E_\gamma \sim 1\,eV})$

Secondary Photons

- Inverse Compton emission:

$$\mathbf{e}^{\pm} + \gamma \rightarrow \mathbf{e}^{\pm} + \gamma^{*}$$

Secondary from DM annihilation or decay

Interstellar radiation field

Up-scattered photon

$$\mathbf{E}_{\gamma^*} = \frac{\mathbf{4}}{\mathbf{3}} \left(\frac{\mathbf{E_e}}{\mathbf{m_e}} \right)^{\mathbf{2}} \mathbf{E}_{\gamma}$$

→ interstellar field radiation: CMB $(\mathbf{E}_{\gamma} \sim \mathbf{2.6 \times 10^{-4}\, eV})$

dust $(\mathbf{E}_{\gamma} \sim \mathbf{10^{-2}\, eV})$

stars $(\mathbf{E}_{\gamma} \sim \mathbf{1\, eV})$

$$\mathbf{E_e} \sim \frac{\mathbf{M}_{\chi}}{\mathbf{10}}$$

Secondary Photons

- Inverse Compton emission:

$$\mathbf{e^{\pm} + \gamma \rightarrow e^{\pm} + \gamma^{*}}$$

Secondary from DM annihilation or decay

Interstellar radiation field

Up-scattered photon

$$\mathbf{E_{\gamma^*} = \frac{4}{3}\left(\frac{E_e}{m_e}\right)^2 E_\gamma}$$

→ interstellar field radiation: CMB $(\mathbf{E_\gamma \sim 2.6 \times 10^{-4}\,eV})$

dust $(\mathbf{E_\gamma \sim 10^{-2}\,eV})$

stars $(\mathbf{E_\gamma \sim 1\,eV})$

$$\mathbf{E_e \sim \frac{M_\chi}{10}}$$

CMB: $\mathbf{E^*_\gamma \sim 10^5\,eV\left(\frac{M_\chi}{100\,GeV}\right)^2 \Rightarrow \vartheta(100\,KeV)\ \ (Xrays)}$

Secondary Photons

- Inverse Compton emission:

$$\mathbf{e^{\pm} + \gamma \rightarrow e^{\pm} + \gamma^*}$$

Secondary from DM annihilation or decay (→ $e^{\pm}$)

Interstellar radiation field (→ γ)

Up-scattered photon (→ γ^*)

$$\mathbf{E_{\gamma^*} = \frac{4}{3}\left(\frac{E_e}{m_e}\right)^2 E_\gamma}$$

→ interstellar field radiation: CMB $\mathbf{(E_\gamma \sim 2.6 \times 10^{-4}\, eV)}$

dust $\mathbf{(E_\gamma \sim 10^{-2}\, eV)}$

stars $\mathbf{(E_\gamma \sim 1\, eV)}$

$$\mathbf{E_e \sim \frac{M_\chi}{10}}$$

CMB: $\mathbf{E^*_\gamma \sim 10^5\, eV \left(\frac{M_\chi}{100\, GeV}\right)^2 \Rightarrow \vartheta(100\, KeV)\ \ (Xrays)}$

NuSTAR
6 - 79 KeV X-ray sky

γ from DM

3) $\chi + \overline{\chi} \rightarrow \gamma + \gamma$

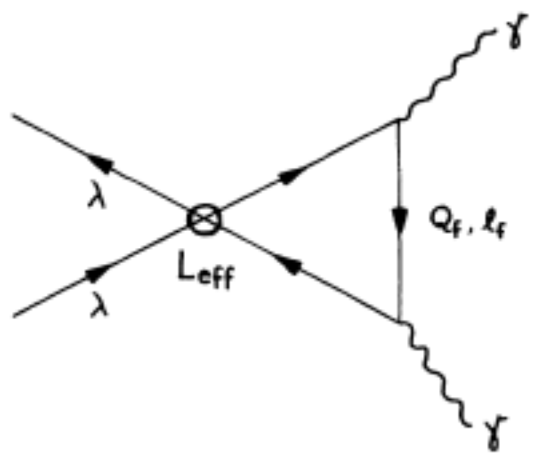

Bergstrom, Snellman, PRD **12**, 1988

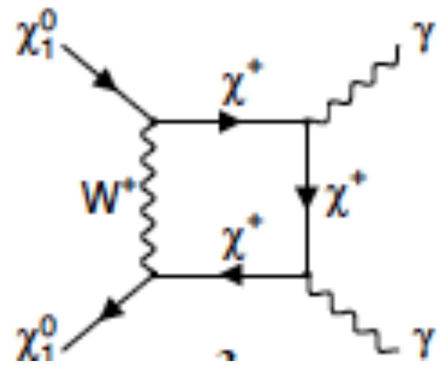

Bergstrom, Ullio, Nuc. Phys. B **504**, 1997

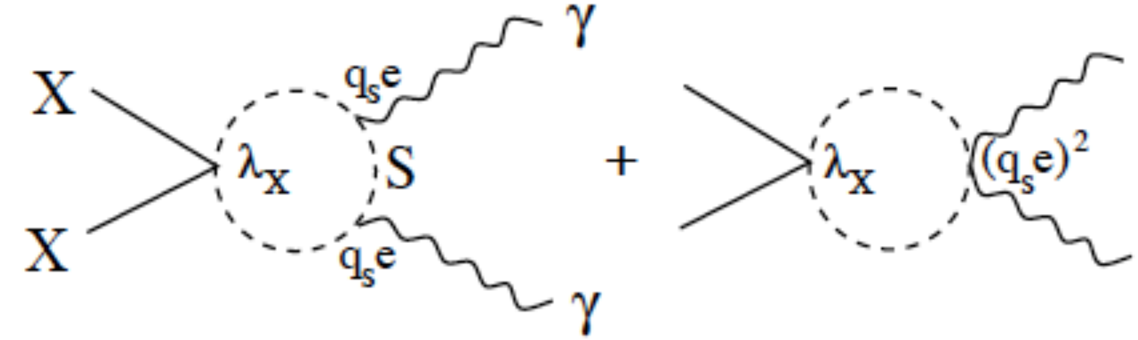

Cline, PRD **86**, 2012

γ from DM

3) $\chi + \overline{\chi} \to \gamma + \gamma$

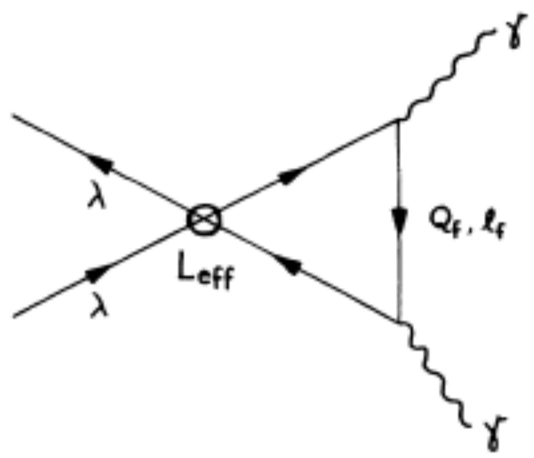

Bergstrom, Snellman, PRD **12**, 1988

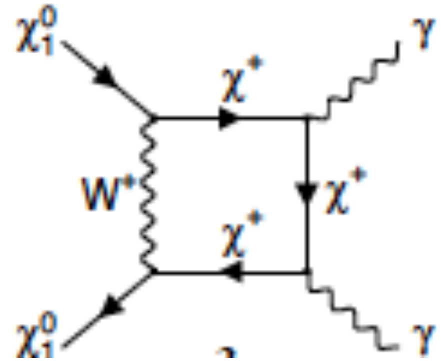

Bergstrom, Ullio, Nuc. Phys. B **504**, 1997

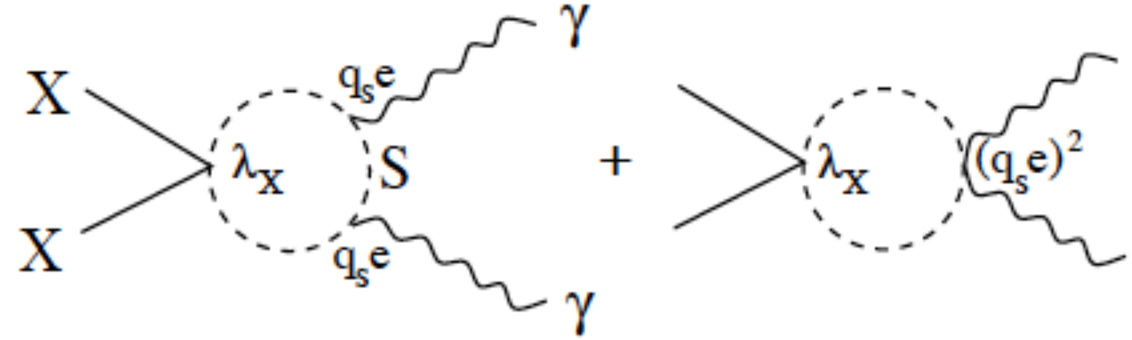

Cline, PRD **86**, 2012

monochromatic line

γ from DM

3) $$\chi + \overline{\chi} \rightarrow \gamma + \gamma$$

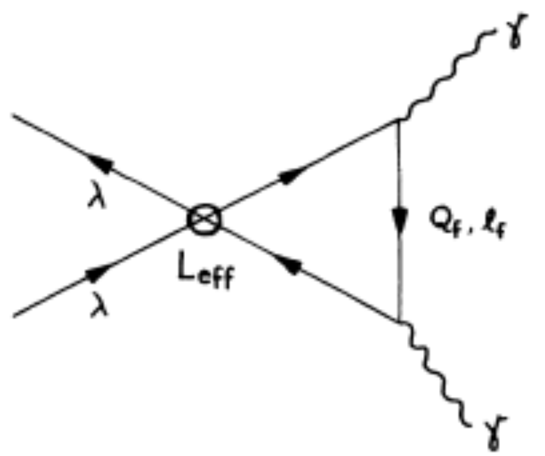

Bergstrom, Snellman, PRD **12**, 1988

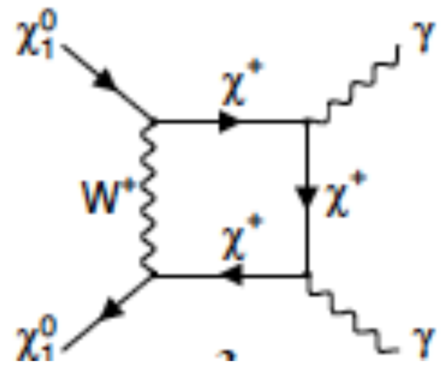

Bergstrom, Ullio, Nuc. Phys. B **504**, 1997

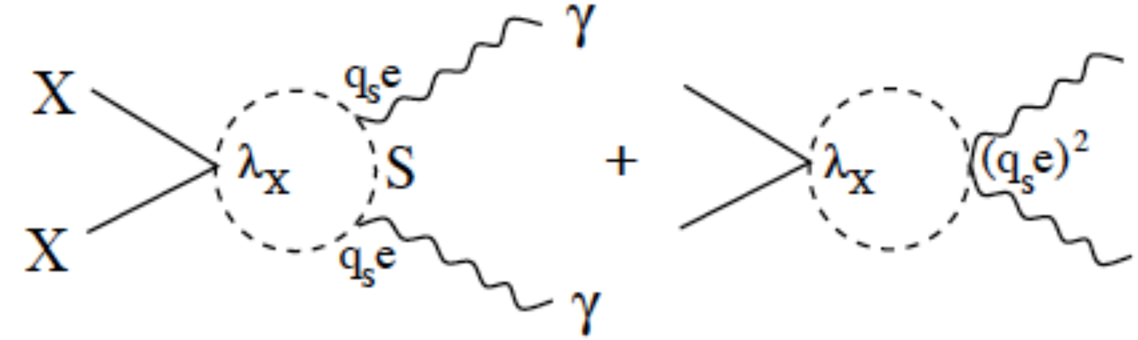

Cline, PRD **86**, 2012

monochromatic line

largely sensitive to DM density profile *

γ from DM

3) $$\chi + \overline{\chi} \rightarrow \gamma + \gamma$$

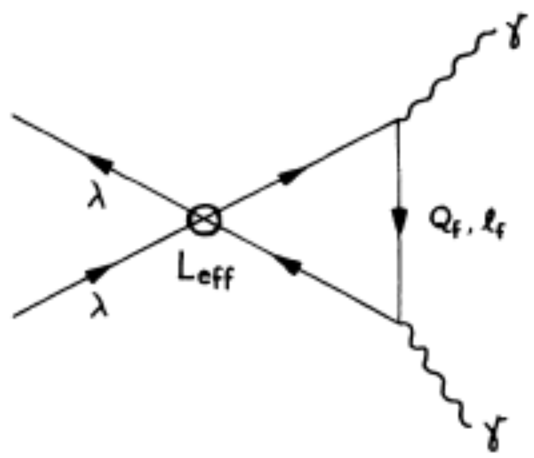

Bergstrom, Snellman, PRD **12**, 1988

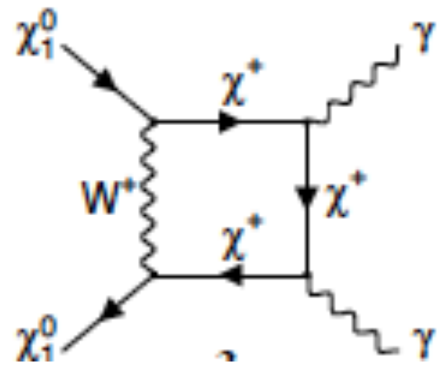

Bergstrom, Ullio, Nuc. Phys. B **504**, 1997

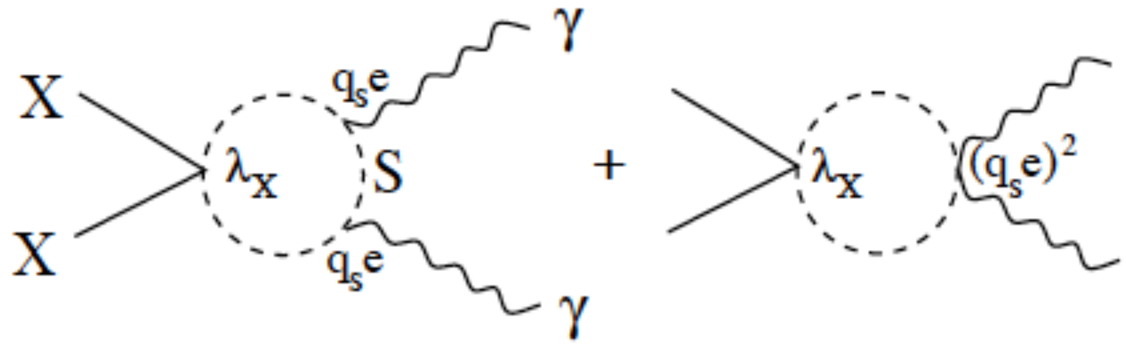

Cline, PRD **86**, 2012

monochromatic line

largely sensitive to DM density profile *

STRONGLY SUPPRESSED!!

Examples of γ Spectra

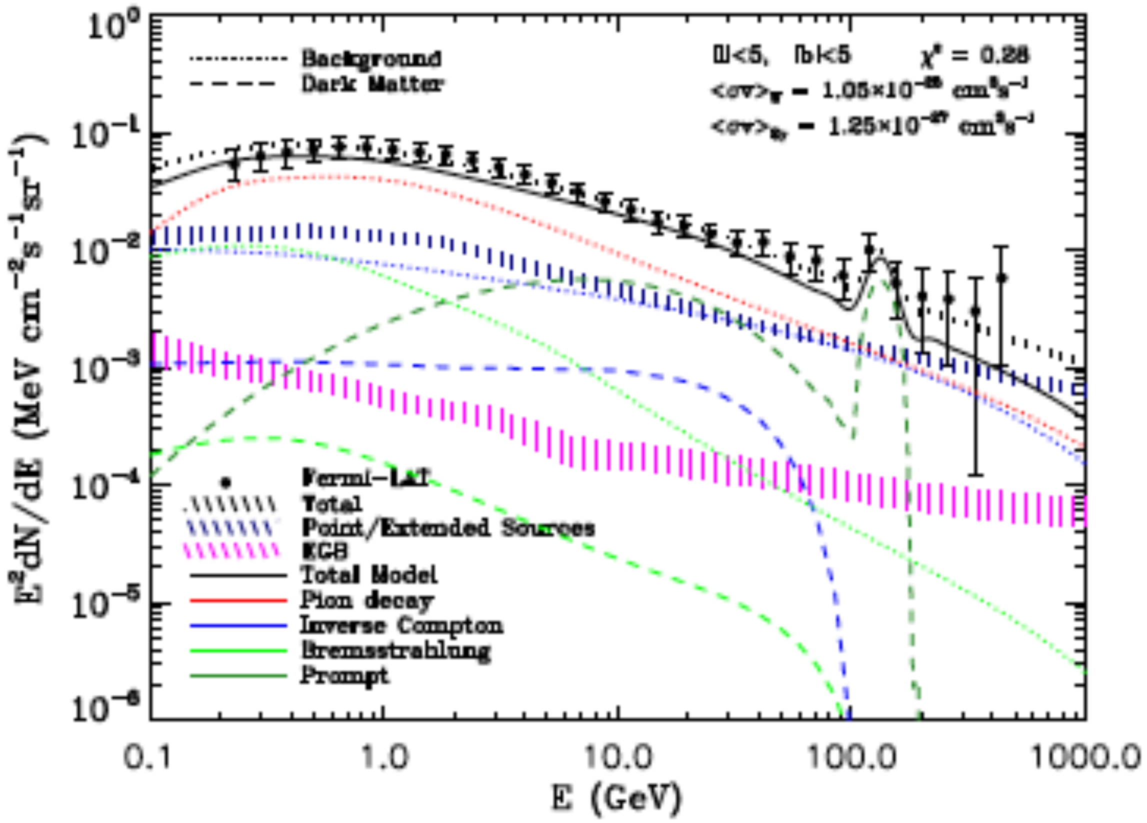

FIG. 1: Case of $m_\chi = 130$ GeV DM particle annihilating to W^+W^- pair with a cross-section of 1.05×10^{-25} cm^{3}s^{-1} a[nd] to a 2γ line with a cross-section of 1.25×10^{-27} cm^{3}s^{-1}. [W...] plot the $|b| < 5°$, $|l| < 5°$.

Cholis, Tavakoli, Ullio, PRD **86**, 2012

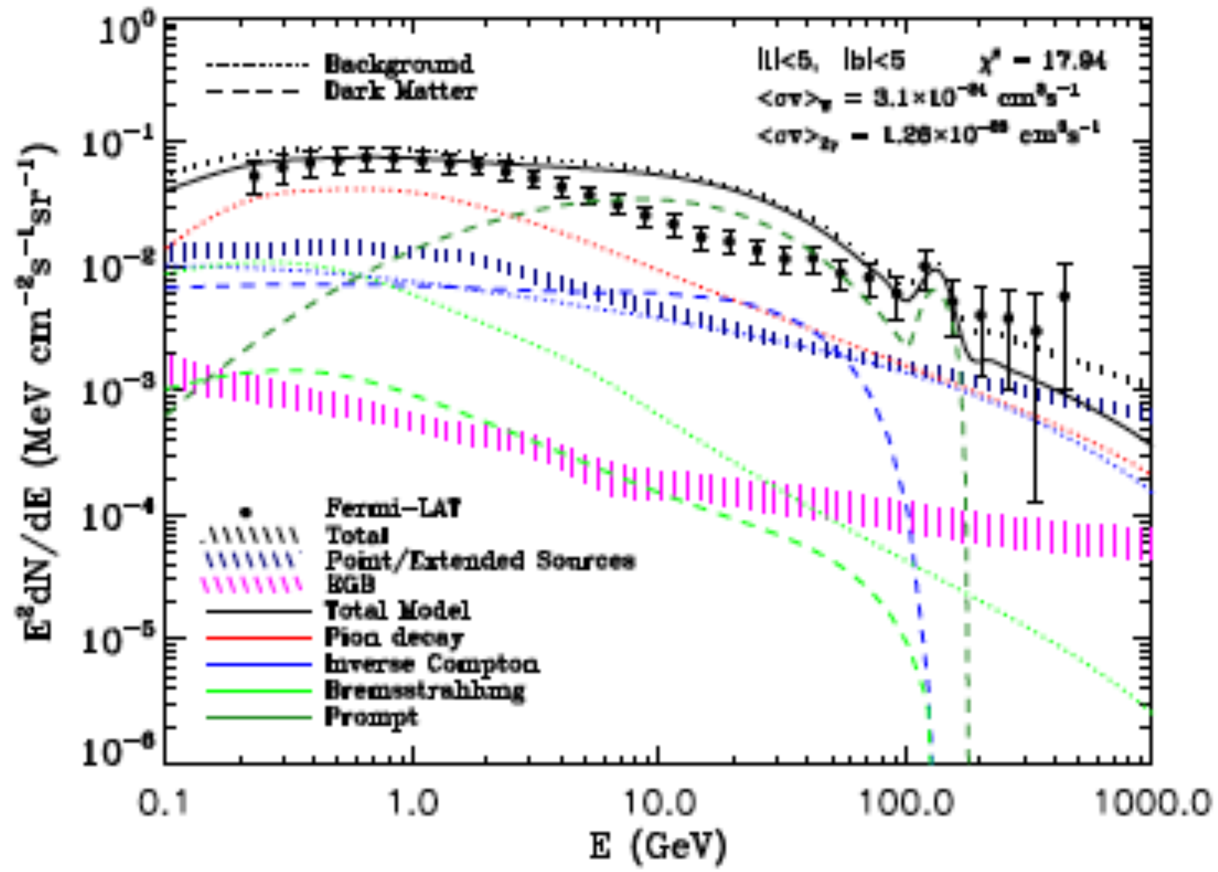

FIG. 6: Wino/Axion model of [30]. $m_\chi = 145$ GeV $\langle\sigma v\rangle_{\chi\chi\rightarrow Z\gamma} = 1.26 \times 10^{-26}$ cm^{3}s^{-1}, $\langle\sigma v\rangle^{tot}_{\chi\chi} = 3.2 \times 10^{-24}$ cm^{3}s^{-1}.

galactic diffuse γ backgrd:
dragon package
http://www.desy.de/~maccione/DRAGON/

[30] Acharya, G. Kane et al., arXiv:1205.5789

γ-ray fluxes

- γ flux from DM annihilation from within a solid angle Ω:

$$\Phi_\gamma = \mathbf{J}\,\frac{<\sigma \mathbf{v}>}{2\,\mathbf{M}_\chi^2}\sum \frac{\mathbf{dN}_\gamma}{\mathbf{dE}}_\gamma$$

Sum over all DM annihilation into γs

$$\mathbf{J}(\Delta\Omega,\psi) = \frac{1}{\Delta\Omega}\int \mathbf{d}\Omega \int_{\mathbf{l.o.s}} \rho^2(\mathbf{l})\mathbf{d}\,\mathbf{l}(\psi) \qquad [\mathbf{J}] = \frac{\mathbf{GeV}}{\mathbf{cm}^5}$$

direction in the sky

$$\rho(\mathbf{r}) = \rho_0 \exp(-\alpha\,\mathbf{f}(\mathbf{r}^\mathbf{n}))$$

γ-ray fluxes

- γ flux from DM annihilation from within a solid angle Ω:

$$\Phi_\gamma \; = \; \mathbf{J} \, \frac{< \sigma \mathbf{v} >}{2 \, \mathbf{M}_\chi^2} \sum \frac{\mathbf{dN}_\gamma}{\mathbf{dE} \;\; \gamma}$$

Sum over all DM annihilation into γs

$$\mathbf{J}(\Delta\Omega, \psi) \; = \; \frac{1}{\Delta\Omega} \int \mathbf{d}\Omega \int_{\mathbf{l.o.s}} \rho^2(\mathbf{l}) \mathbf{d} \; \mathbf{l}(\psi) \qquad [\mathbf{J}] \; = \; \frac{\mathbf{GeV}}{\mathbf{cm}^5}$$

ψ → direction in the sky

- NFW density profile:

$$\rho(\mathbf{r}) \frac{\rho_\mathbf{s}}{\frac{\mathbf{r}}{\mathbf{R_s}} \left(1 + \frac{\mathbf{r}}{\mathbf{R_S}}\right)^2}$$

$\rho(\mathbf{r})$ and $\mathbf{R_s}$ are halo parameters

$$\rho(\mathbf{r}) \; = \; \rho_0 \exp(-\alpha \, \mathbf{f}(\mathbf{r}^\mathbf{n}))$$

γ-ray fluxes

- γ flux from DM annihilation from within a solid angle Ω:

$$\Phi_\gamma = J \frac{< \sigma v >}{2 M_\chi^2} \sum \frac{dN_\gamma}{dE_\gamma}$$

Sum over all DM annihilation into γs

$$J(\Delta\Omega, \psi) = \frac{1}{\Delta\Omega} \int d\Omega \int_{l.o.s} \rho^2(l) d\, l(\psi) \qquad [J] = \frac{GeV}{cm^5}$$

↓ direction in the sky

- NFW density profile: $\rho(r) \frac{\rho_s}{\frac{r}{R_s}\left(1 + \frac{r}{R_S}\right)^2}$

$\rho(r)$ and R_s are halo parameters

$$\rho(r) = \rho_0 \exp(-\alpha\, f(r^n))$$

Ω => depends on telescope, source, fov => should be optimized to maximize signal/noise

γ-ray fluxes

- γ flux from DM annihilation from within a solid angle Ω:

$$\Phi_\gamma = J \frac{<\sigma v>}{2 M_\chi^2} \sum \frac{dN_\gamma}{dE_\gamma}$$

Sum over all DM annihilation into γs

$$J(\Delta\Omega, \psi) = \frac{1}{\Delta\Omega} \int d\Omega \int_{l.o.s} \rho^2(l) d\, l(\psi) \qquad [J] = \frac{GeV}{cm^5}$$

ψ → direction in the sky

- NFW density profile: $\rho(r) \frac{\rho_s}{\frac{r}{R_s}\left(1 + \frac{r}{R_s}\right)^2}$

$\rho(r)$ and R_s are halo parameters

- Einasto density profile: $\rho(r) = \rho_0 \exp(-\alpha\, f(r^n))$

Ω => depends on telescope, source, fov => should be optimized to maximize signal/noise

Good γ Locations

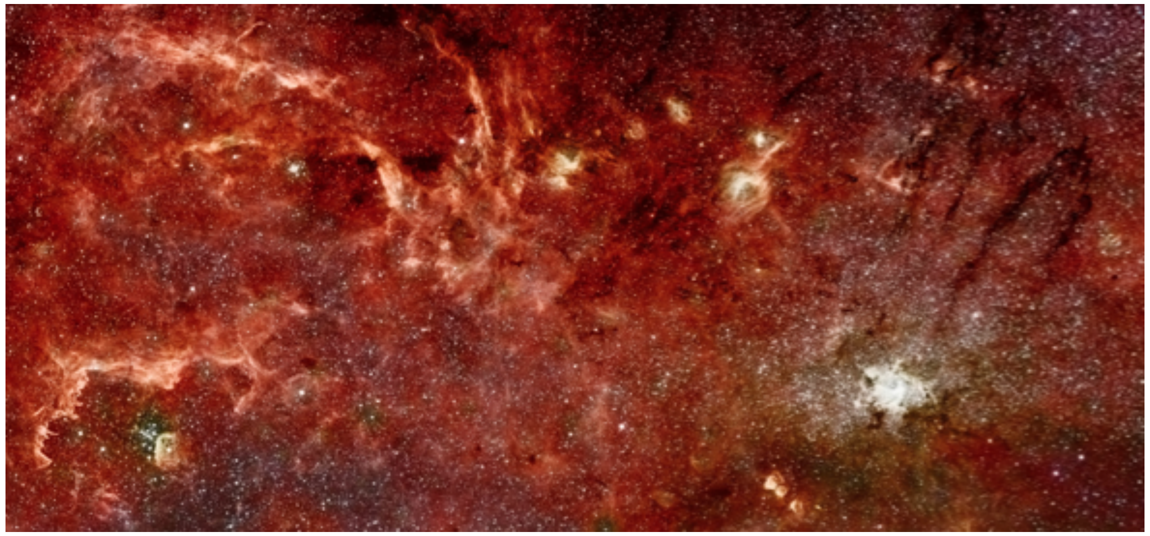

Galactic Center

Good statistics

Huge Background

Good γ Locations

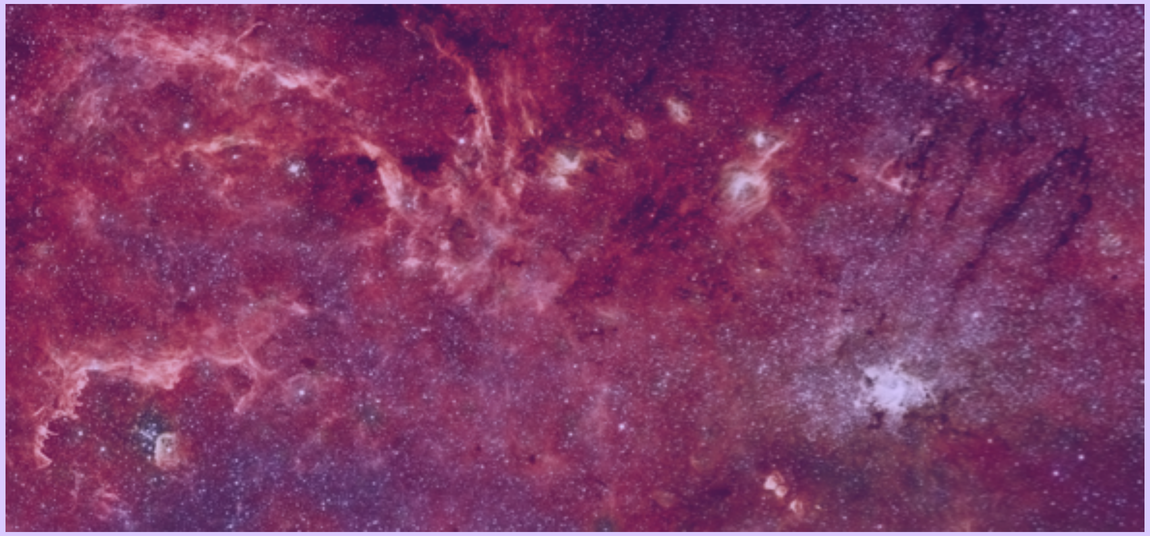

Galactic Center

Good statistics

Huge Background

Good γ Locations

Dwarf galaxies

(Fornax dwarf spheroidal galaxy)

Large mass/light ratio
(no gas detected)

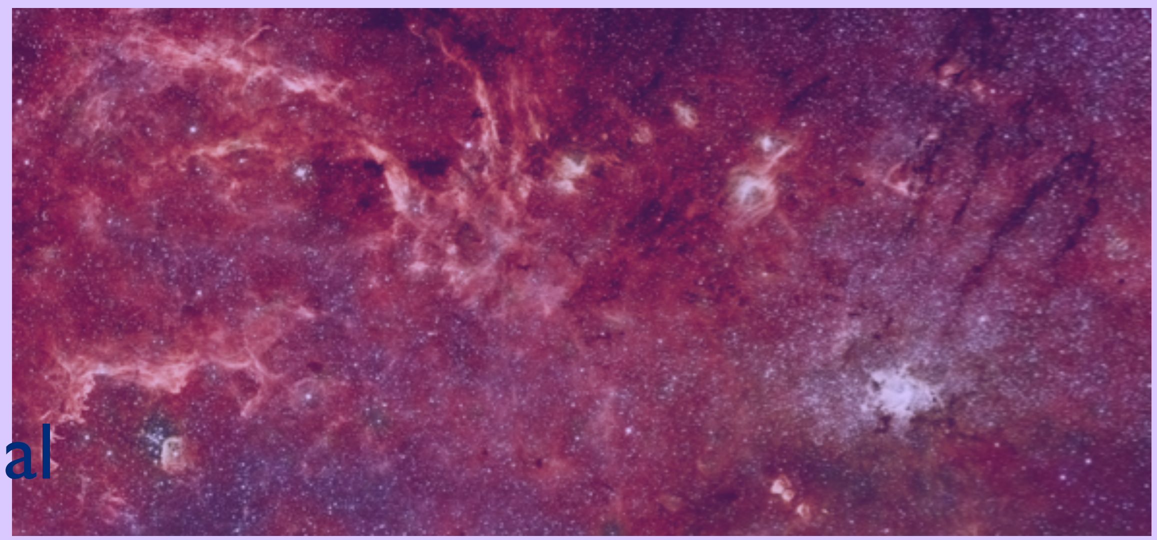

Galactic Center

Good statistics

Huge Background

Good γ Locations

Dwarf galaxies

(Fornax dwarf spheroidal galaxy)

Large mass/light ratio (no gas detected)

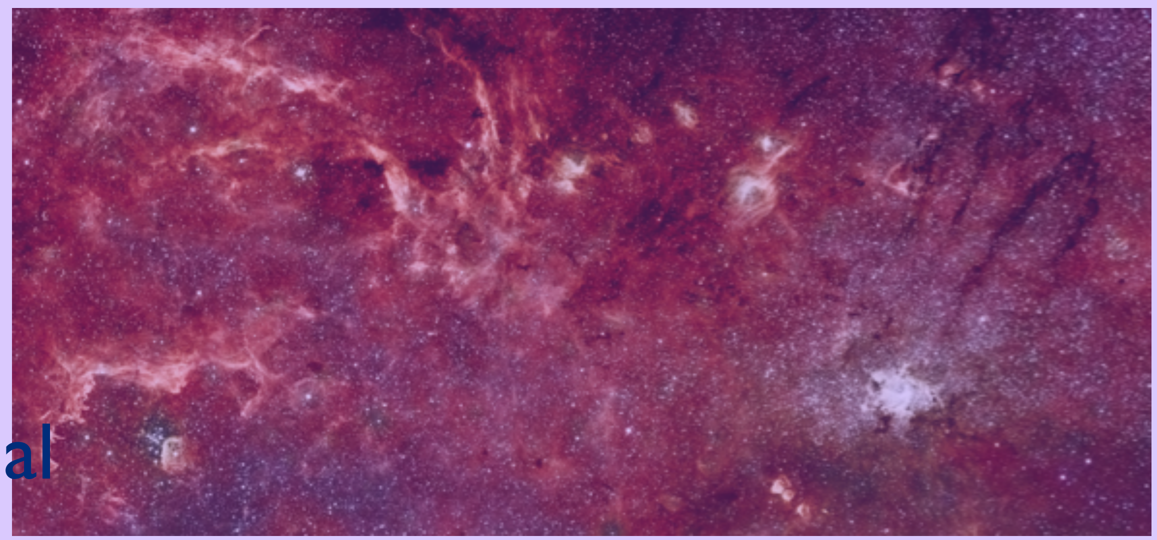

Galactic Center

Good statistics

Huge Background

Cluster of galaxies

Coma Cluster

Good γ Locations

Dwarf galaxies

(Fornax dwarf spheroidal galaxy)

Large mass/light ratio
(no gas detected)

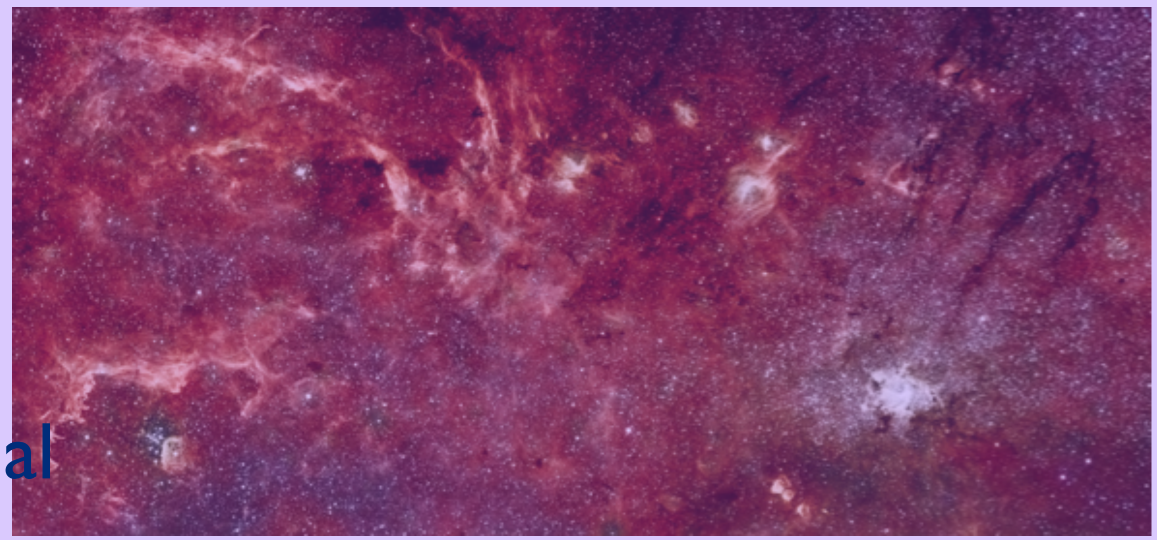

Galactic Center

Good statistics

Huge Background

Cluster of galaxies

Coma Cluster

Spectral lines:
excellent identification
rare events => low sensitivity

J Factors

$\Delta\Omega = 1^o$ and NFW profile

Name	$[\langle R\rangle, \langle P\rangle]$	$\left[\langle R^2\rangle - \langle R\rangle^2, \langle P^2\rangle - \langle P\rangle^2, \langle RP\rangle - \langle R\rangle\langle P\rangle\right]$ $R \equiv \log_{10}(r_s/kpc)$, $P \equiv \log_{10}(\rho_s/M_\odot\, kpc^{-3})$	J^{NFW} $(10^{19}\frac{GeV^2}{cm^5})$
Ursa Major II	[−0.78, 8.54]	[0.0417, 0.0986, −0.0554]	$0.58^{+0.91}_{-0.35}$
Coma Berenices	[−0.79, 8.41]	[0.0603, 0.132, −0.0820]	$0.16^{+0.22}_{-0.08}$
Bootes I	[−0.57, 8.31]	[0.0684, 0.165, −0.0931]	$0.16^{+0.35}_{-0.13}$
Usra Minor	[−0.19, 7.99]	[0.0430, 0.116, −0.0697]	$0.64^{+0.25}_{-0.18}$
Sculptor	[−0.021, 7.57]	[0.0357, 0.0798, −0.0528]	$0.24^{+0.06}_{-0.06}$
Draco	[0.32, 7.41]	[0.0236, 0.0364, −0.0286]	$1.20^{+0.31}_{-0.25}$
Sextans	[−0.43, 7.93]	[0.0302, 0.109, −0.0570]	$0.06^{+0.03}_{-0.02}$
Fornax	[−0.24, 7.82]	[0.0474, 0.140, −0.0798]	$0.06^{+0.03}_{-0.03}$

Dwarfs

FermiLat (Ackermann et al.), Astrophy. J. **712**, 2010

large mass/light ratio
low bckg (no gas detected)

Cluster	RA	Dec.	z	J $(10^{17}$ GeV^2 cm$^{-5})$
AWM 7	43.6229	41.5781	0.0172	$1.4^{+0.1}_{-0.1}$
Fornax	54.6686	-35.3103	0.0046	$6.8^{+1.0}_{-0.9}$
M49	187.4437	7.9956	0.0033	$4.4^{+0.2}_{-0.1}$
NGC 4636	190.7084	2.6880	0.0031	$4.1^{+0.3}_{-0.3}$
Centaurus (A3526)	192.1995	-41.3087	0.0114	$2.7^{+0.1}_{-0.1}$
Coma	194.9468	27.9388	0.0231	$1.7^{+0.1}_{-0.1}$

Clusters

FermiLat (Ackermann et al.), JCAP **1005**, 2010

Galactic center: $J \sim 10^{21}\ \mathrm{GeV}^2\mathrm{cm}^{-5}$

PAMELA Telescope

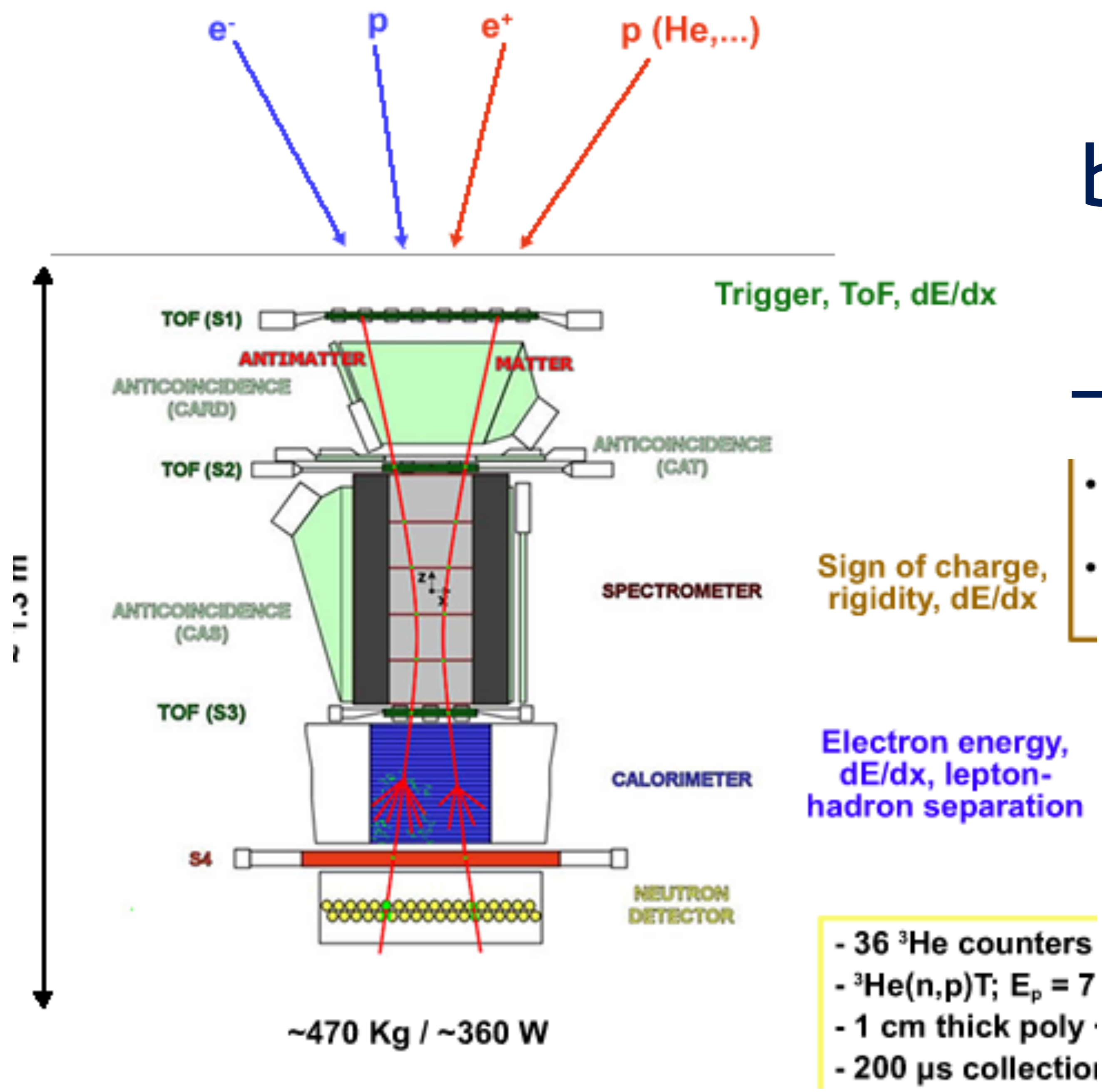

- magnetic spectrometer: bending depends on electric charge and rigidity
→ momentum is determined

- calorimeter: $e^{\pm}$ separation from $p^{\pm}$

- satellite in an elliptical orbit at an altitude between 350 and 610 Km

a Payload for Antimatter Matter Exploration and Light Nuclei Astrophysics

Fermi-LAT Telescope

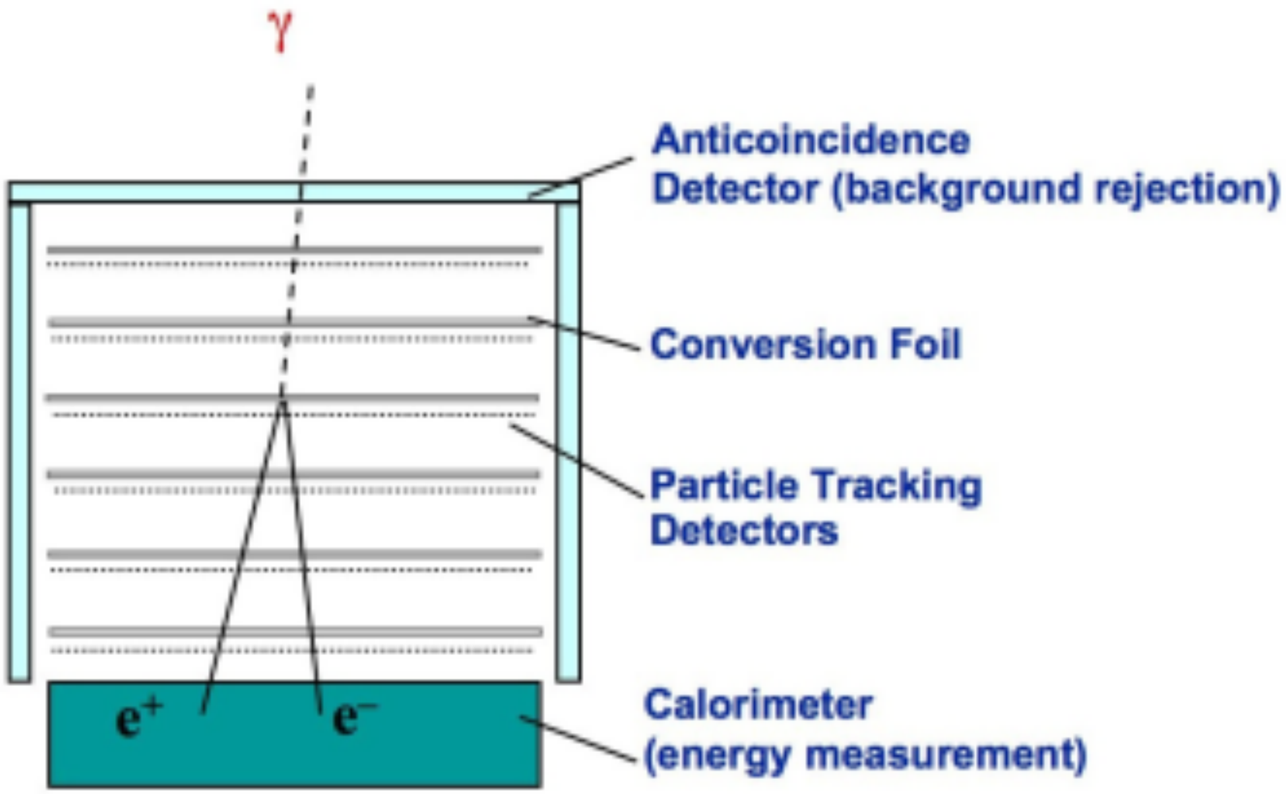

- γ rays go freely through plastic anti-coincidence detector

→charged particles (CR) cause a flash of light

γ rays convert into e^+e^-

e^+e^- reconstruction: energy and direction incident γ-ray

Quantity	LAT (Minimim Spec.)	EGRET
Energy Range	20 MeV - 300 GeV	20 MeV - 30 GeV
Peak Effective Area[1]	> 8000 cm^2	1500 cm^2
Field of View	> 2 sr	0.5 sr
Angular Resolution[2]	< 3.5° (100 MeV) < 0.15° (>10 GeV)	5.8° (100 MeV)
Energy Resolution[3]	< 10%	10%
Deadtime per Event	< 100 μs	100 ms
Source Location Determination[4]	< 0.5'	15'
Point Source Sensitivity[5]	< 6 x 10^{-9} cm^{-2} s^{-1}	~ 10^{-7} cm^{-2} s^{-1}

Fermi-LAT $e^- + e^+$ measurement

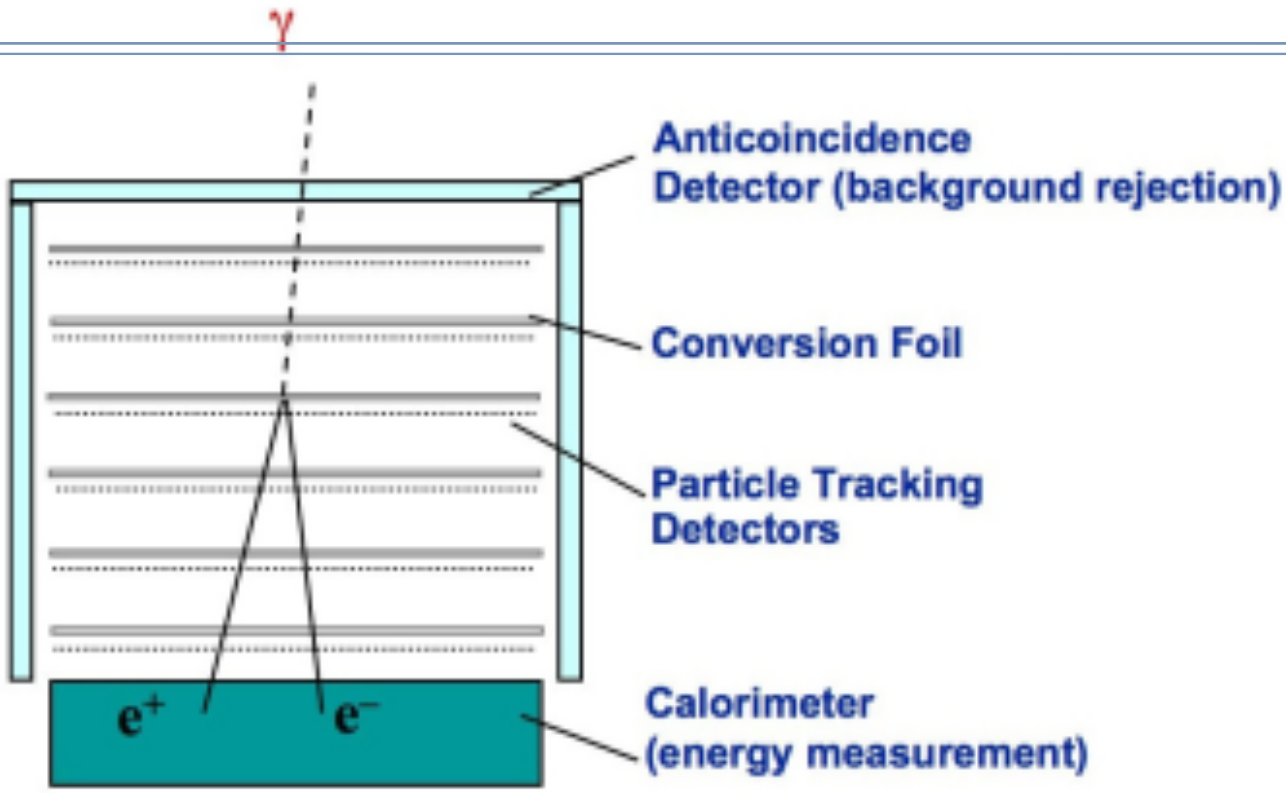

Abdo et al. (FermiLat Coll.), PRL **102**, 2009

Fermi-LAT $e^- + e^+$ measurement

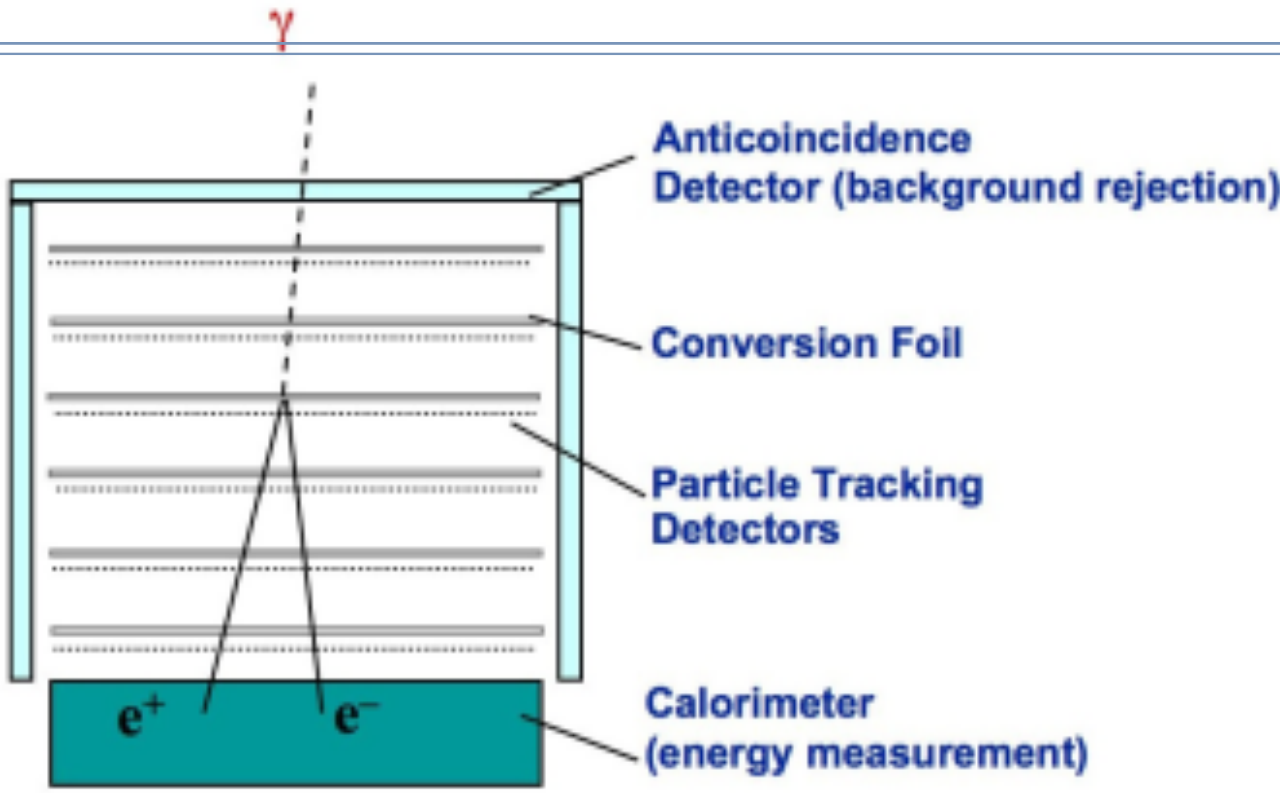

→ fails AC veto

Abdo et al. (FermiLat Coll.), PRL **102**, 2009

Fermi-LAT $e^- + e^+$ measurement

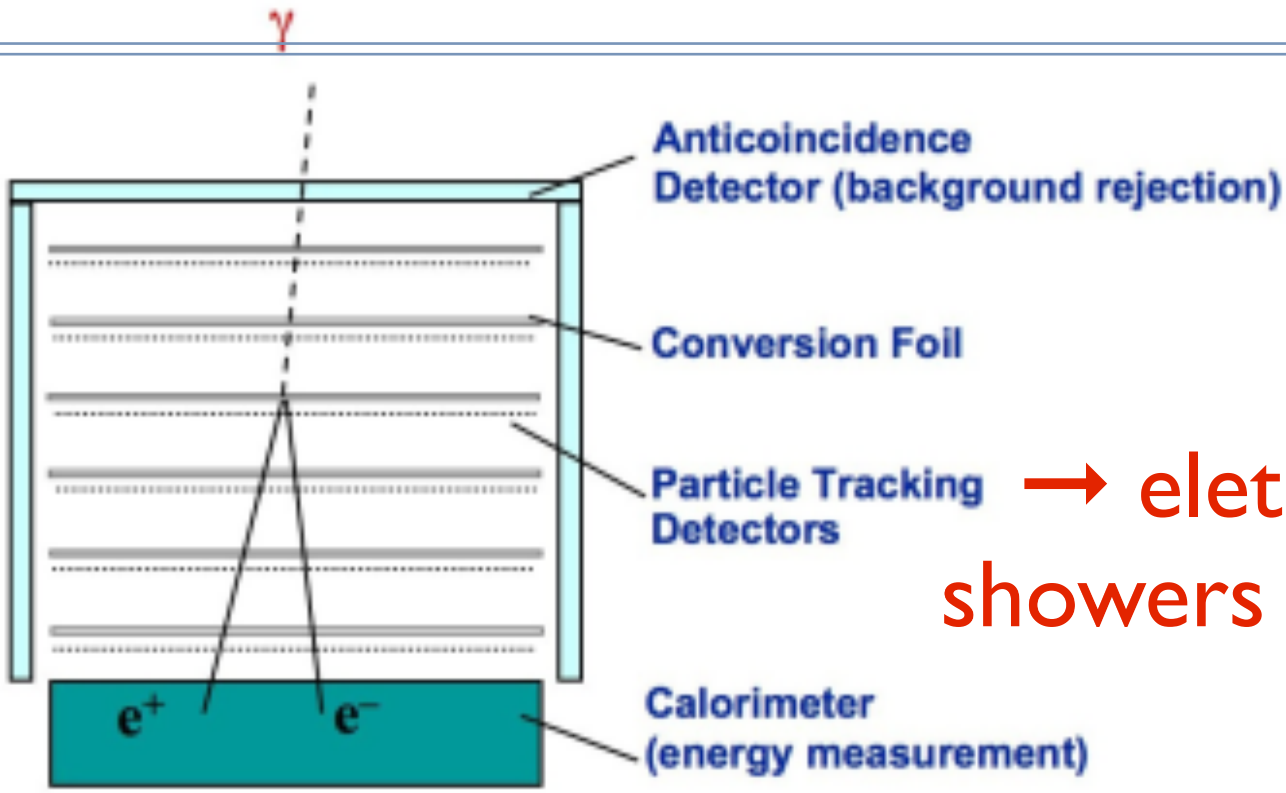

→ fails AC veto

→ eletromagnetic/hadron showers have different shapes

Abdo et al. (FermiLat Coll.), PRL **102**, 2009

Fermi-LAT $e^- + e^+$ measurement

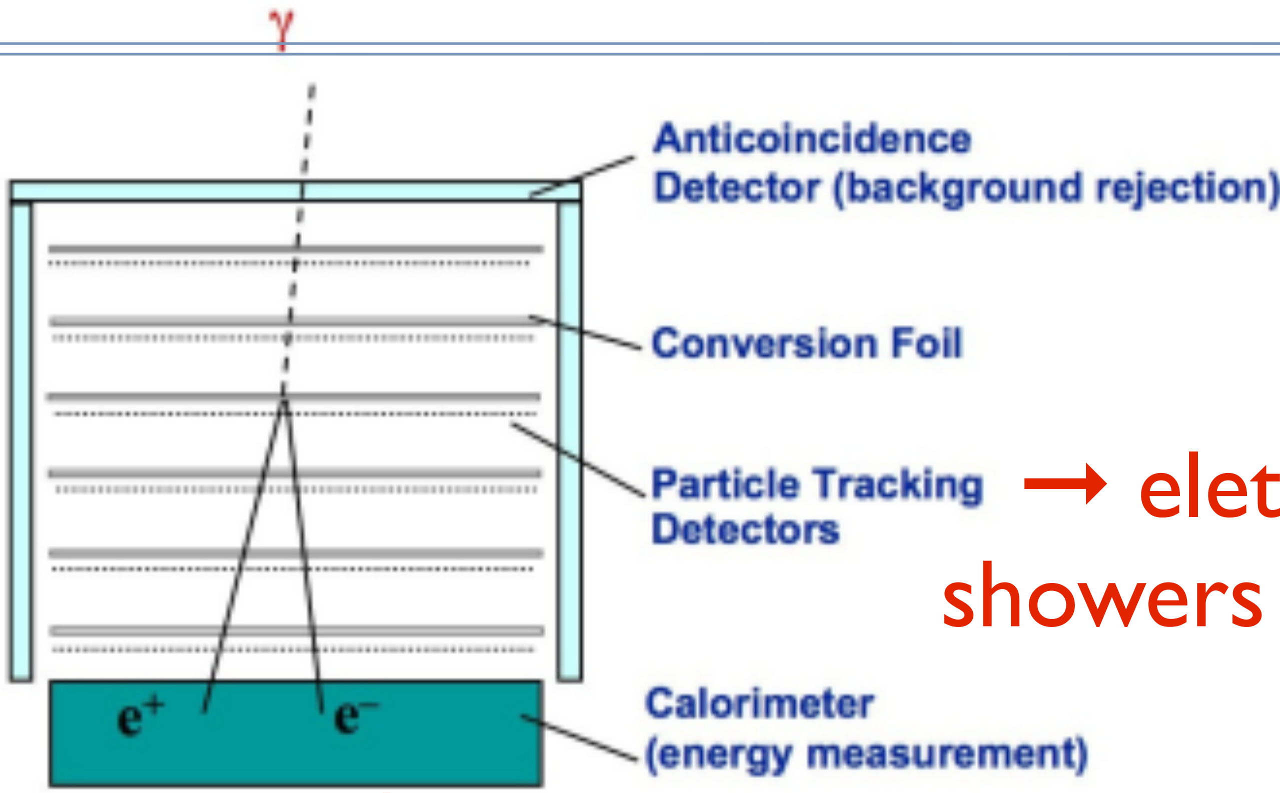

→ fails AC veto

→ eletromagnetic/hadron showers have different shapes

↳ > 20 GeV: large fraction of the event energy falls out of the Cal

Abdo et al. (FermiLat Coll.), PRL **102**, 2009

Fermi-LAT $e^- + e^+$ measurement

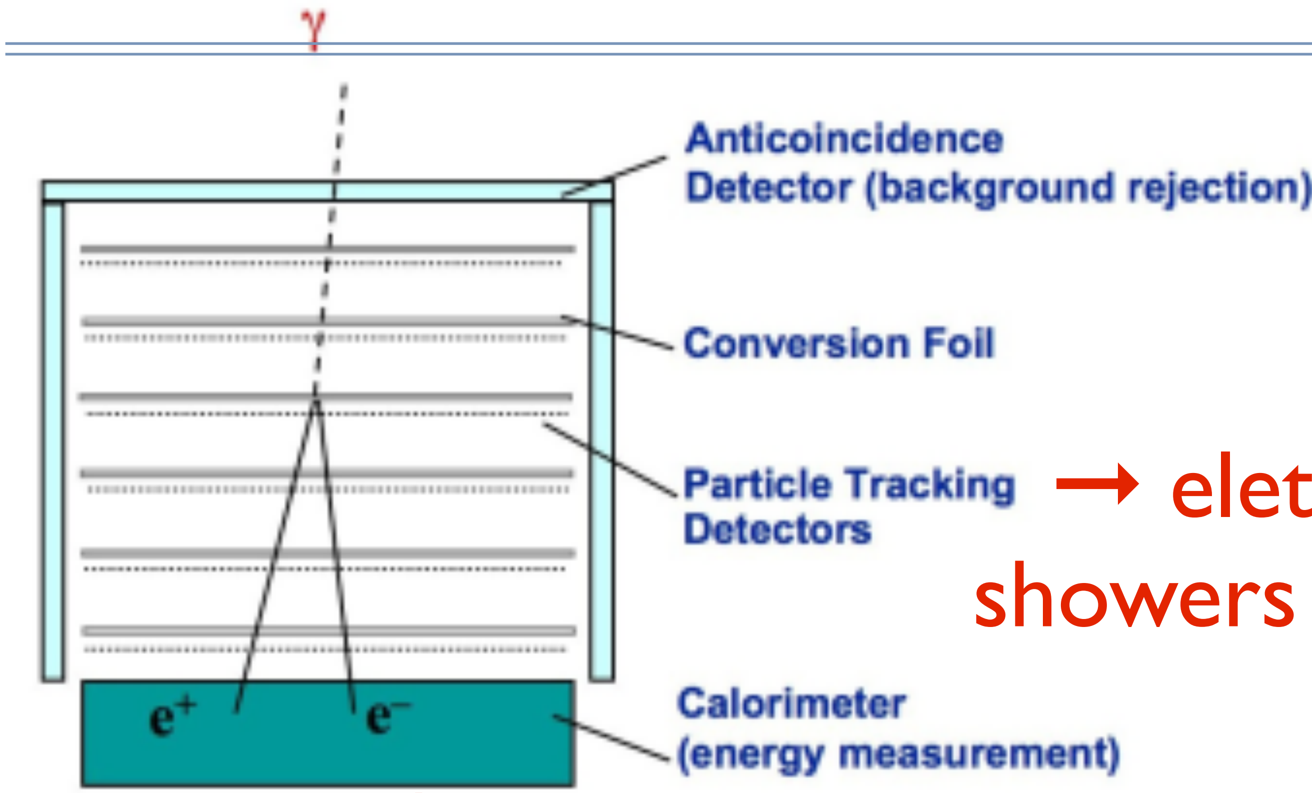

→ fails AC veto

→ eletromagnetic/hadron showers have different shapes

↳ > 20 GeV: large fraction of the event energy falls out of the Cal

→ energy reconstruction depends on Monte Carlo

Abdo et al. (FermiLat Coll.), PRL **102**, 2009

Fermi-LAT $e^- + e^+$ measurement

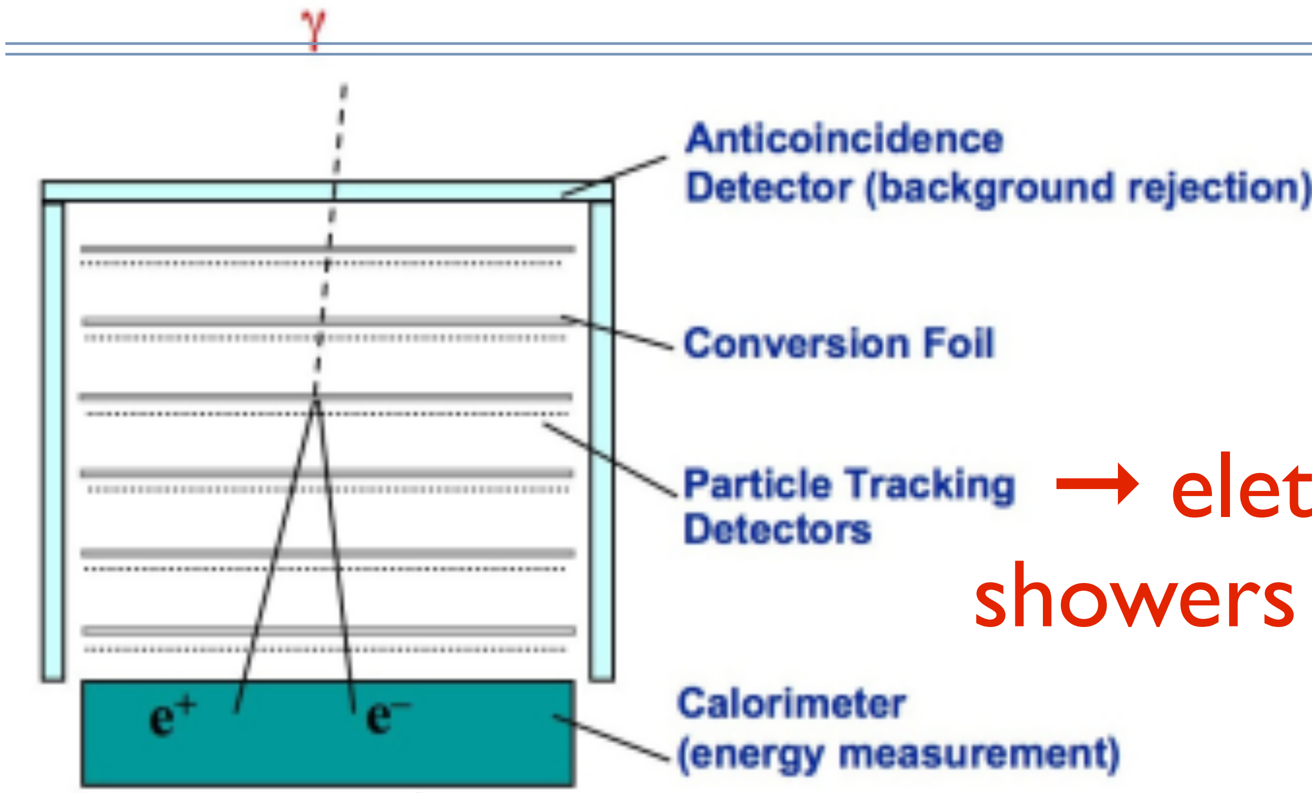

→ fails AC veto

→ eletromagnetic/hadron showers have different shapes

↳ > 20 GeV: large fraction of the event energy falls out of the Cal

→ energy reconstruction depends on Monte Carlo

→ beam test data for electrons and hadrons up to 282 GeV

Abdo et al. (FermiLat Coll.), PRL **102**, 2009

Fermi-LAT $e^- + e^+$ measurement

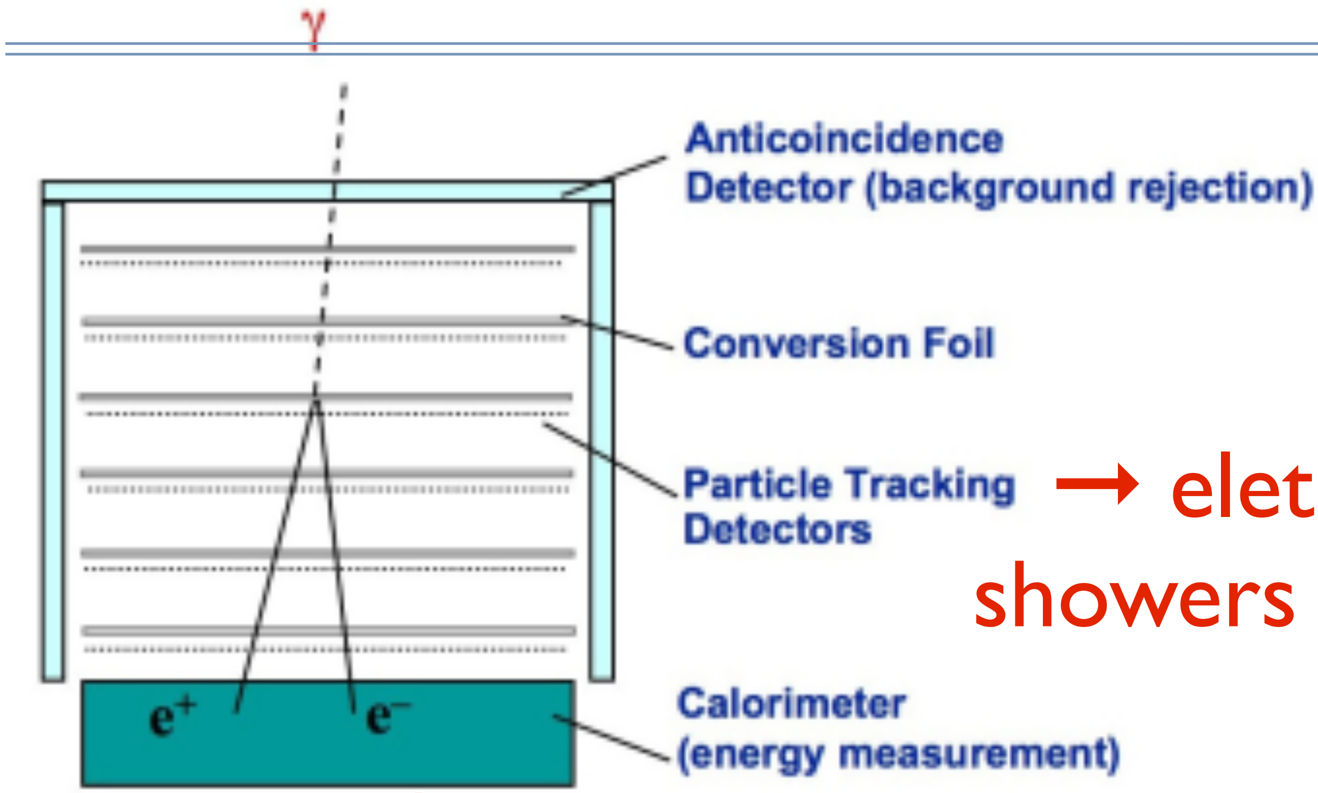

→ fails AC veto

→ eletromagnetic/hadron showers have different shapes

↳ > 20 GeV: large fraction of the event energy falls out of the Cal

→ energy reconstruction depends on Monte Carlo

→ beam test data for electrons and hadrons up to 282 GeV

Abdo et al. (FermiLat Coll.), PRL **102**, 2009

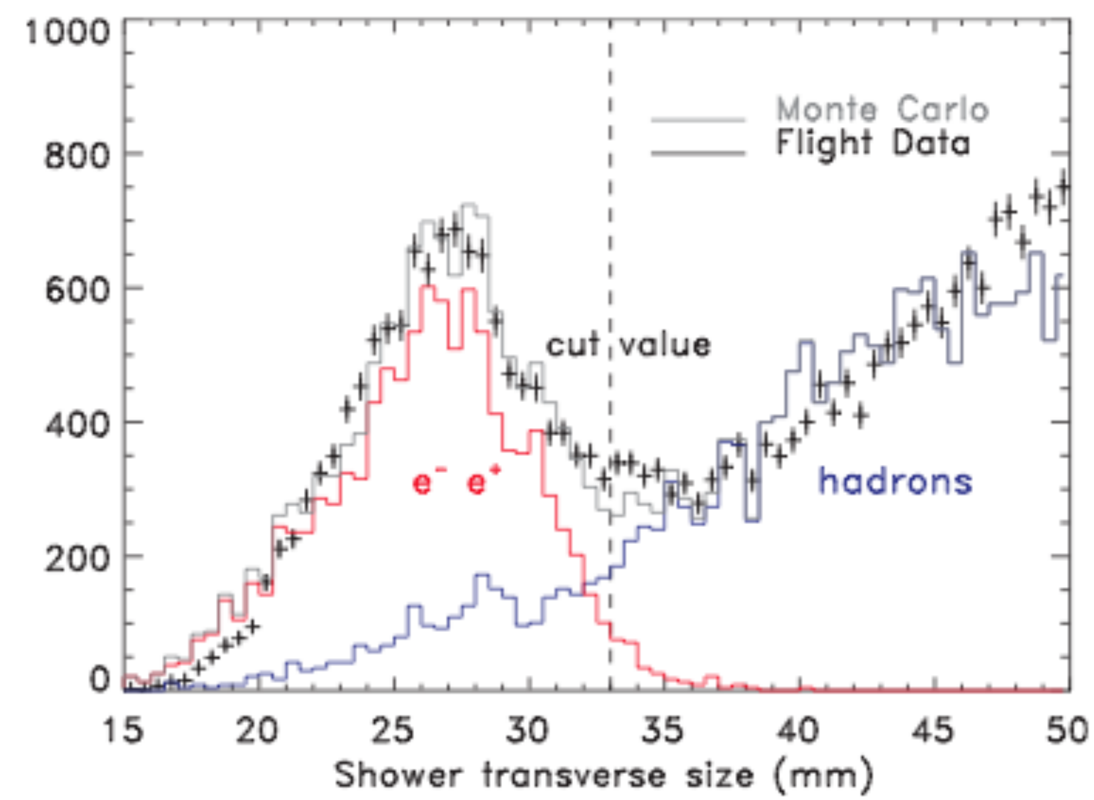

Bits of Light

Hints from from electromagnetic fluxes

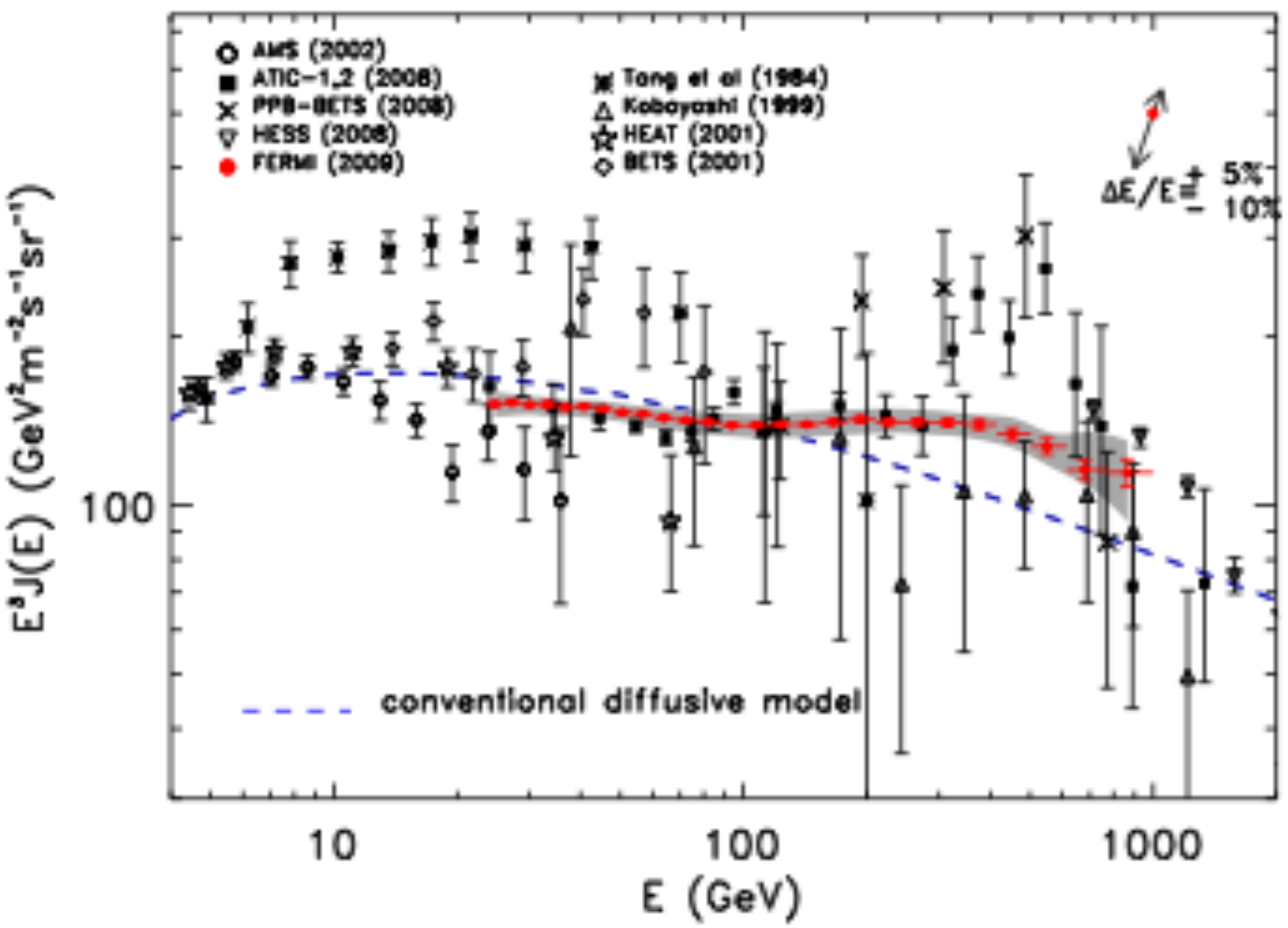

e$^-$ + e$^+$ spectrum from Fermi-Lat (2009)

--- expected diff spectrum

Abdo et al. (FermiLat Coll.), PRL **102**, 2009

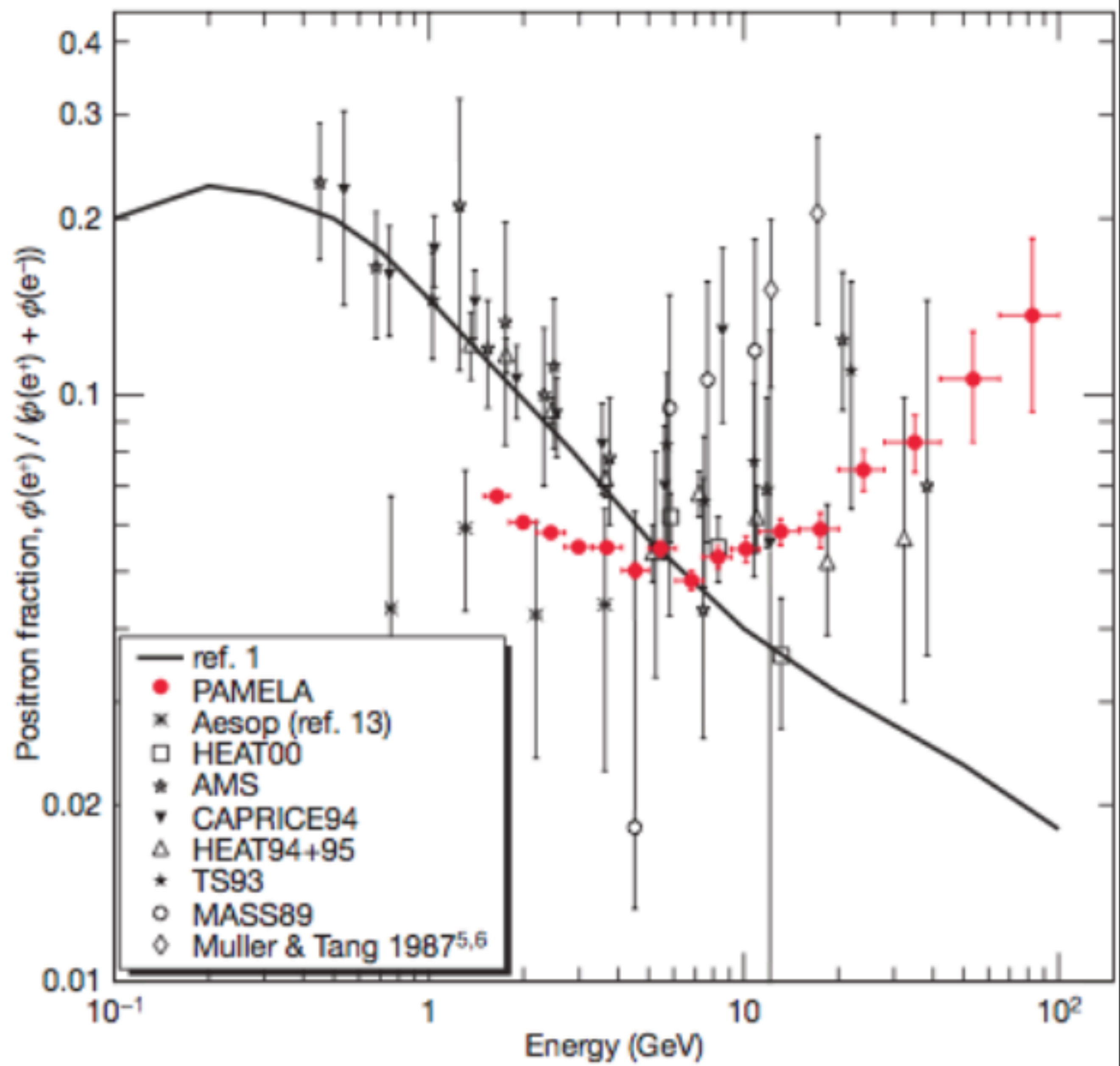

Pamela - Nature 458 (2009)

— expected secondary spec

Fermi-LAT e^- e^+ separated fluxes

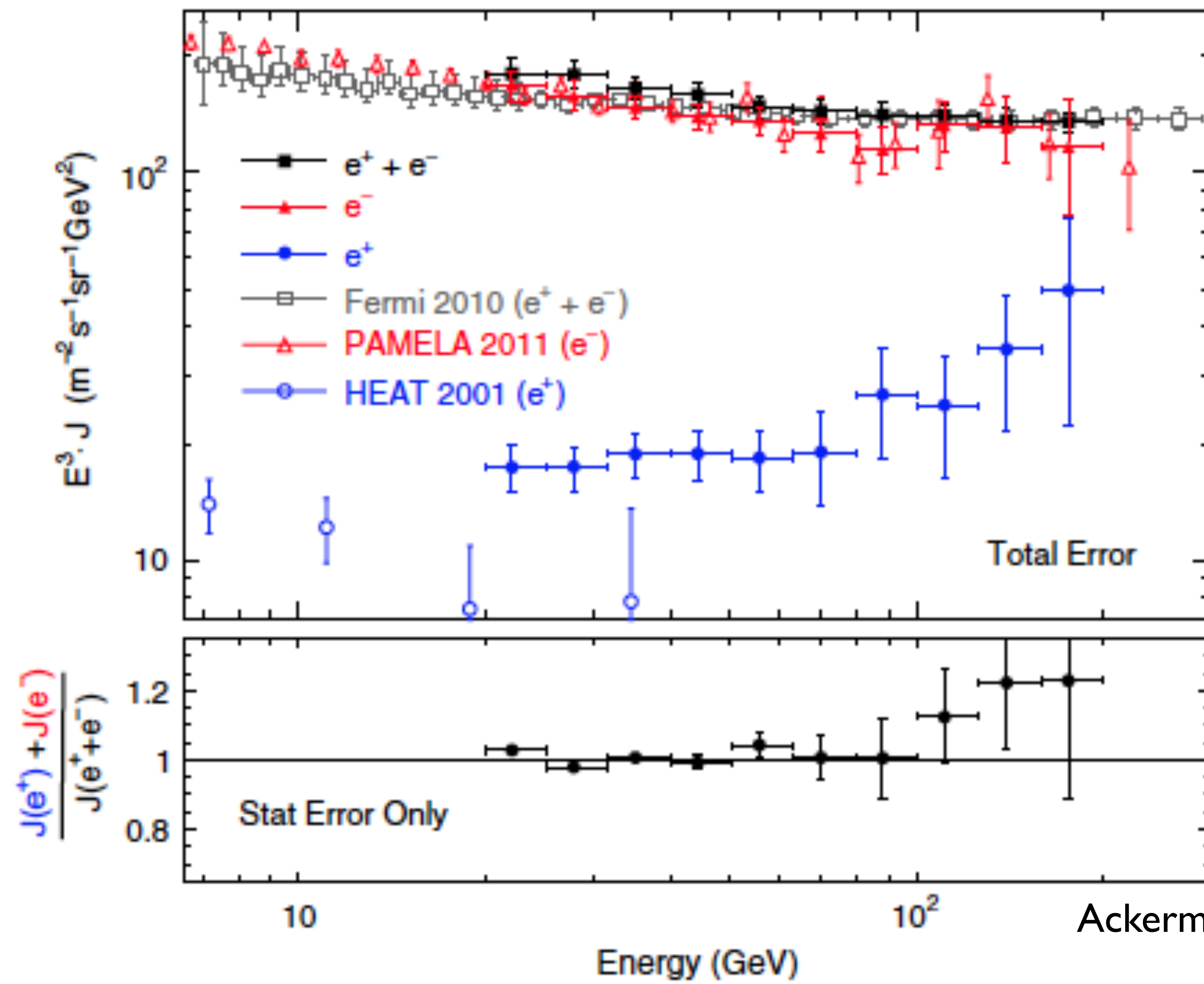

Ackermann et al. (FermiLat Coll.), PRL **108**, 2012

Fermi-LAT e^- e^+ separated fluxes

no magnet => effect of Earth magnetic field (20 to 200 GeV)

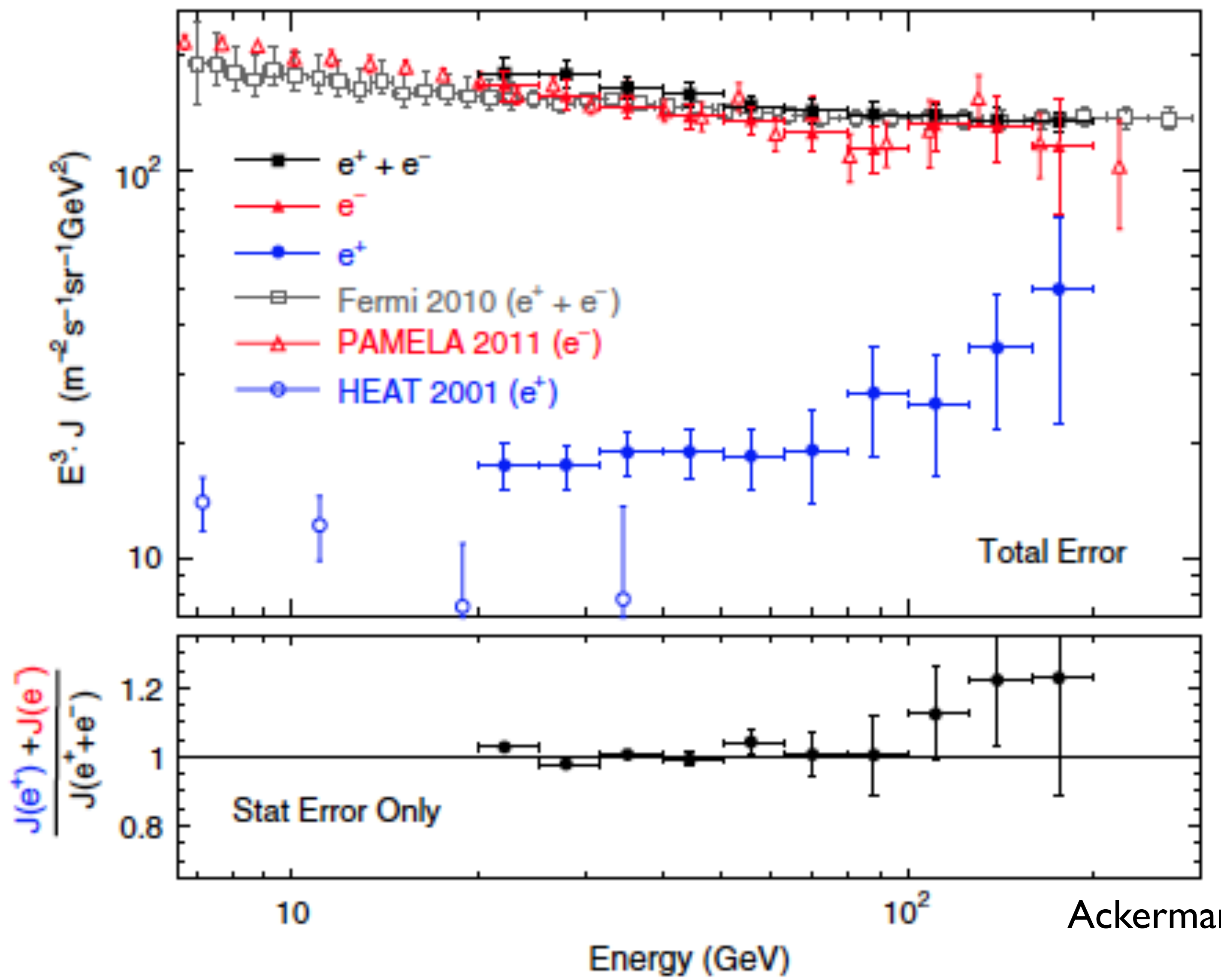

Ackermann et al. (FermiLat Coll.), PRL **108**, 2012

Fermi-LAT e^- e^+ separated fluxes

no magnet => effect of Earth magnetic field (20 to 200 GeV)

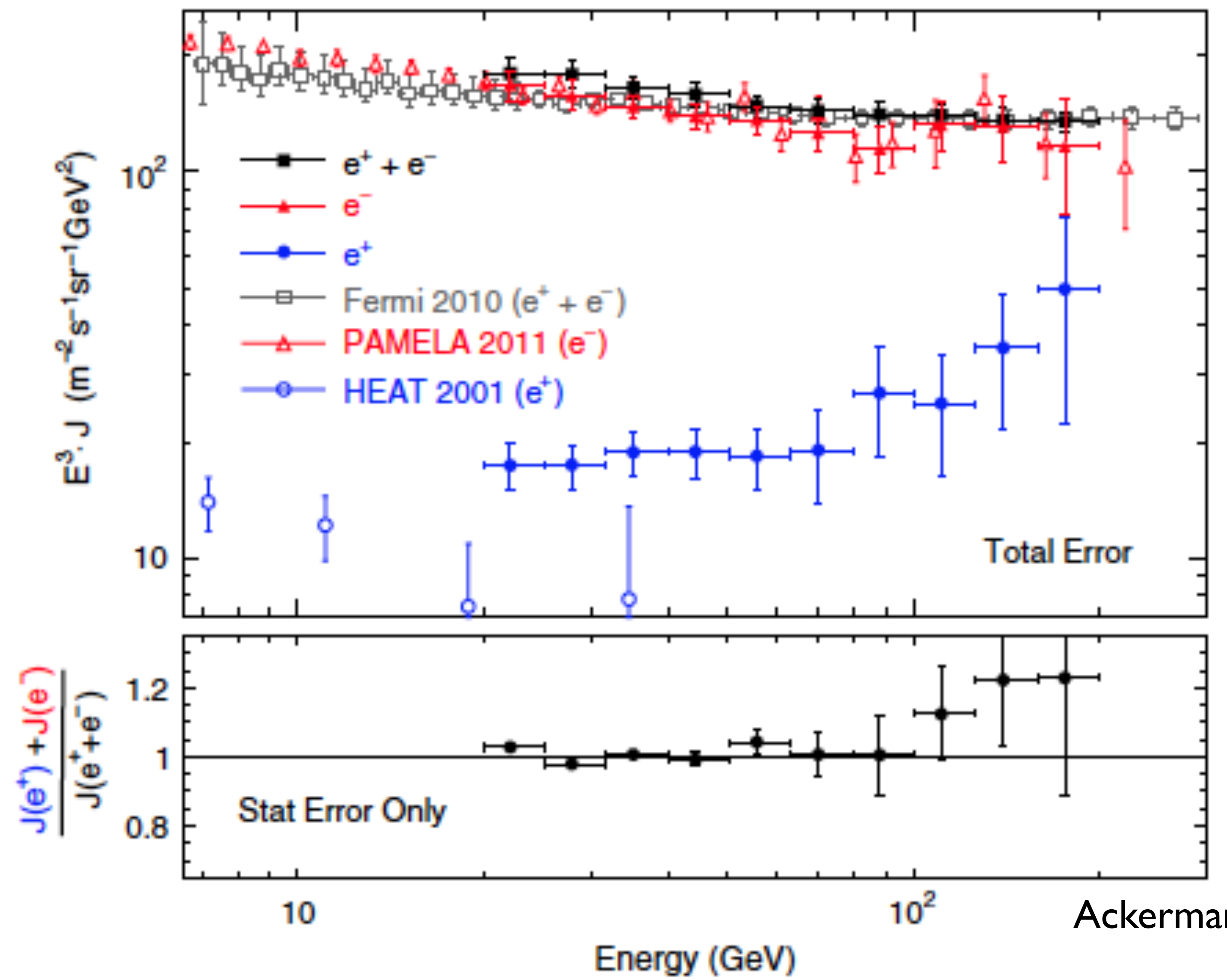

Ackermann et al. (FermiLat Coll.), PRL **108**, 2012

consistent with previous measurement + with PAMELA

AMS Results

Alpha Magnetic Spectrometer

1.03 TeV
electron

~1.4 KG

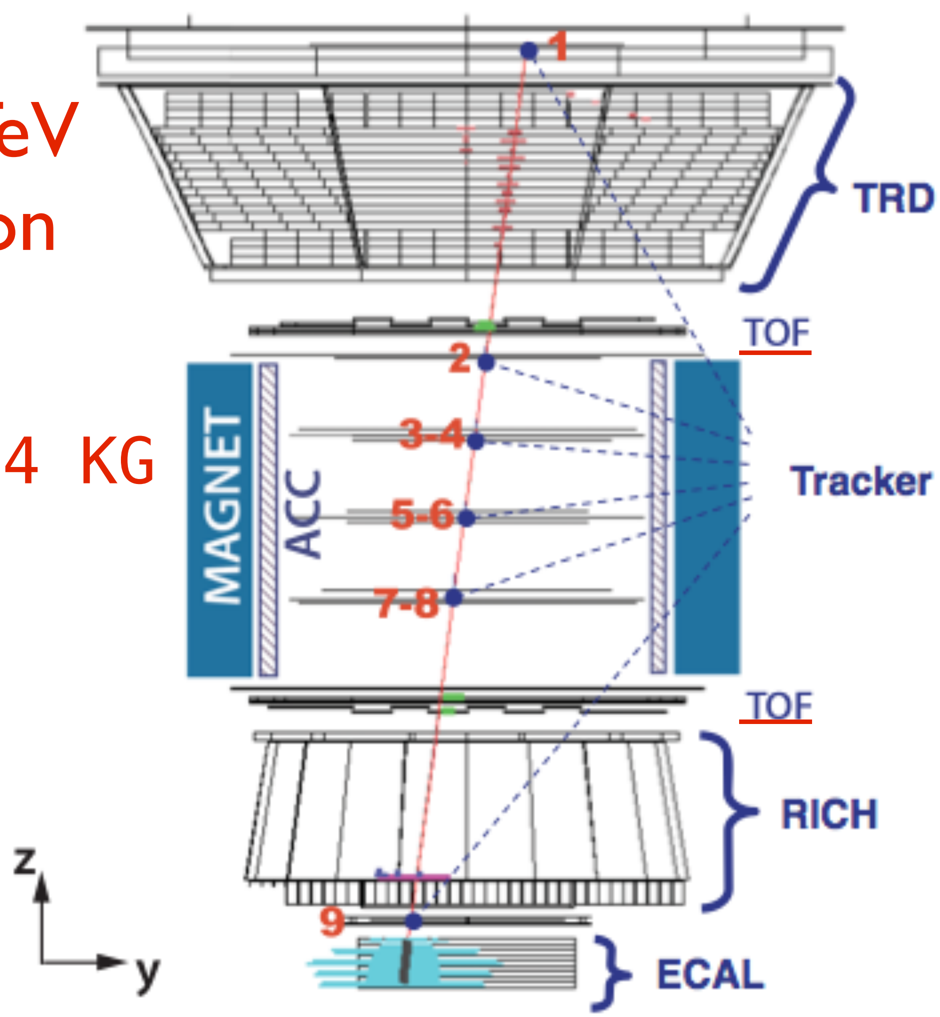

AMS Results

Alpha Magnetic Spectrometer

1.03 TeV
electron

~1.4 KG

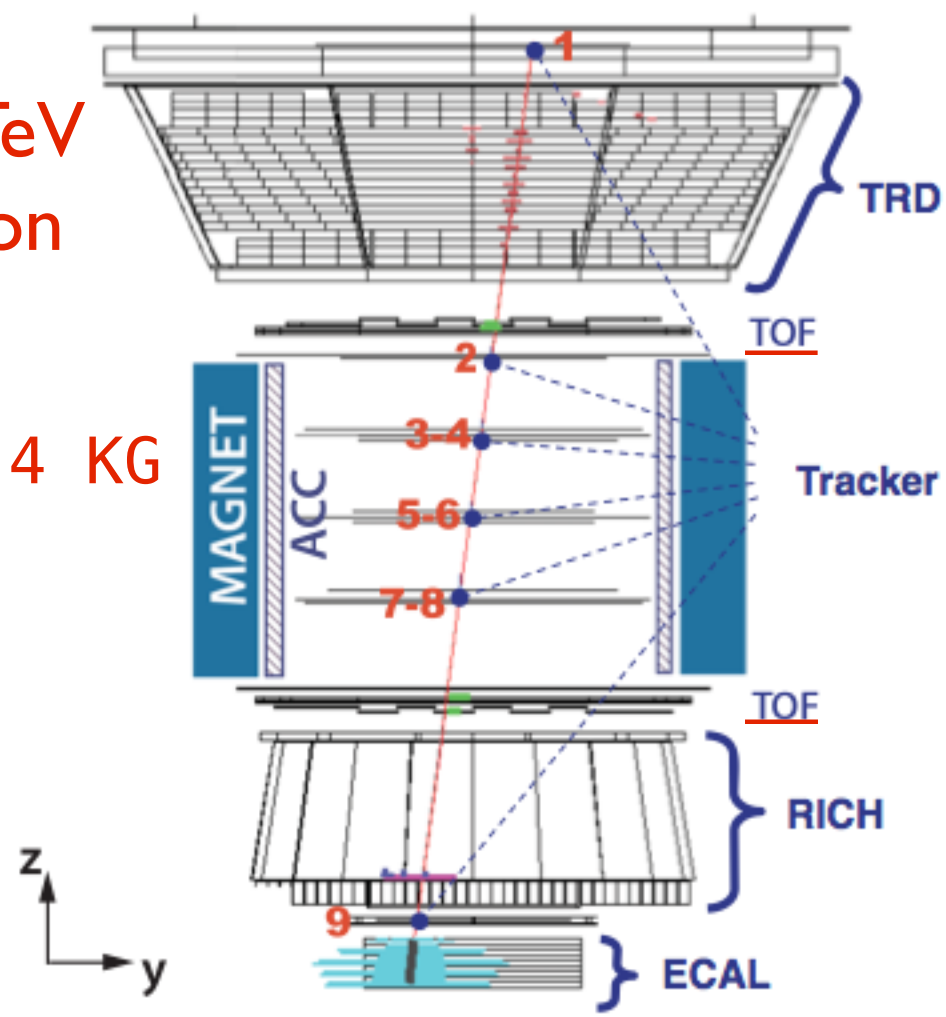

→ electron id vs proton or nuclei
p/e^+ rejection > 10^2

AMS Results

Alpha Magnetic Spectrometer

1.03 TeV
electron

~1.4 KG

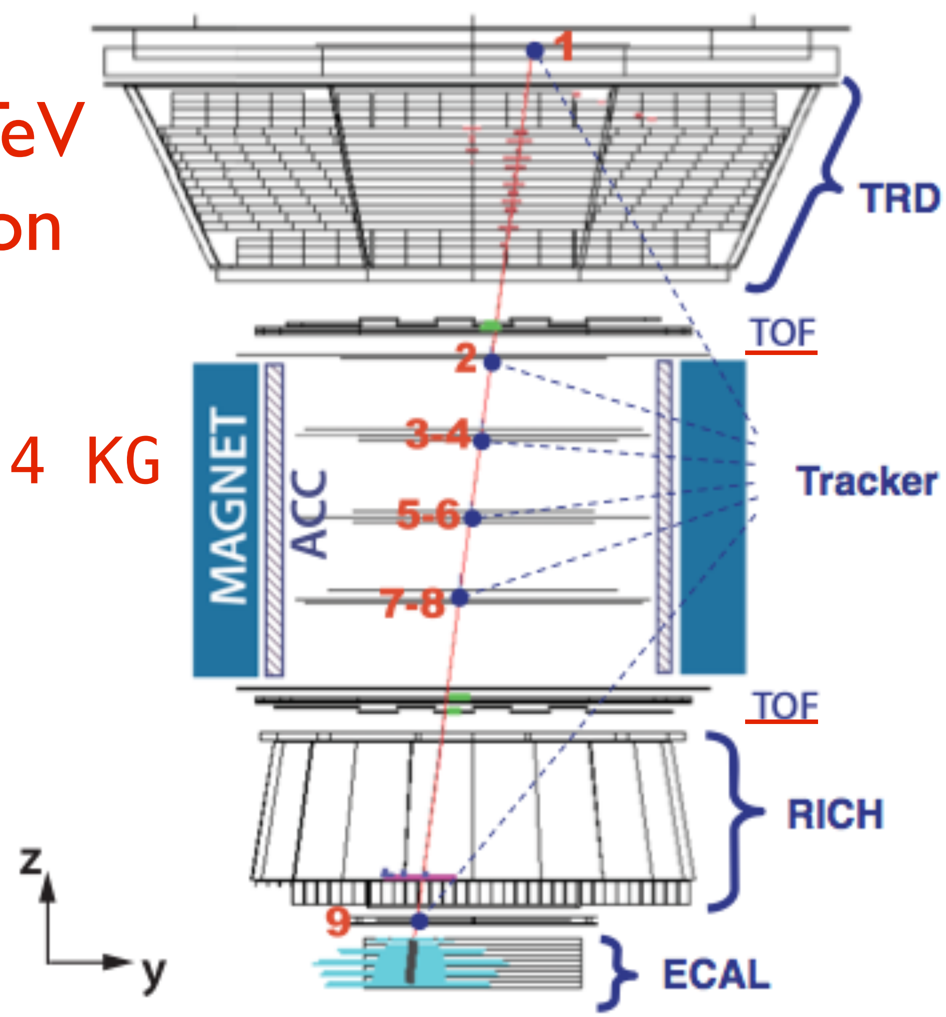

→ electron id vs proton or nuclei
p/e^+ rejection > 10^2

→ particle charge and momentum

AMS Results

Alpha Magnetic Spectrometer

1.03 TeV
electron

~1.4 KG

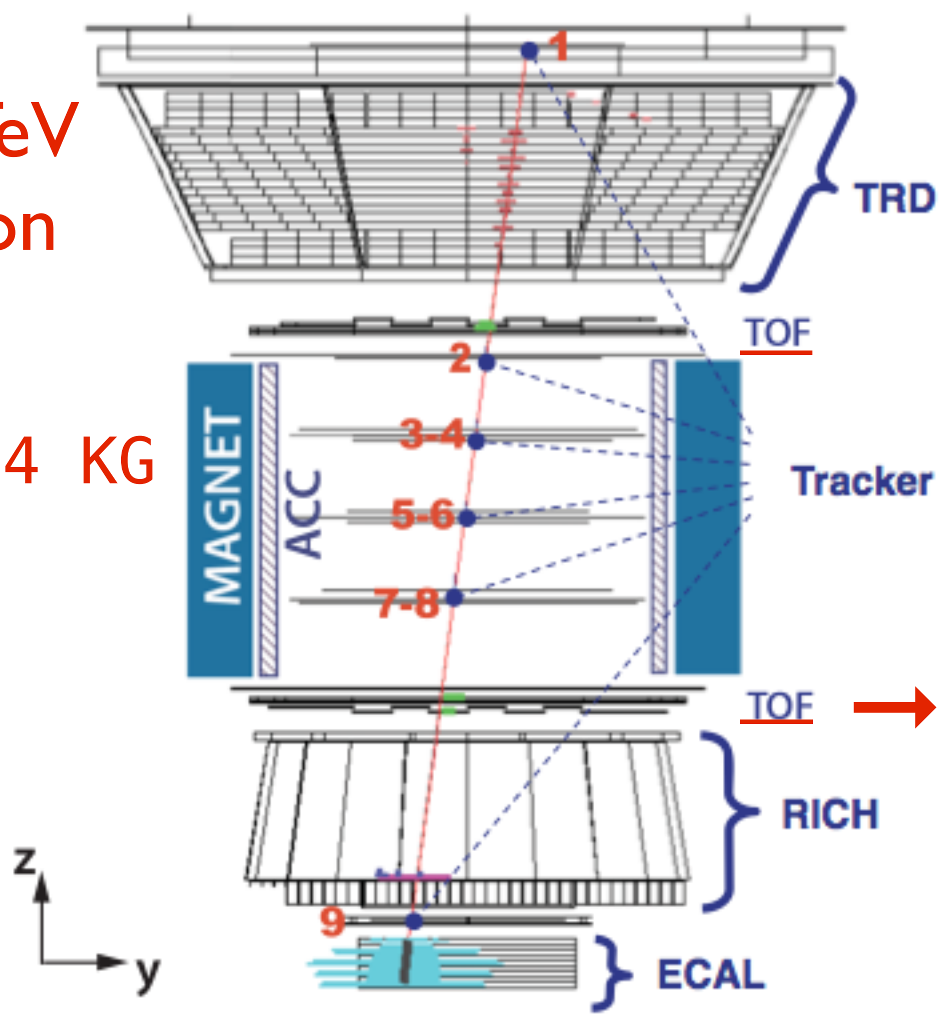

→ electron id vs proton or nuclei
p/e^+ rejection > 10^2

→ particle charge and momentum

→ velocity and if down-going

AMS Results

Alpha Magnetic Spectrometer

1.03 TeV
electron

~1.4 KG

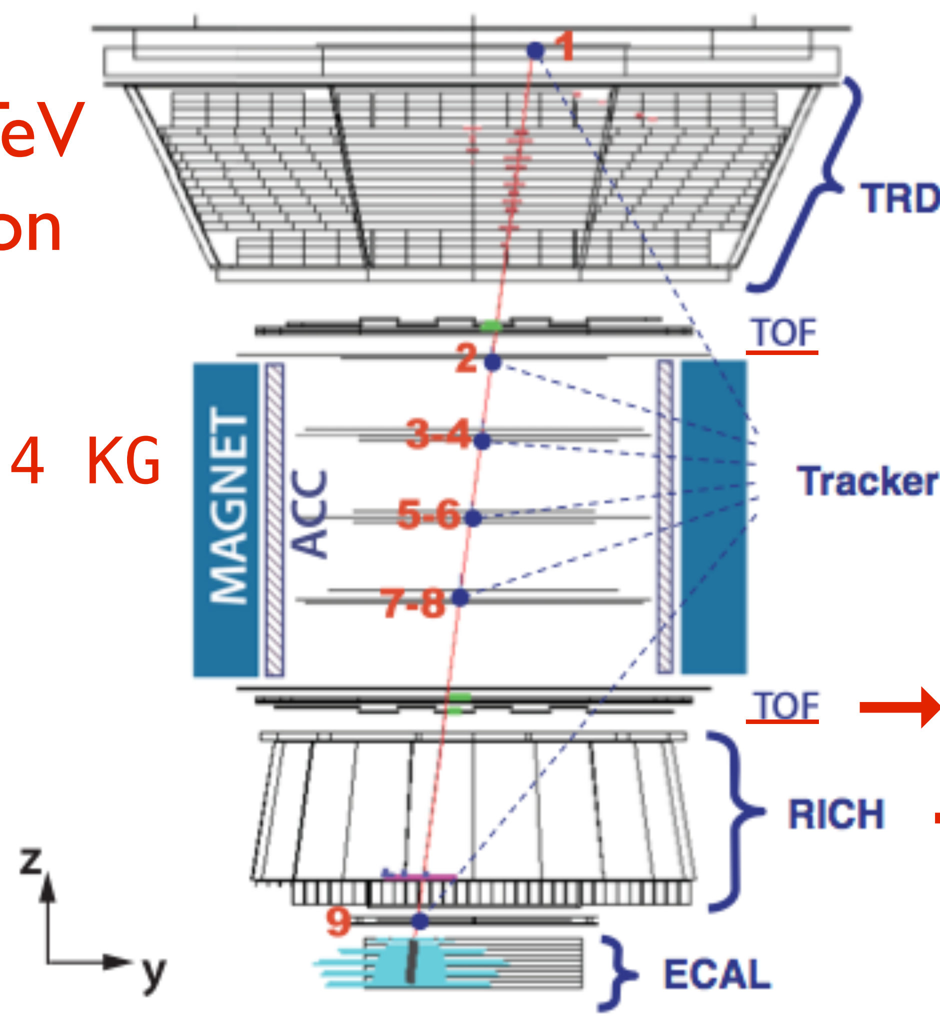

→ electron id vs proton or nuclei
p/e^+ rejection > 10^2

→ particle charge and momentum

→ velocity and if down-going

→ charge and velocity

AMS Results

Alpha Magnetic Spectrometer

1.03 TeV
electron

~1.4 KG

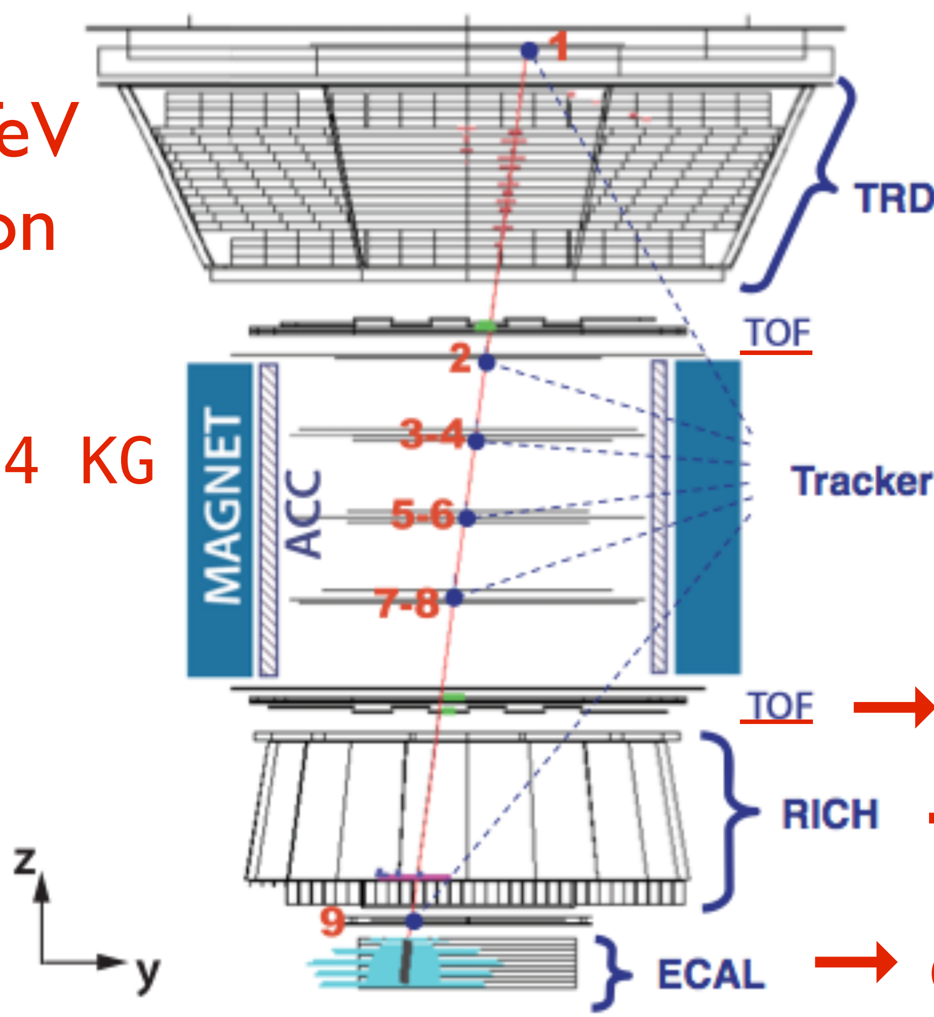

→ electron id vs proton or nuclei
p/e$^+$ rejection > 10^2

→ particle charge and momentum

→ velocity and if down-going

→ charge and velocity

→ energy
p/e$^+$ rejection > 10^4

AMS Results

Alpha Magnetic Spectrometer

1.03 TeV electron

~1.4 KG

anti-coincidence counters (also sweeps alway e^+ produced in TRD)

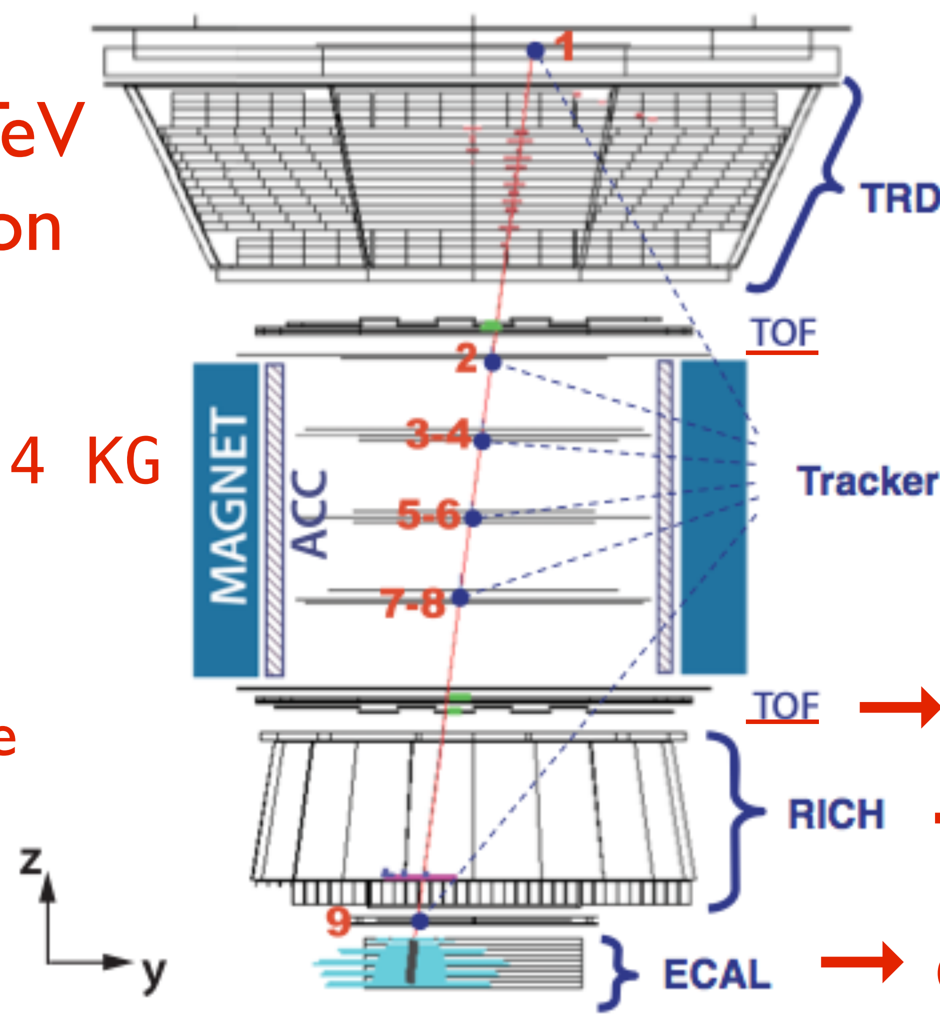

→ electron id vs proton or nuclei p/e^+ rejection > 10^2

→ particle charge and momentum

→ velocity and if down-going

→ charge and velocity

→ energy

p/e^+ rejection > 10^4

AMS Positron Fraction

6.8 x 10^6 e^+ e^-

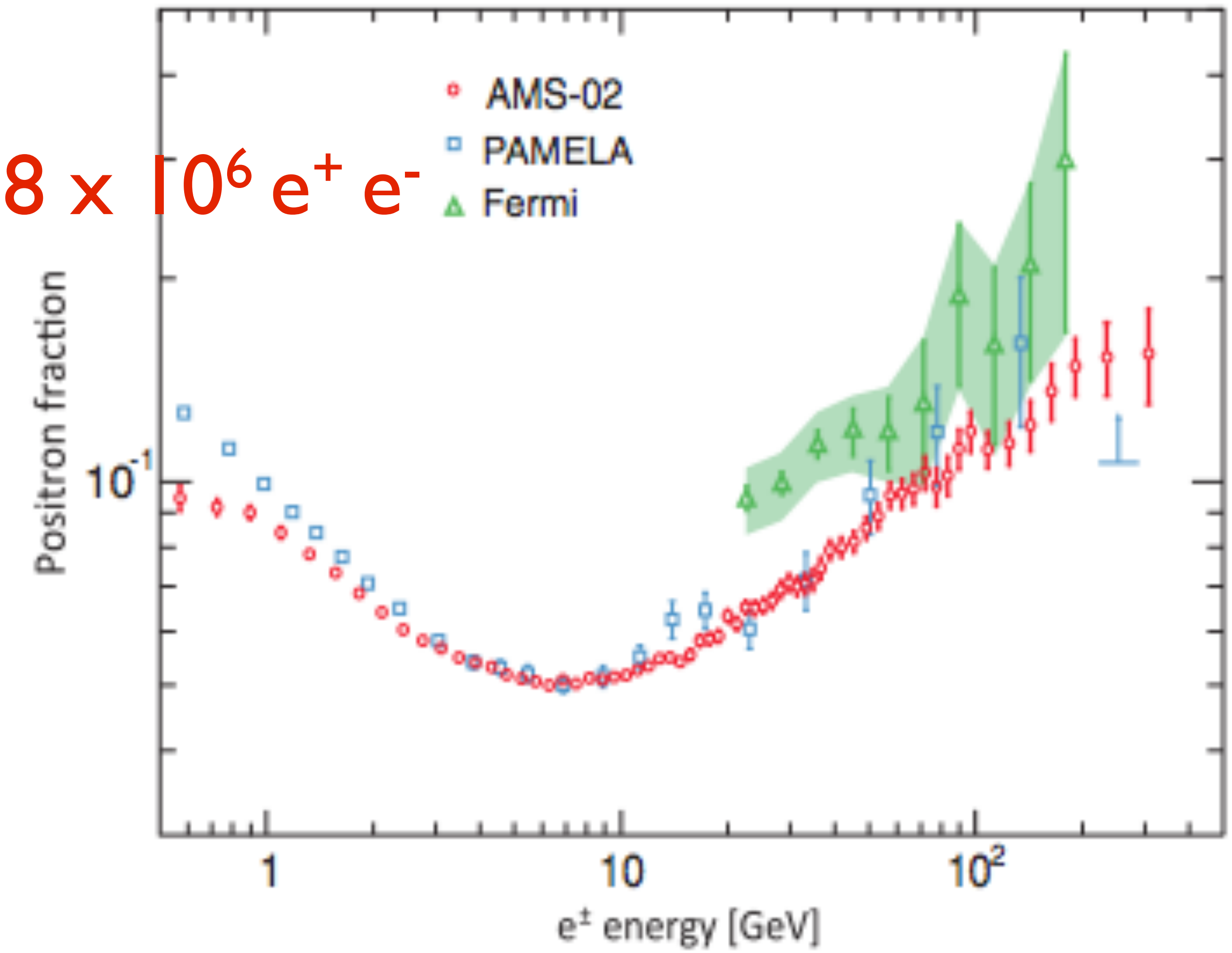

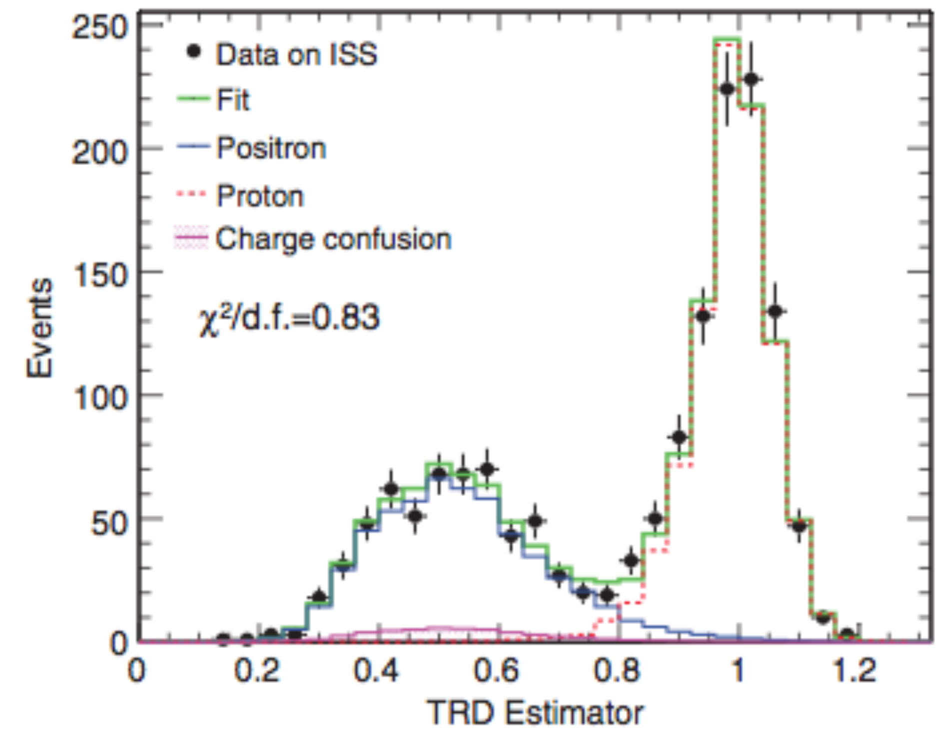

Aguilar et al. (AMS Coll.), PRL **110**, 2013

AMS Positron Fraction

$6.8 \times 10^6\ e^+ e^-$

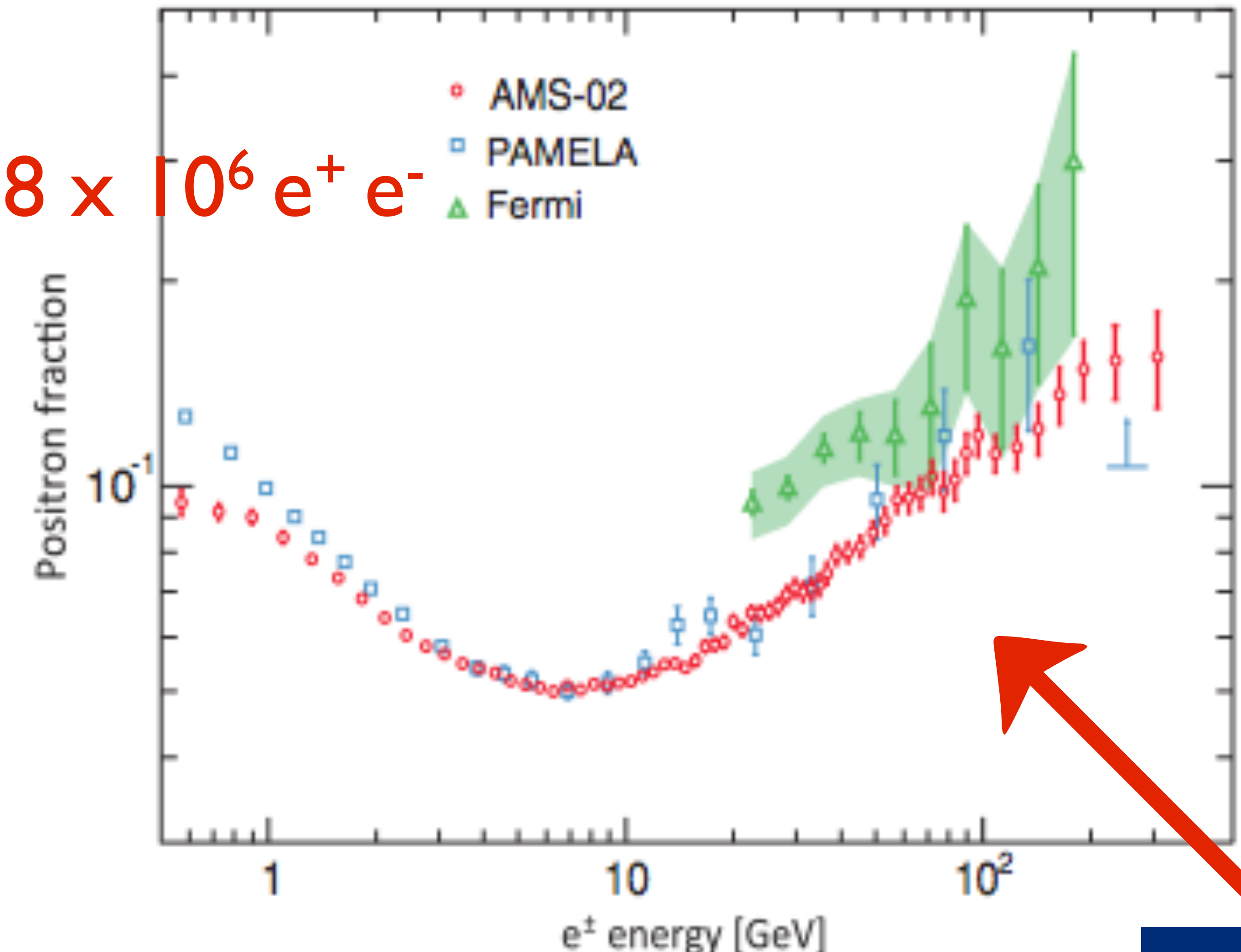

Aguilar et al. (AMS Coll.), PRL **110**, 2013

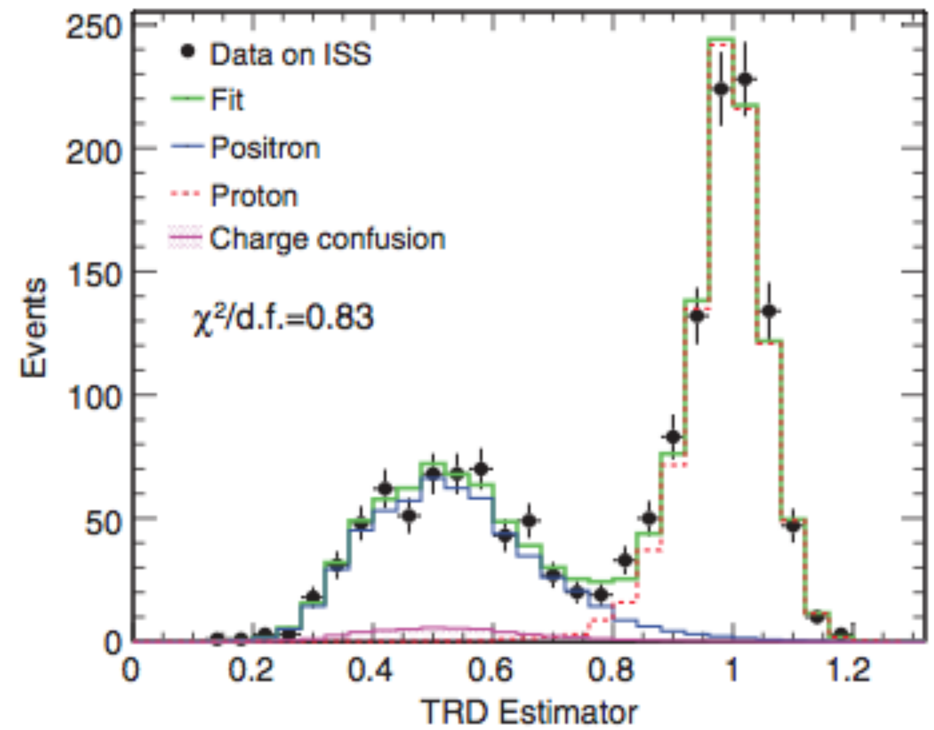

Increase in slope as seen by Fermi and Pamela

AMS Positron Fraction

6.8 x 10^6 e^+ e^-

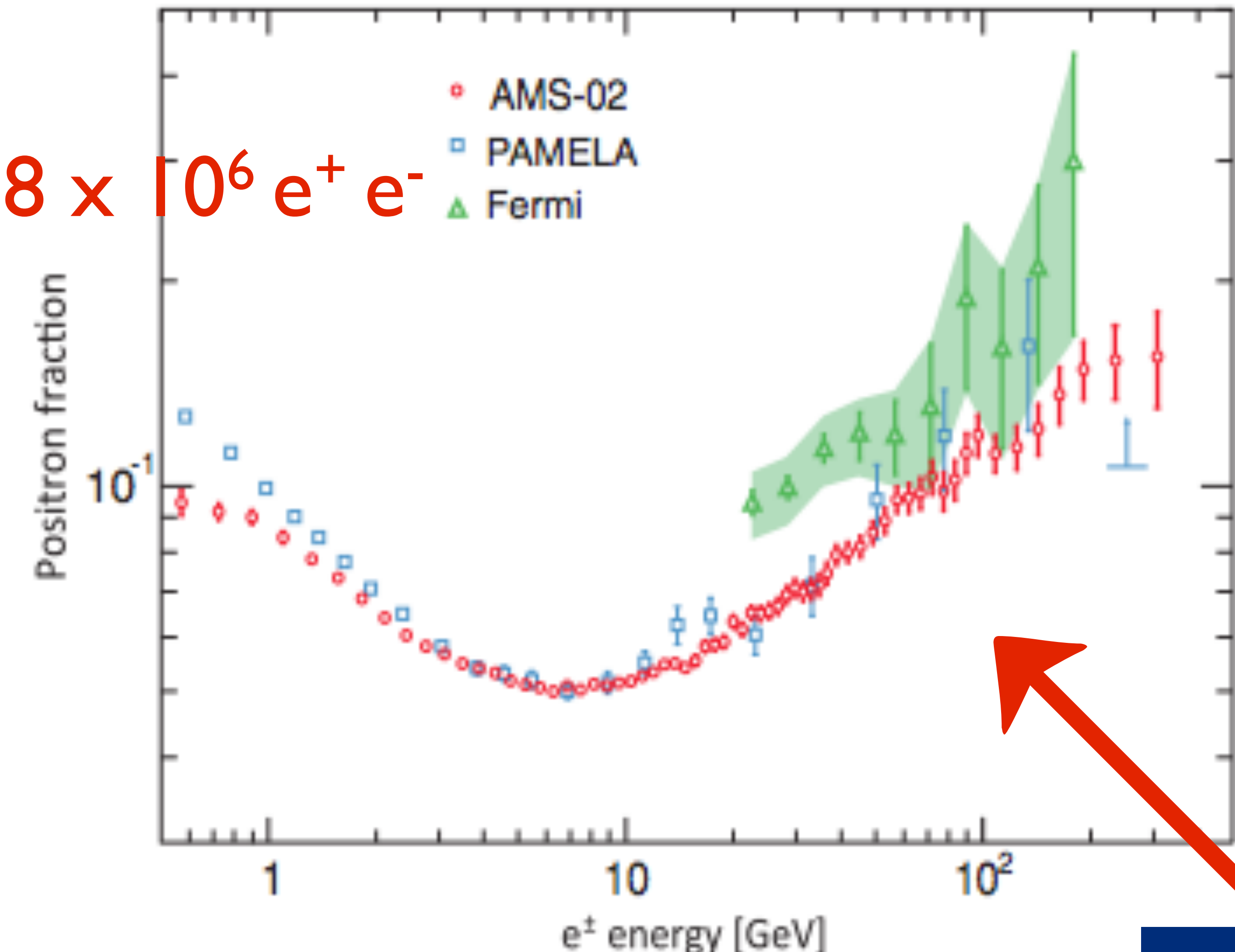

Aguilar et al. (AMS Coll.), PRL **110**, 2013

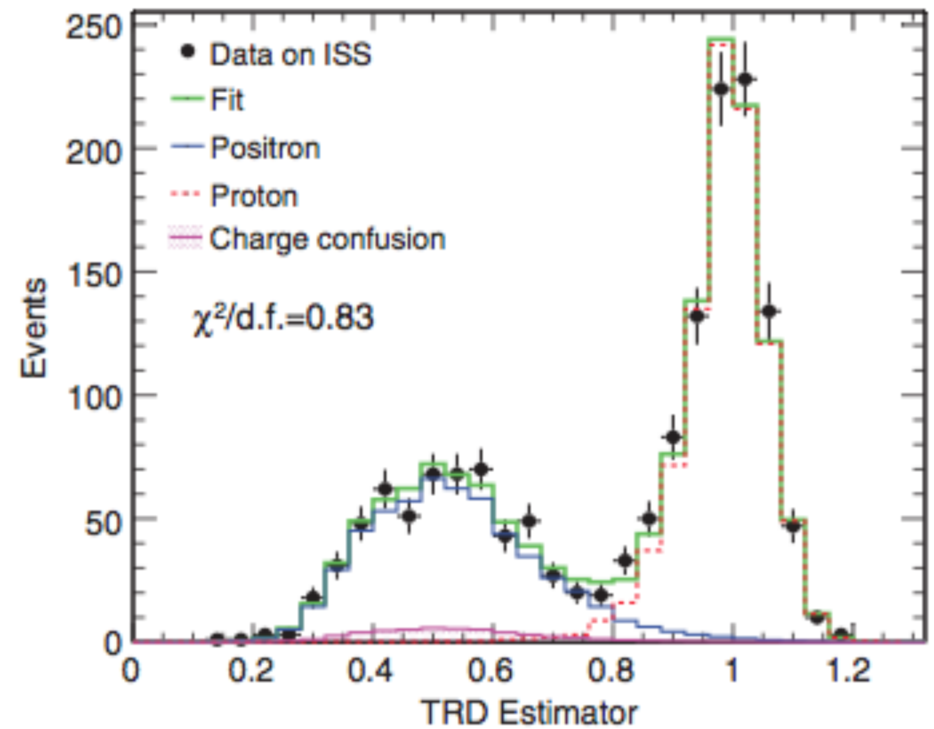

Increase in slope as seen by Fermi and Pamela

consistent with new physics (either from particle or astrophysics)

Possible Scenarios

- STANDARD solutions:

  → pulsars (S. Profumo - arXiv:0812.4457)

  → secondaries from shock accelerated hadrons
  (Blasi - PRL 103 - 2009)

- DM solutions:

$$\chi\overline{\chi} \rightarrow (t\bar{t}, b\bar{b}, \ldots) \rightarrow \text{hadrons}$$
$$\Rightarrow \quad \text{leptons}$$
$$\gamma s$$

Anti Proton Spectrum

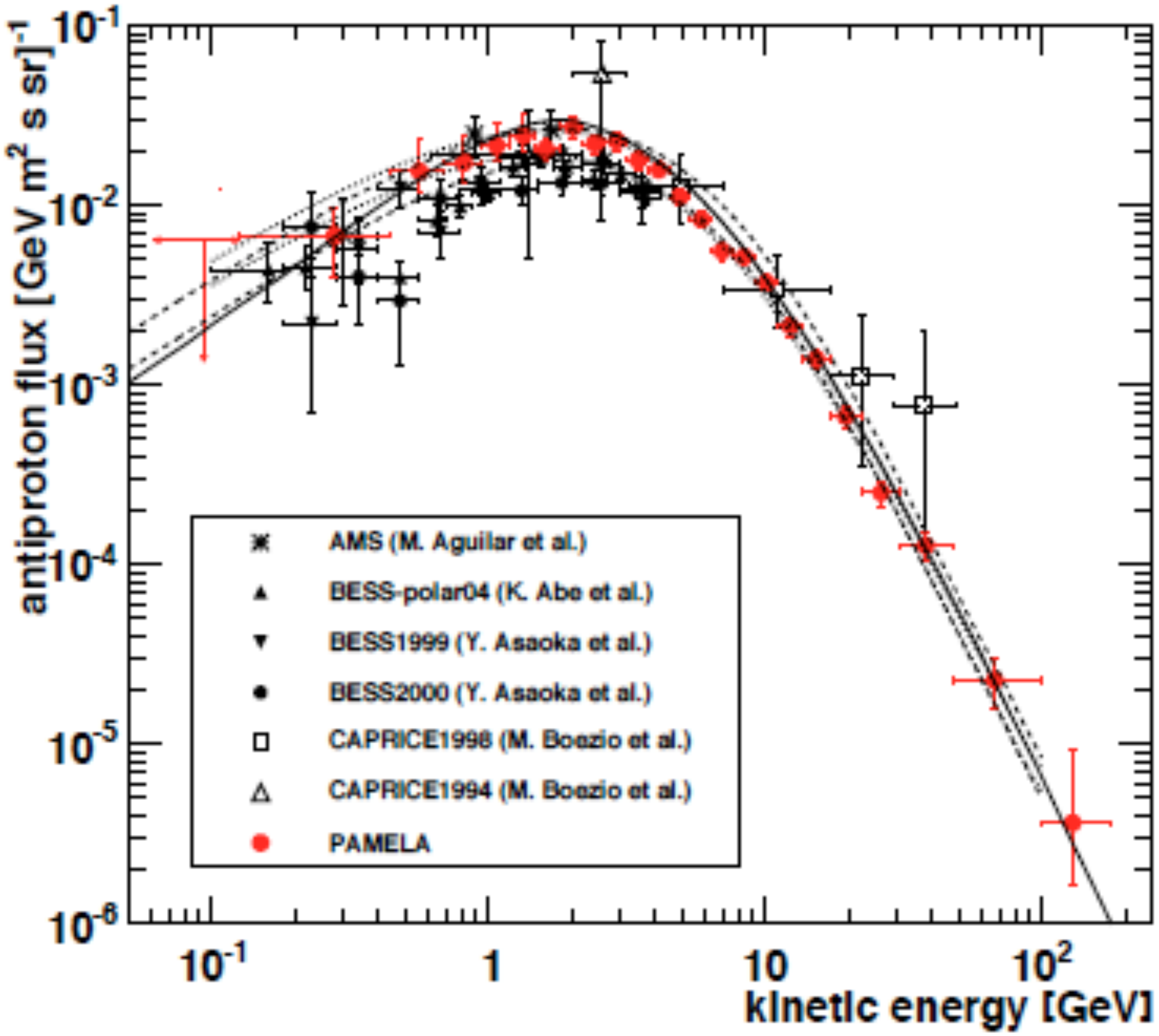

O.~Adriani et al. (PAMELA), Phys. Rev. Lett., 105 (2010).

$$\chi\bar{\chi} \;\rightarrow\; (t\bar{t}, b\bar{b}) \;\rightarrow\; \text{hadrons}$$

Anti Proton Spectrum

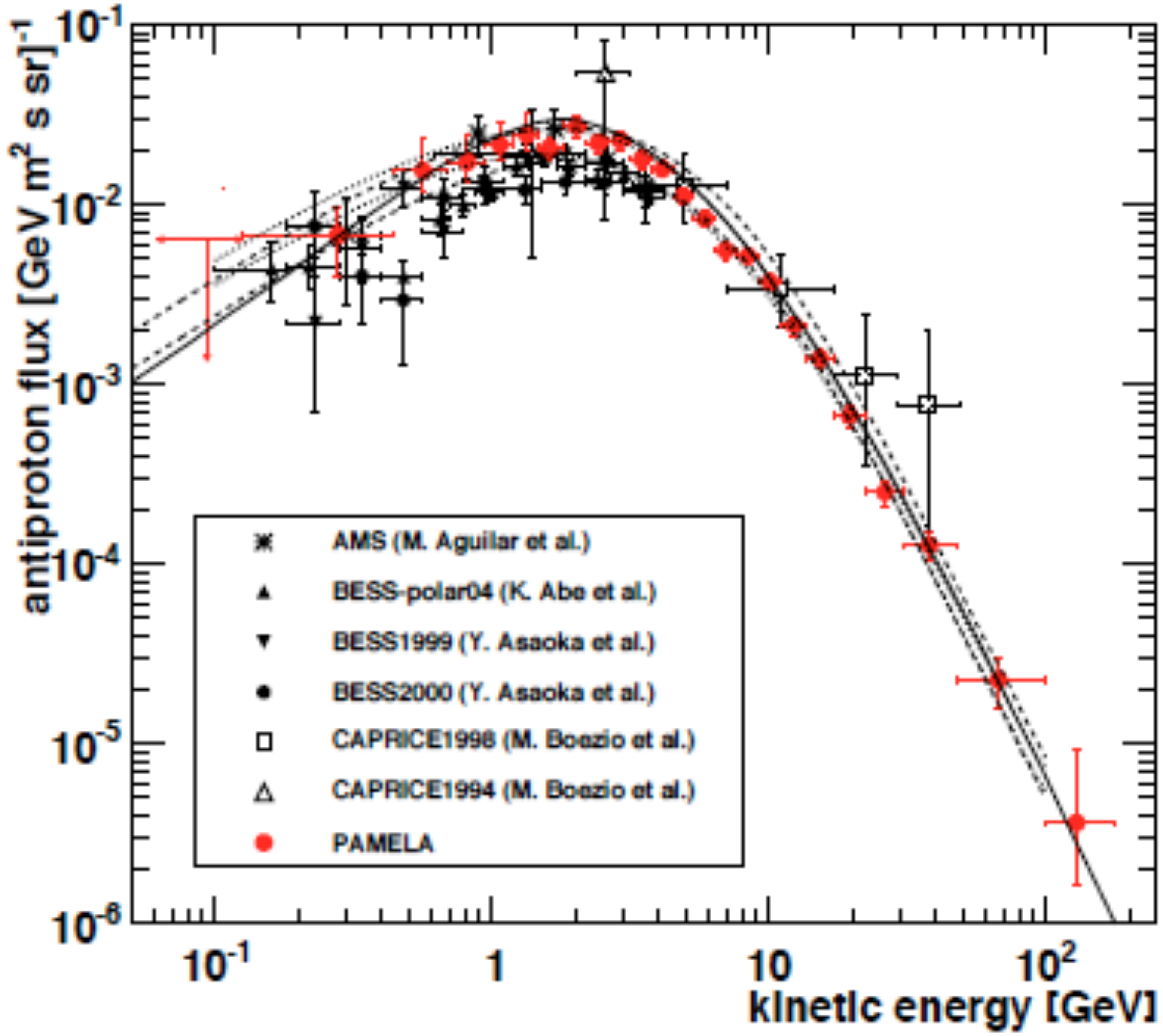

O.~Adriani et al. (PAMELA), Phys. Rev. Lett., 105 (2010).

$$\chi\bar{\chi} \rightarrow (t\bar{t}, b\bar{b}) \rightarrow \text{hadrons}$$

DM can explain excess

Two Examples

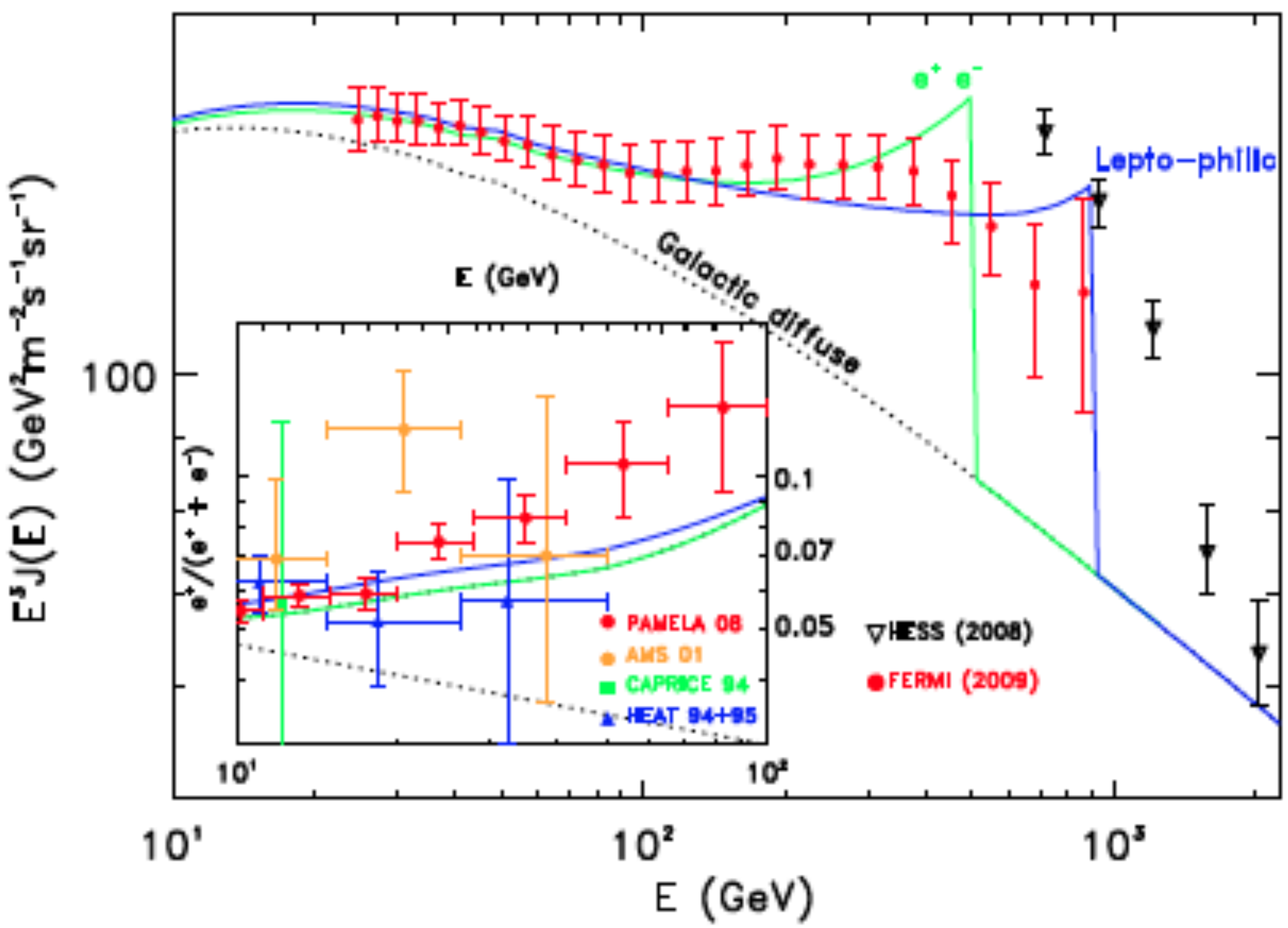

Extracted from D. Grasso *et al.* Nucl.Instrum.Meth. A630, 48-51 (2011).

Fig. 11. Predictions for the CRE spectrum from two specific dark matter models, compared to current measurements. The same large scale Galactic CRE components (dotted line) as in Figs. 4 and 6 (model 0 in Table 1) is used here. Note that the theoretical model curves showed in this plot do not account for the smearing due the finite experimental energy resolution.

Lepto-philic models: pair annihilation into $e^{\pm}, \mu^{\pm}, \tau^{\pm}$

P.Fox, E. Poppitz (PRD 79 - 2009)

Annihilation into $e^{\pm}$

Finkbeiner, N. Weiner (PRD 76 - 2007)

DM Fit

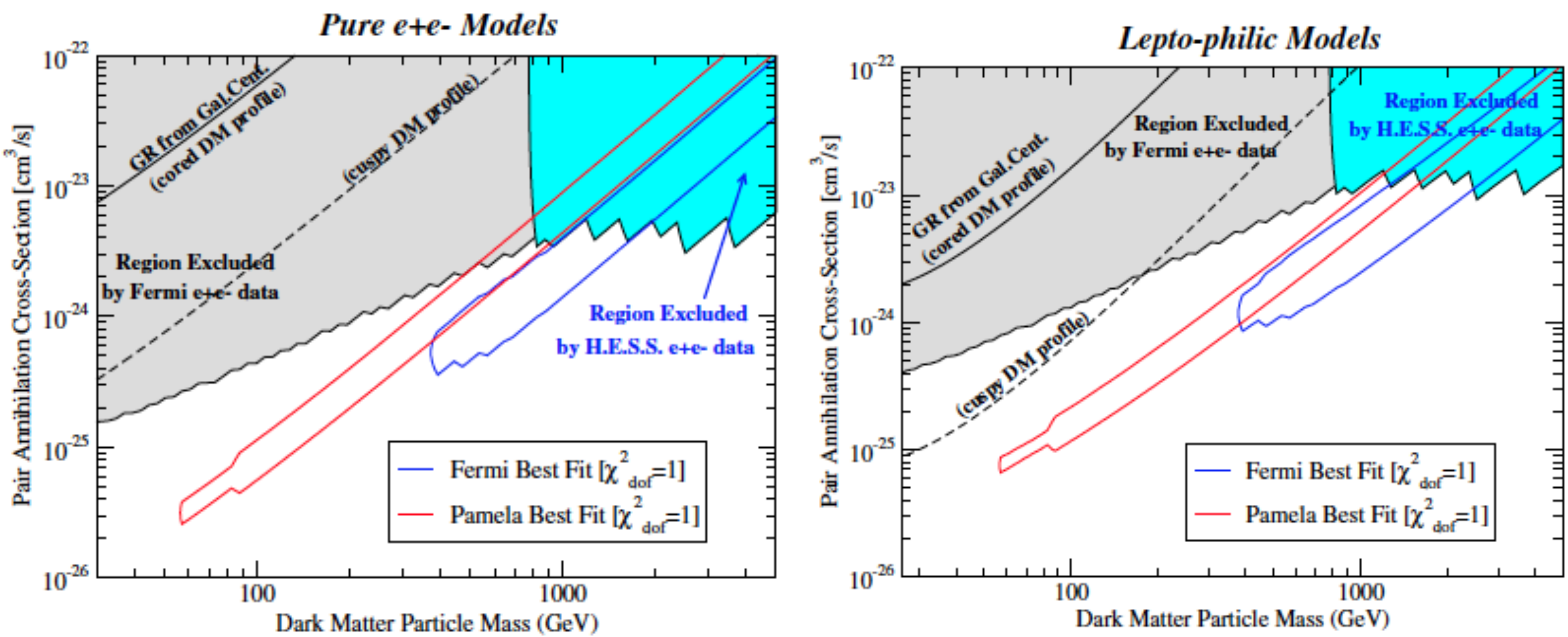

D. Grasso *et al.*,
Nucl.Instrum.Meth.
A630, 48-51 (2011)

Exclusion at 2σ level

DM Fit

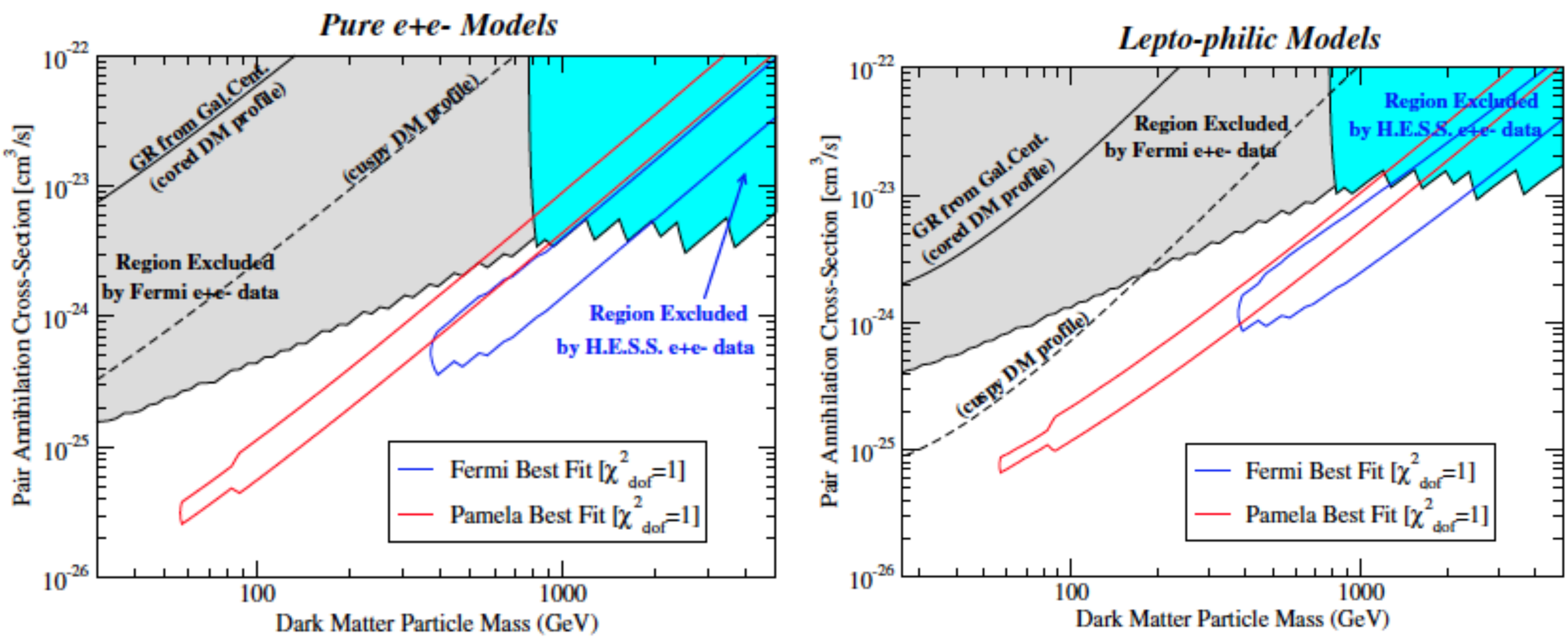

D. Grasso *et al.*, Nucl.Instrum.Meth. A630, 48-51 (2011)

Exclusion at 2σ level

these candidates are thermal relics!

$$\langle \sigma \mathbf{v} \rangle = \mathbf{3} \times \mathbf{10^{-26}} \mathrm{cm}^3/\mathrm{s}$$

DM Fit

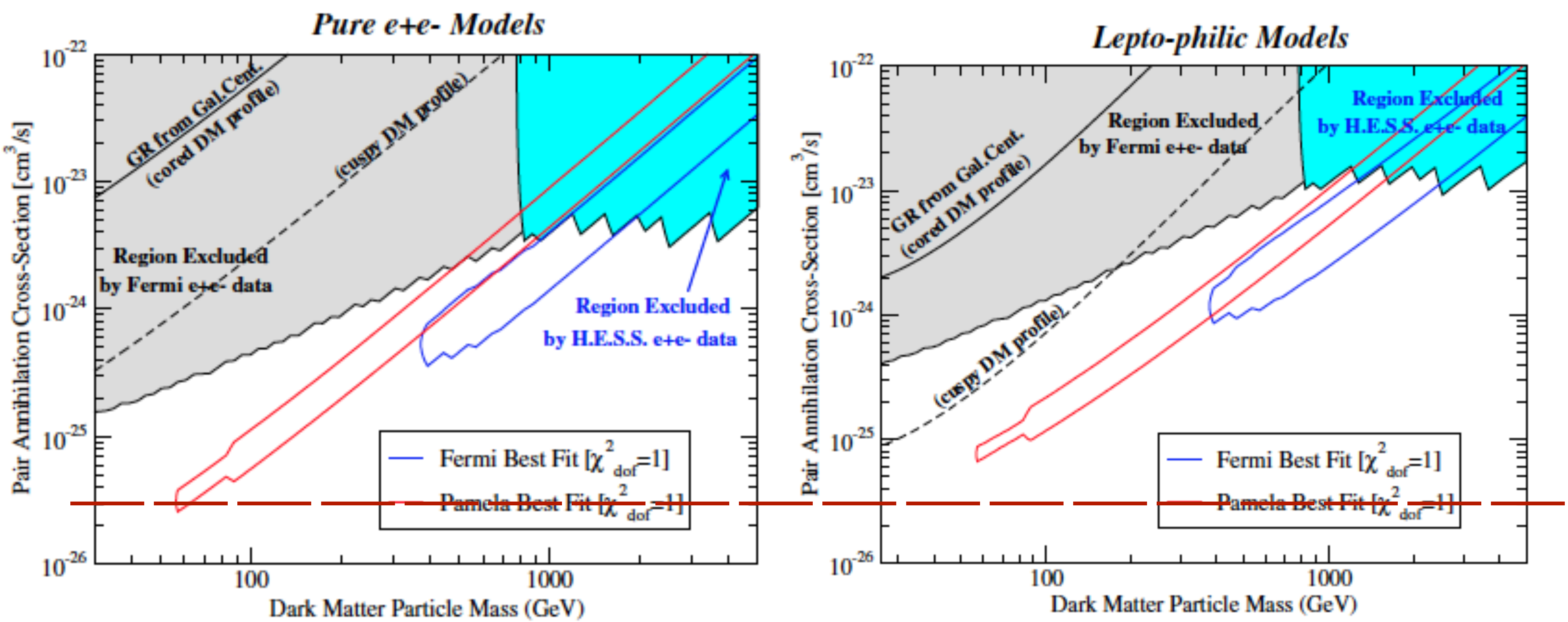

D. Grasso *et al.*,
Nucl.Instrum.Meth. A630, 48-51 (2011)

Exclusion at 2σ level

these candidates are thermal relics!

$$\langle \sigma v \rangle = \mathbf{3} \times \mathbf{10}^{\mathbf{-26}} \mathrm{cm}^3/\mathrm{s}$$

Boost on Γ_A is necessary!!

– Γ_A can be enhanced in several ways:

=> DM substructures in the halo

=> Annihilation XS is enhanced

* Sommerfeld enhancement

=> combination of both effects

Fermi-LAT constraints on Galactic DM

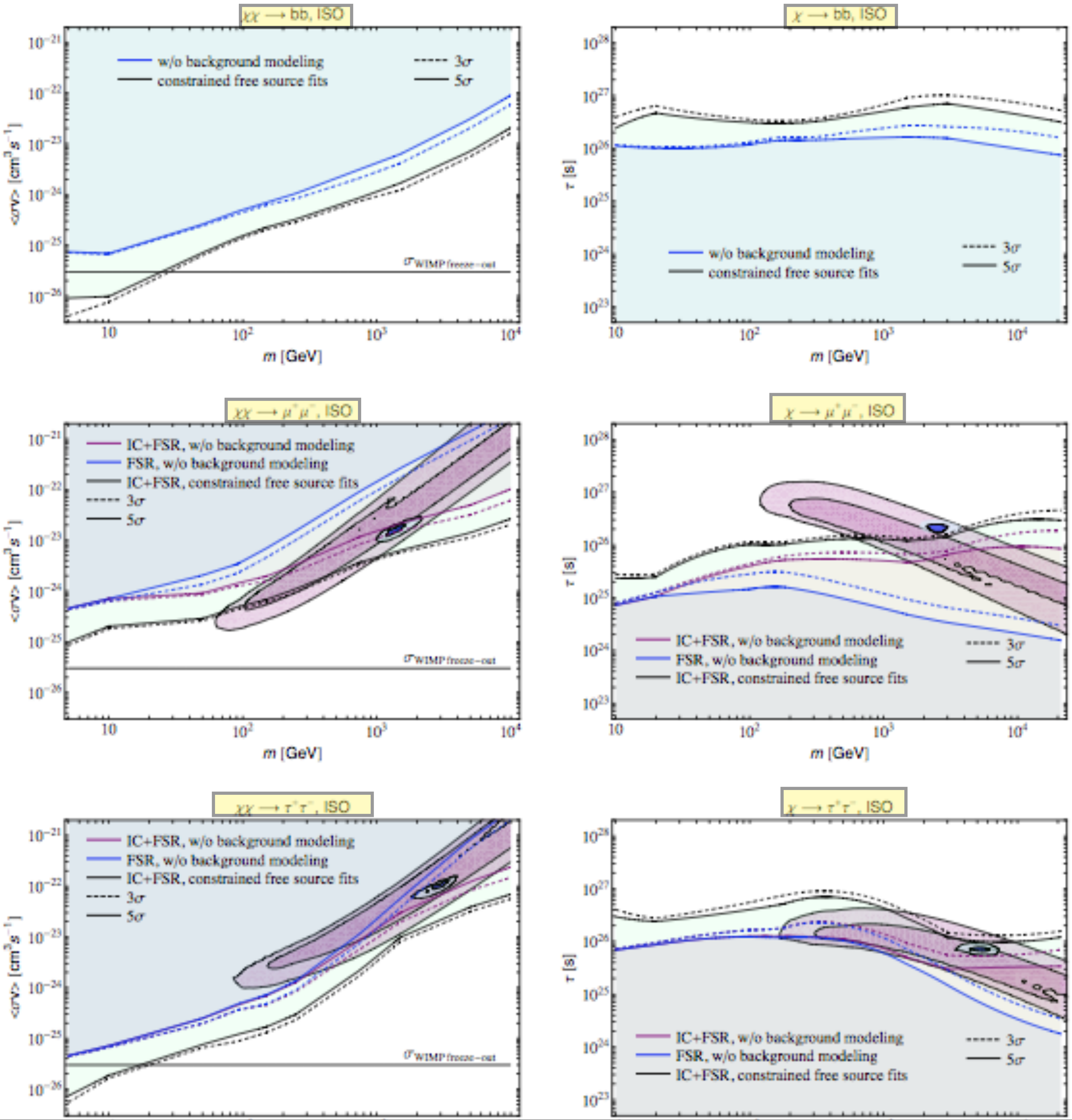

diffuse γ-ray emission at intermediate galactic latitudes => conservative limits assuming DM signal does not exceed the observed diffuse limit

Fermi-LAT constraints on Galactic DM

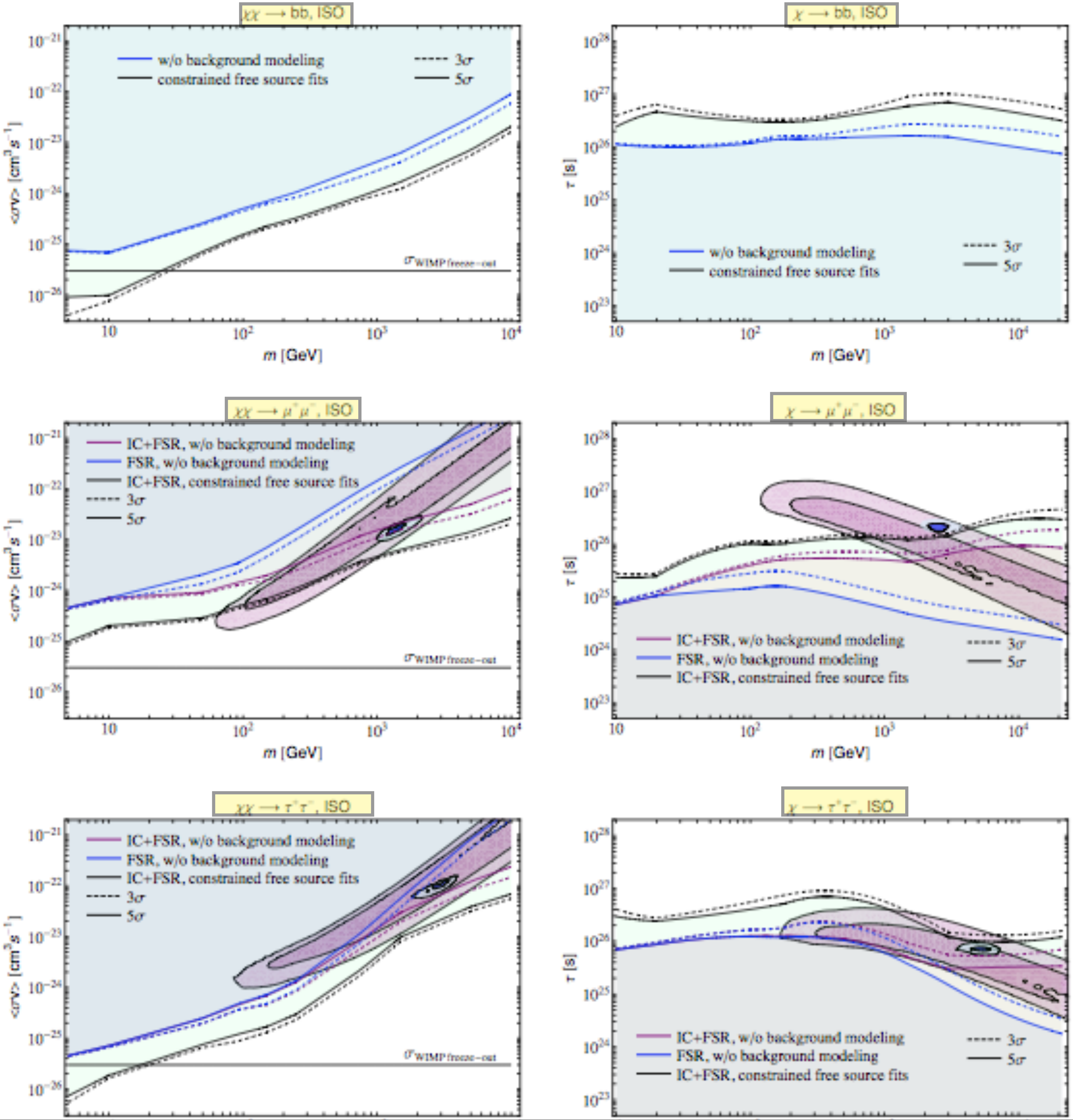

W/O backgrd modeling: compares expected counts from DM with event counts after all triggers

diffuse γ-ray emission at intermediate galactic latitudes => conservative limits assuming DM signal does not exceed the observed diffuse limit

Fermi-LAT constraints on Galactic DM

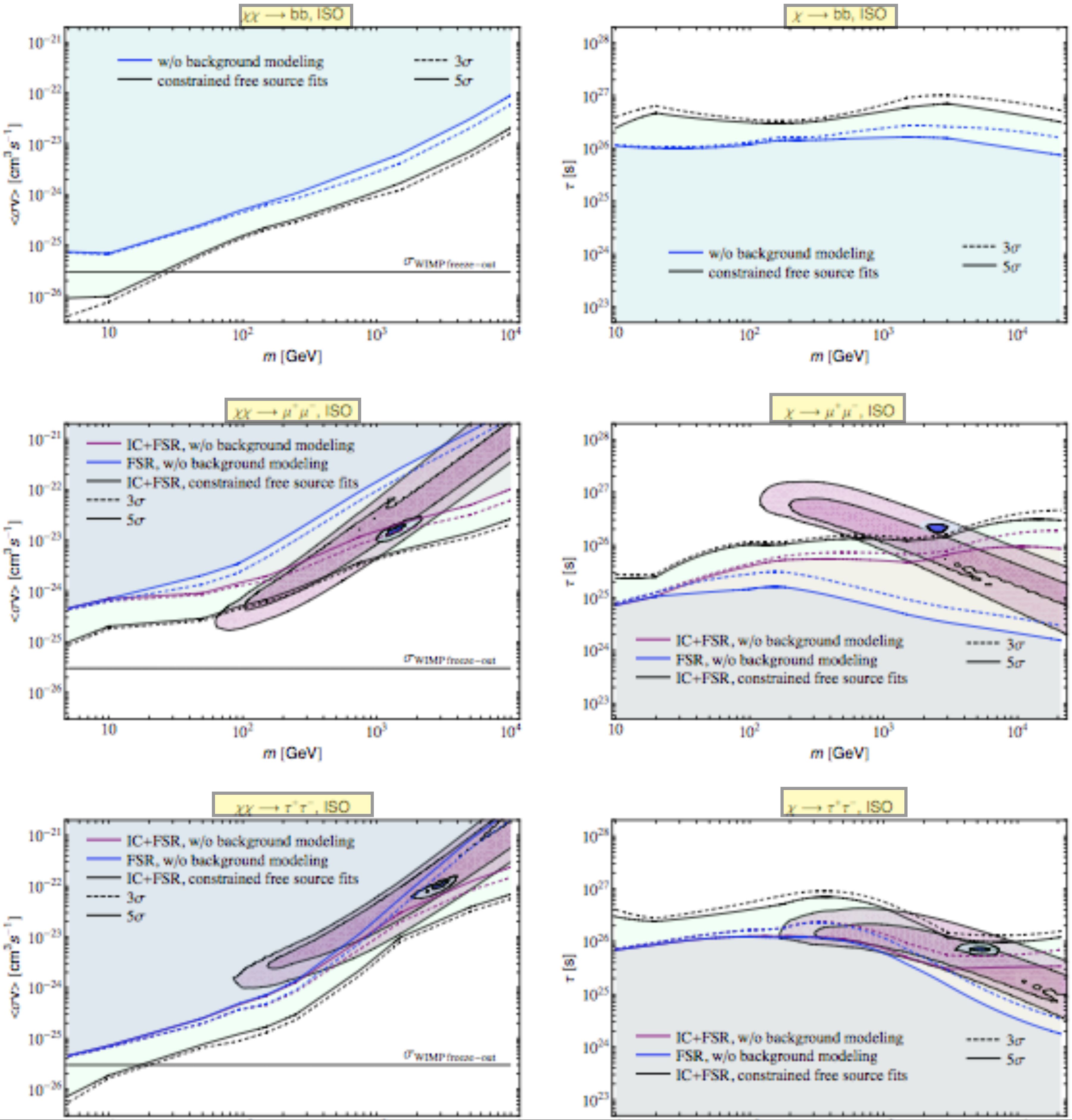

W/O backgrd modeling: compares expected counts from DM with event counts after all triggers

constrained fit: linear fit to all expected backgrounds
IC: Inverse Compton
FSR: Final State Radiation

diffuse γ-ray emission at intermediate galactic latitudes => conservative limits assuming DM signal does not exceed the observed diffuse limit

Fermi-LAT constraints on Galactic DM

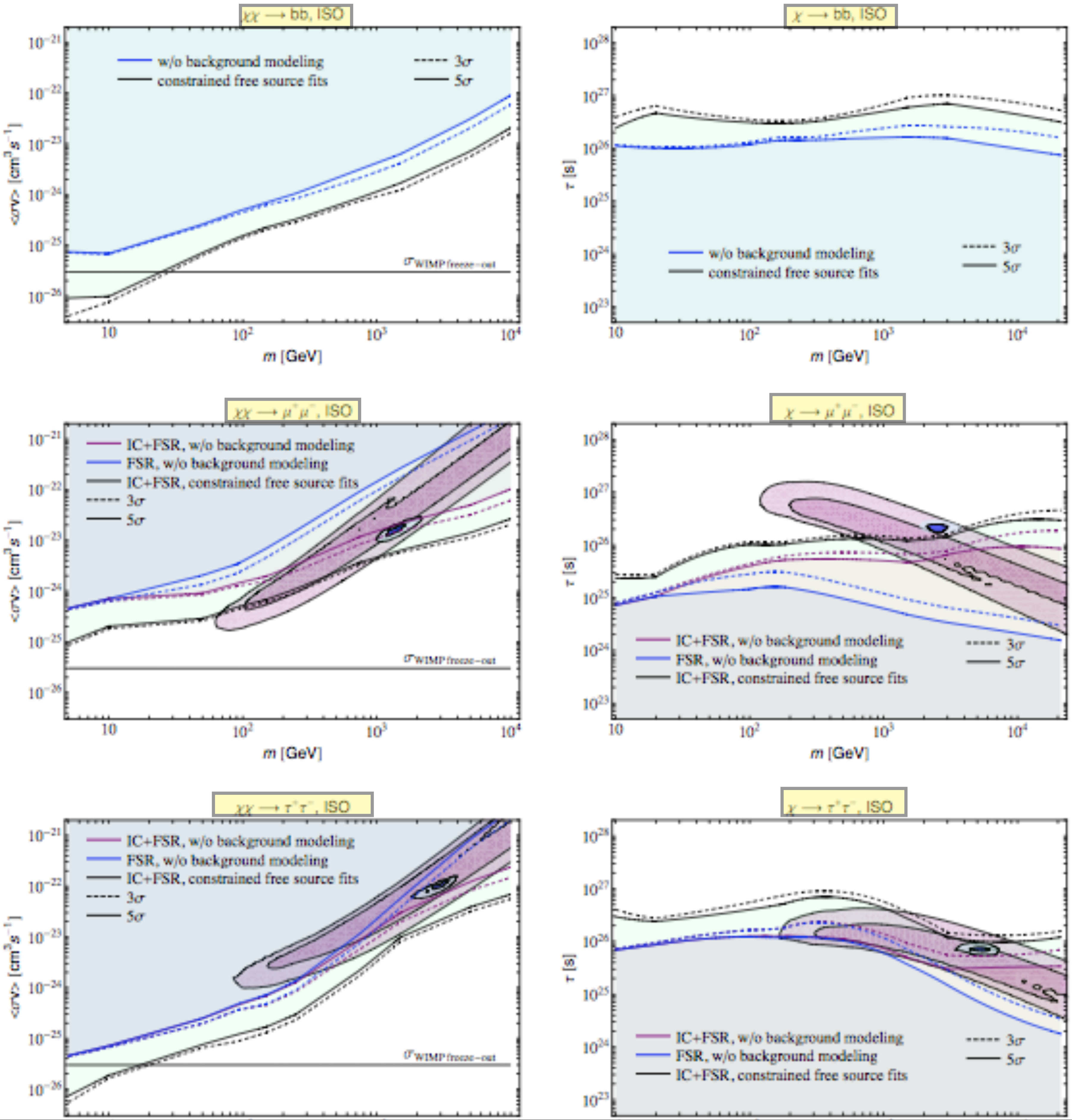

W/O backgrd modeling: compares expected counts from DM with event counts after all triggers

constrained fit: linear fit to all expected backgrounds
IC: Inverse Compton
FSR: Final State Radiation

Good fit to PAMELA e^+e^- results

diffuse γ-ray emission at intermediate galactic latitudes => conservative limits assuming DM signal does not exceed the observed diffuse limit

Fermi-LAT constraints on Galactic DM

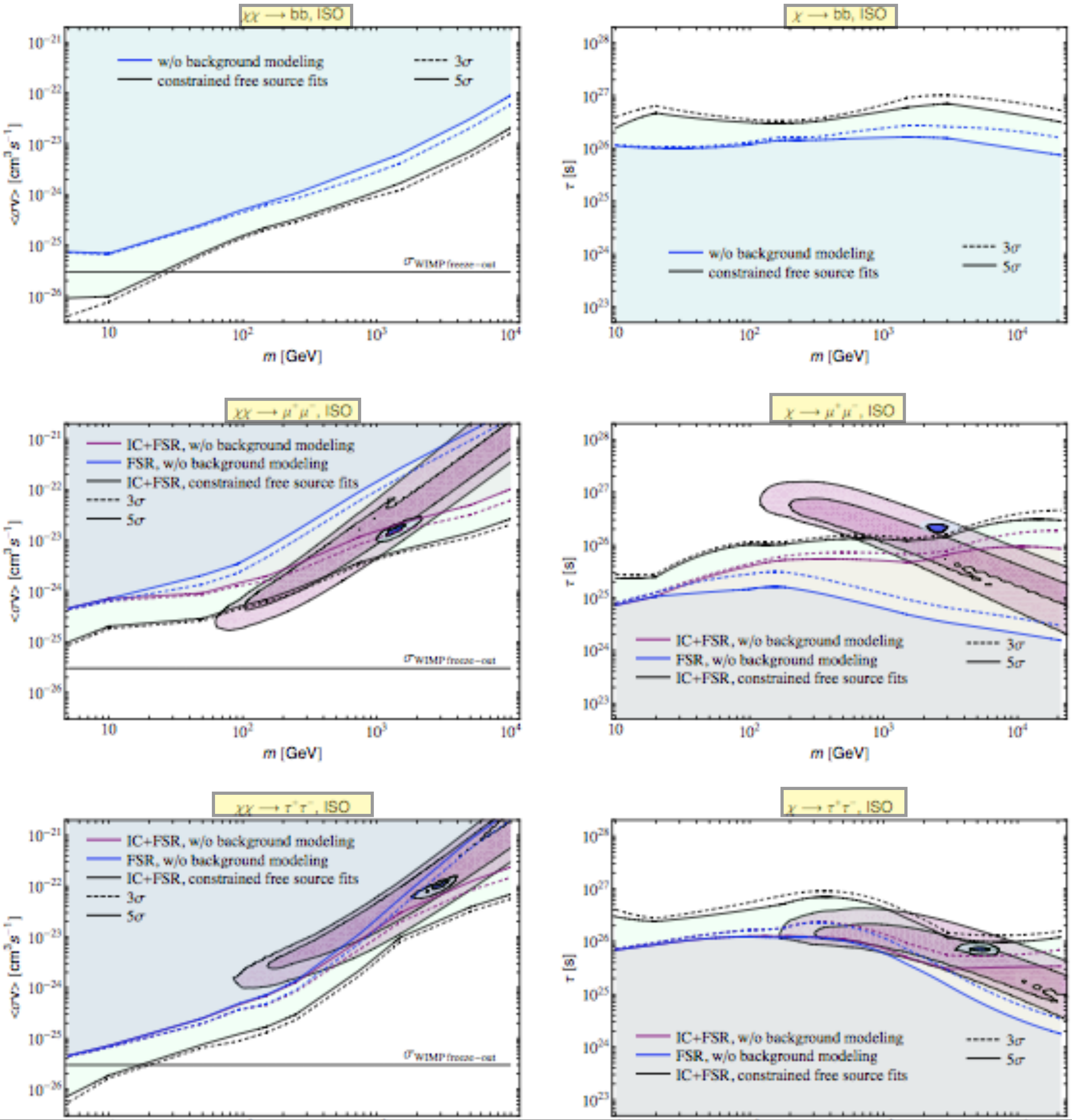

W/O backgrd modeling: compares expected counts from DM with event counts after all triggers

constrained fit: linear fit to all expected backgrounds
IC: Inverse Compton
FSR: Final State Radiation

Good fit to PAMELA e^+e^- results

Good fit to Fermi e^+e^- results

diffuse γ-ray emission at intermediate galactic latitudes => conservative limits assuming DM signal does not exceed the observed diffuse limit

Fermi-LAT constraints on Galactic DM

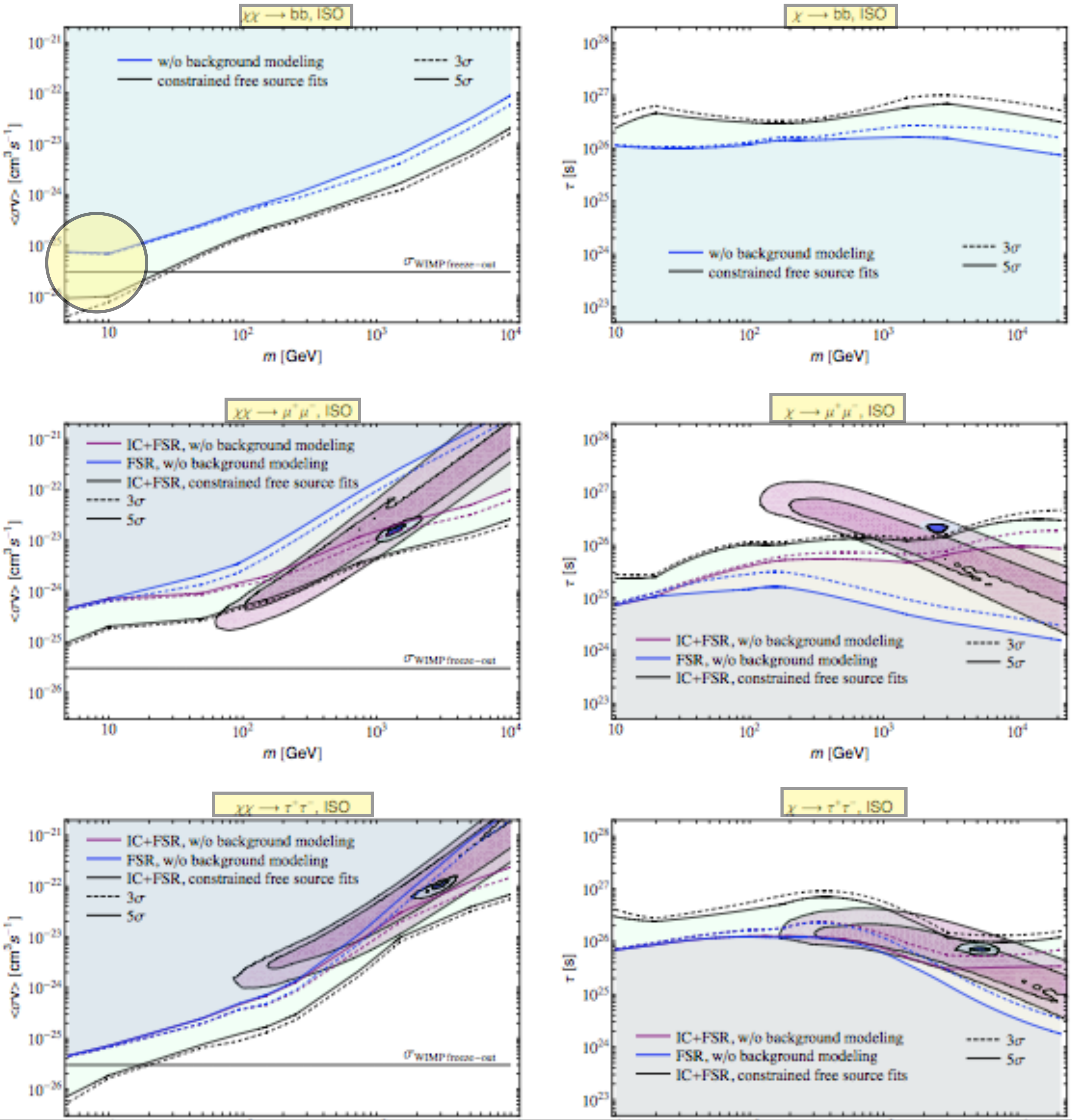

W/O backgrd modeling: compares expected counts from DM with event counts after all triggers

constrained fit: linear fit to all expected backgrounds
IC: Inverse Compton
FSR: Final State Radiation

Good fit to PAMELA e^+e^- results

Good fit to Fermi e^+e^- results

diffuse γ-ray emission at intermediate galactic latitudes => conservative limits assuming DM signal does not exceed the observed diffuse limit

Indirect Searches

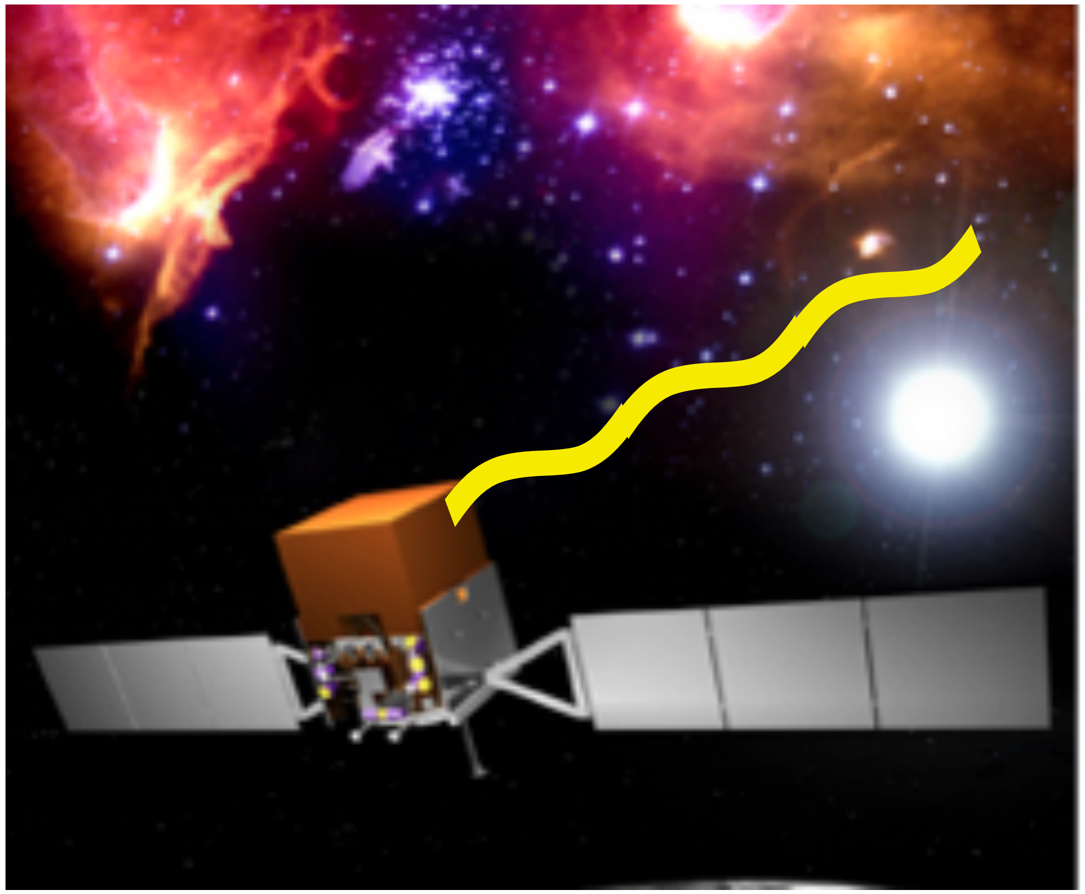

Boost on annihilation XS

Should also boost neutrino flux (Delaunay, Fox, Perez JHeP 05 2009)

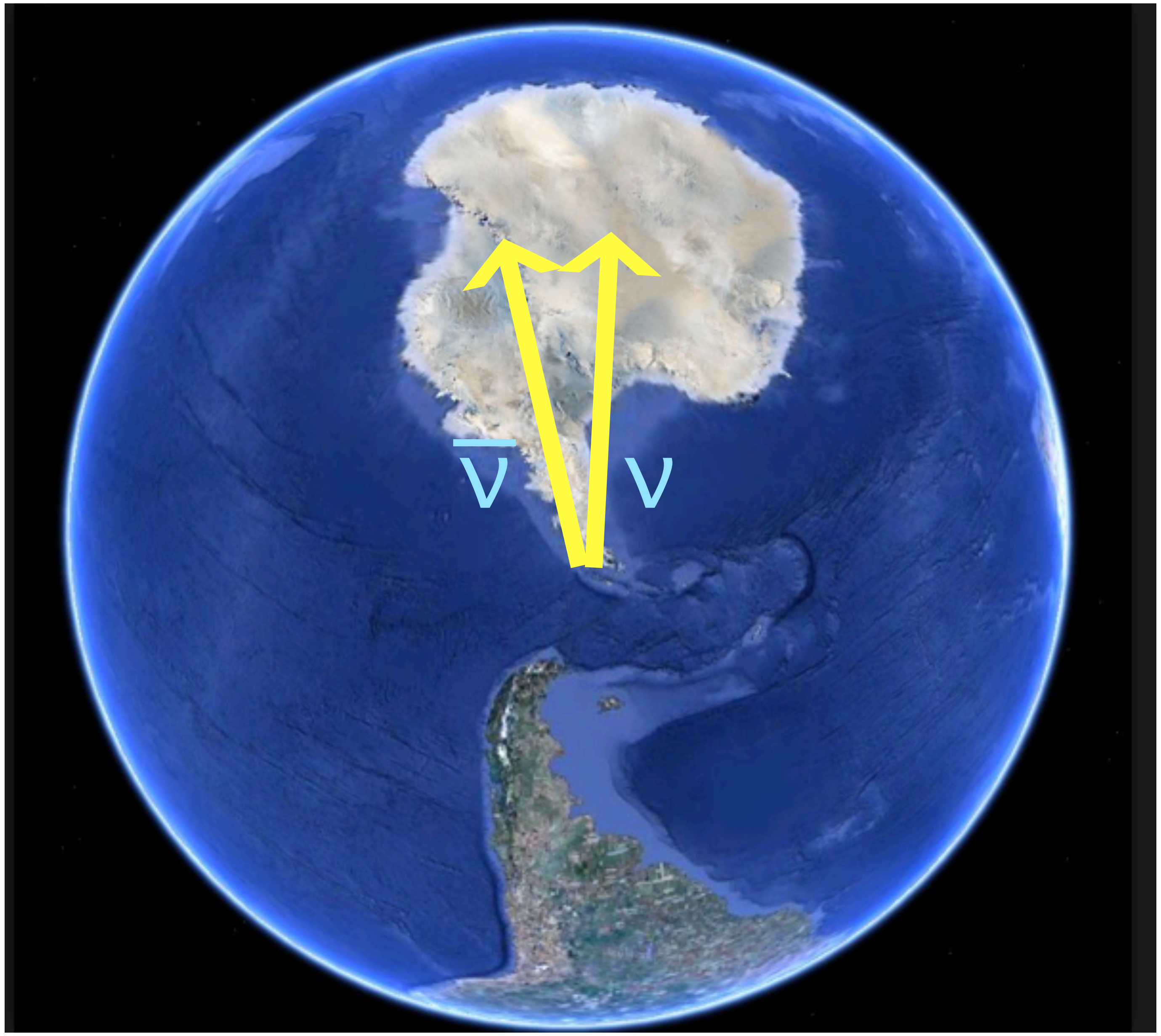

Indirect Searches

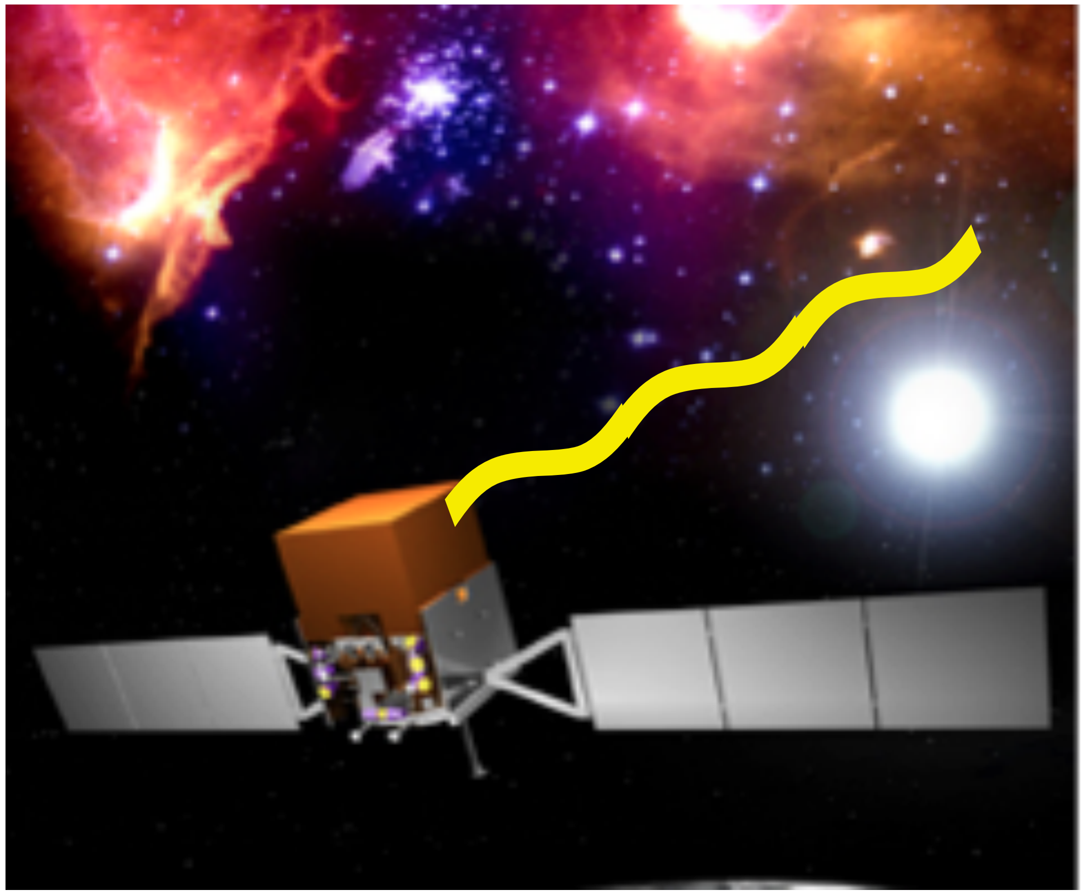

Boost on annihilation XS

Capture and annihilation equilibrium is accelerated

Should also boost neutrino flux (Delaunay, Fox, Perez JHeP 05 2009)

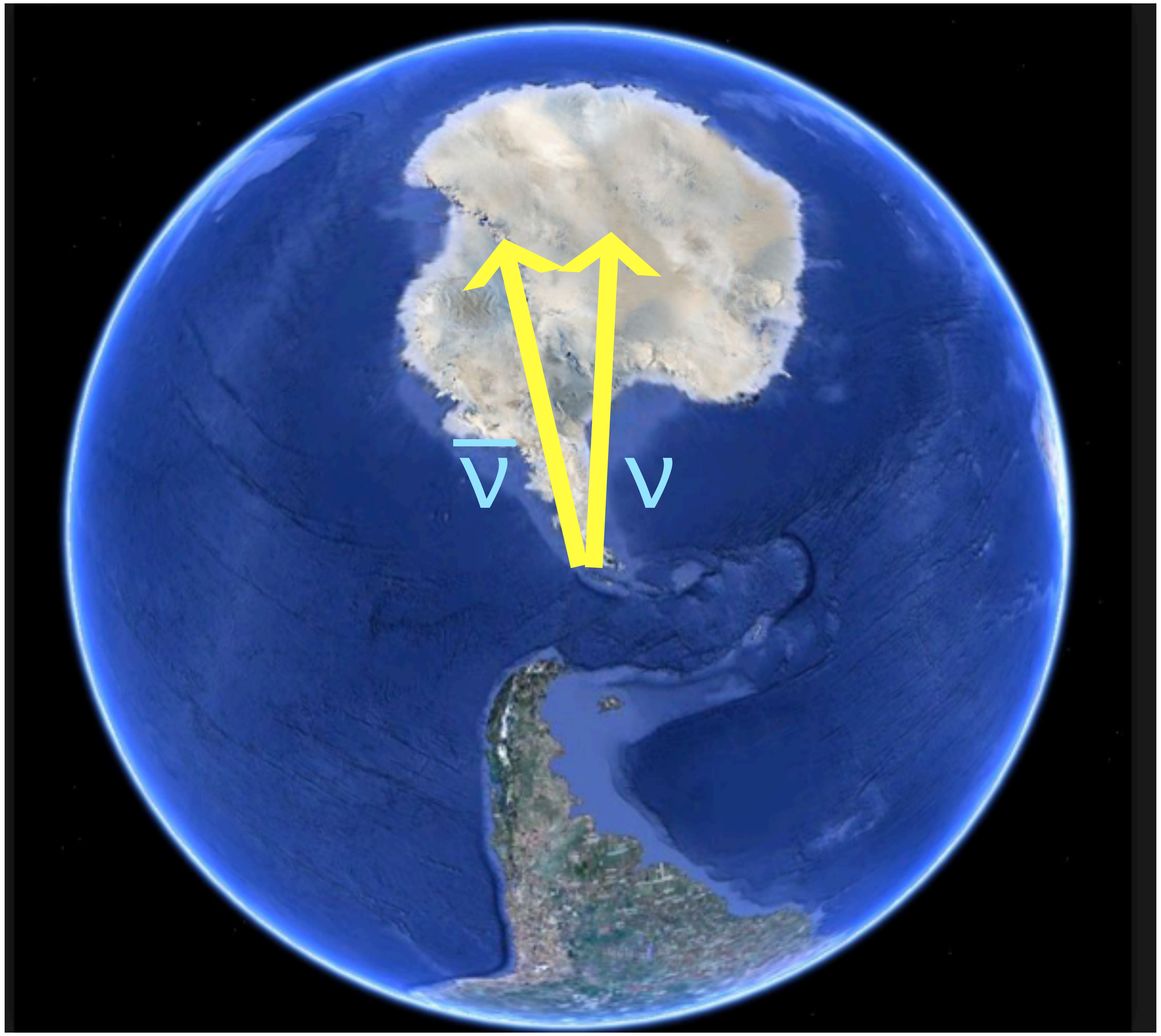

Boost on annihilation XS

Γ_A enhanced by boost B_f over XS:

$$\langle \sigma v \rangle \; = \; B_f \, \langle \sigma v \rangle_R$$

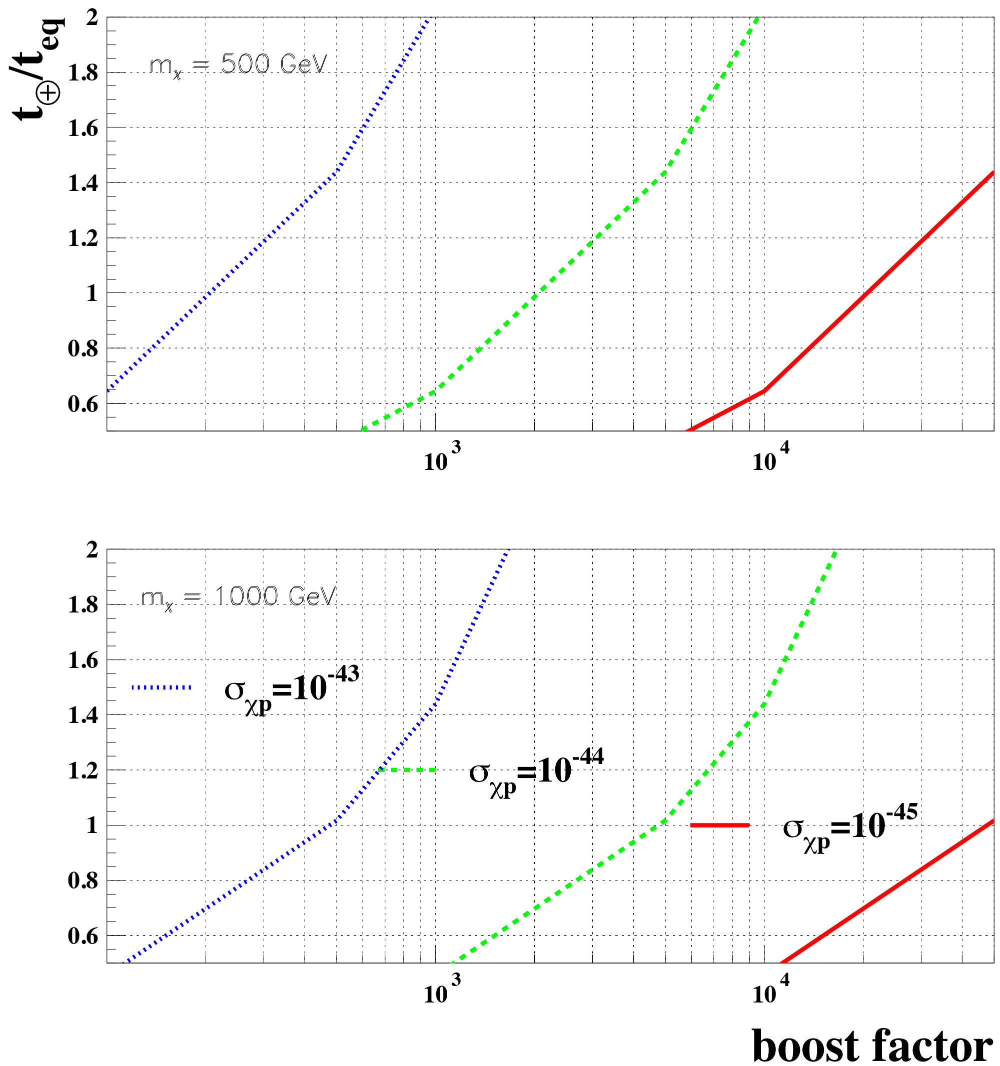

Boost on annihilation XS

Γ_A enhanced by boost B_f over XS:

$$\langle \sigma v \rangle \; = \; B_f \, \langle \sigma v \rangle_R$$

Today Earth is far from equilibrium
Enhancement is effective if accelerates equilibrium

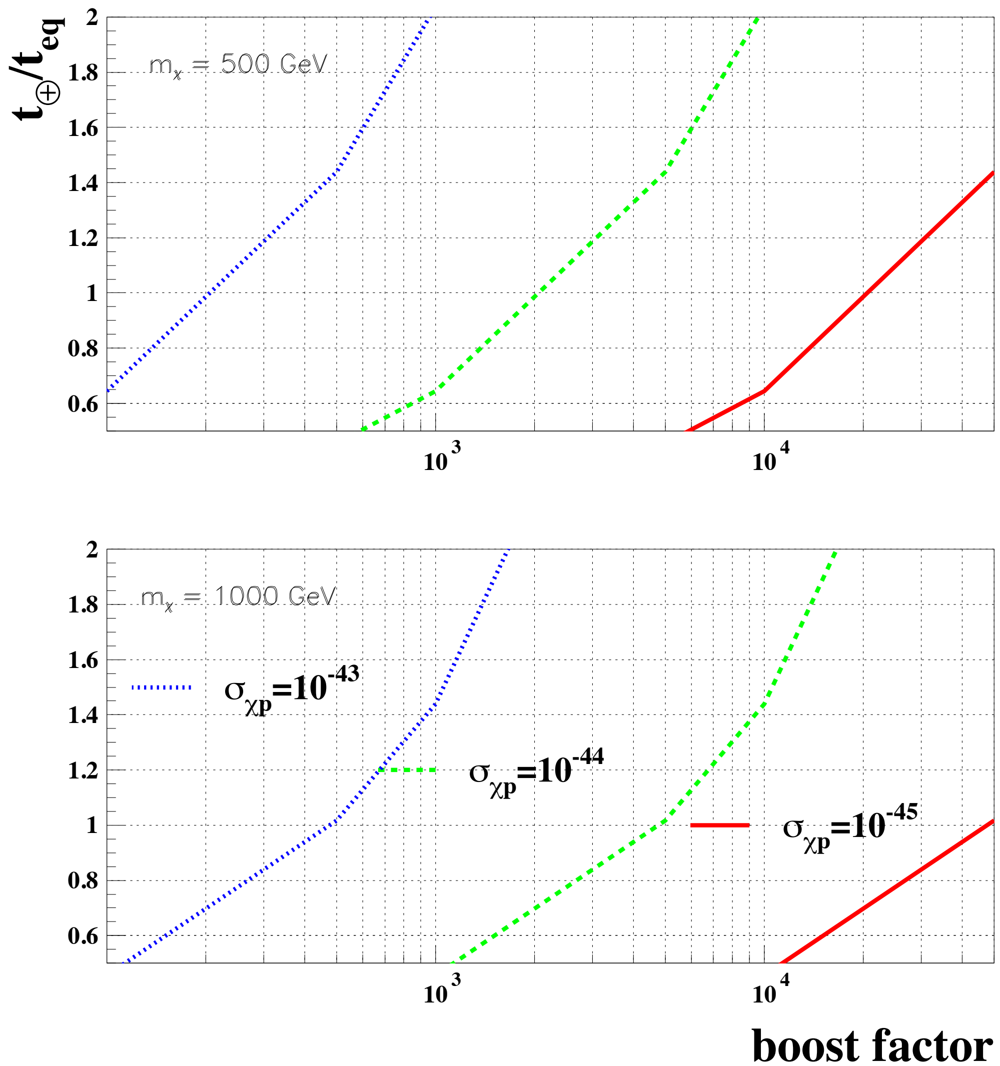

DM Annihilation in the Earth

$$\chi\,\overline{\chi} \to f_{\nu\overline{\nu}}\,\nu_\mu\,\overline{\nu}_\mu$$

- primary flux from the center of the Earth:

$$\frac{d\phi_\nu}{dE_\nu\,dA\,dt\,d\Omega} = \frac{f_{\nu\overline{\nu}}\,\Gamma_A}{4\,\pi\,R_\oplus^2}\,\frac{dN_\nu}{dE_\nu}$$

$$\mathbf{m}_\chi = 500 \text{ and } 1000 \text{ GeV}$$

- monochromatic ν flux

- secondary ν are too low in energy (Delaunay, Fox, Perez JHeP 05 2009)

ν production and propagation

- Monte Carlo Simulation: WIMPSIM code

(M. Blennow, J. Edsjo, T. Ohlsson - JCAP **01** 2008)

=> CC and NC interactions

=> ν oscillations

ν production and propagation

- Monte Carlo Simulation: WIMPSIM code

(M. Blennow, J. Edsjo, T. Ohlsson - JCAP **01** 2008)

=> CC and NC interactions

=> ν oscillations

- Output: ν_μ flux $\left(\frac{\mathbf{d}\phi_\nu}{\mathbf{dE}_\nu}\right)$ at the detector

ν production and propagation

- Monte Carlo Simulation: WIMPSIM code

(M. Blennow, J. Edsjo, T. Ohlsson - JCAP **01** 2008)

=> CC and NC interactions

=> ν oscillations

- Output: ν_μ flux $\left(\frac{d\phi_\nu}{dE_\nu}\right)$ at the detector

- Number of μ at given angular region Ω at IceCube*:

$$\int \left(\frac{d\phi_\nu}{dE_\nu \, dA \, dt \, d\Omega} \right) dE_\nu \, t_{exp} \, A_{eff} \, \Omega$$

DM ν_s angular distribution

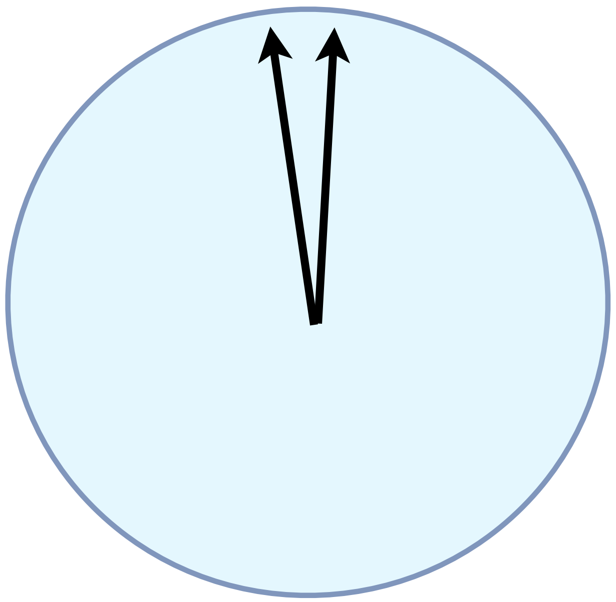

ν_μ angular distribution

(from WIMPSIM)

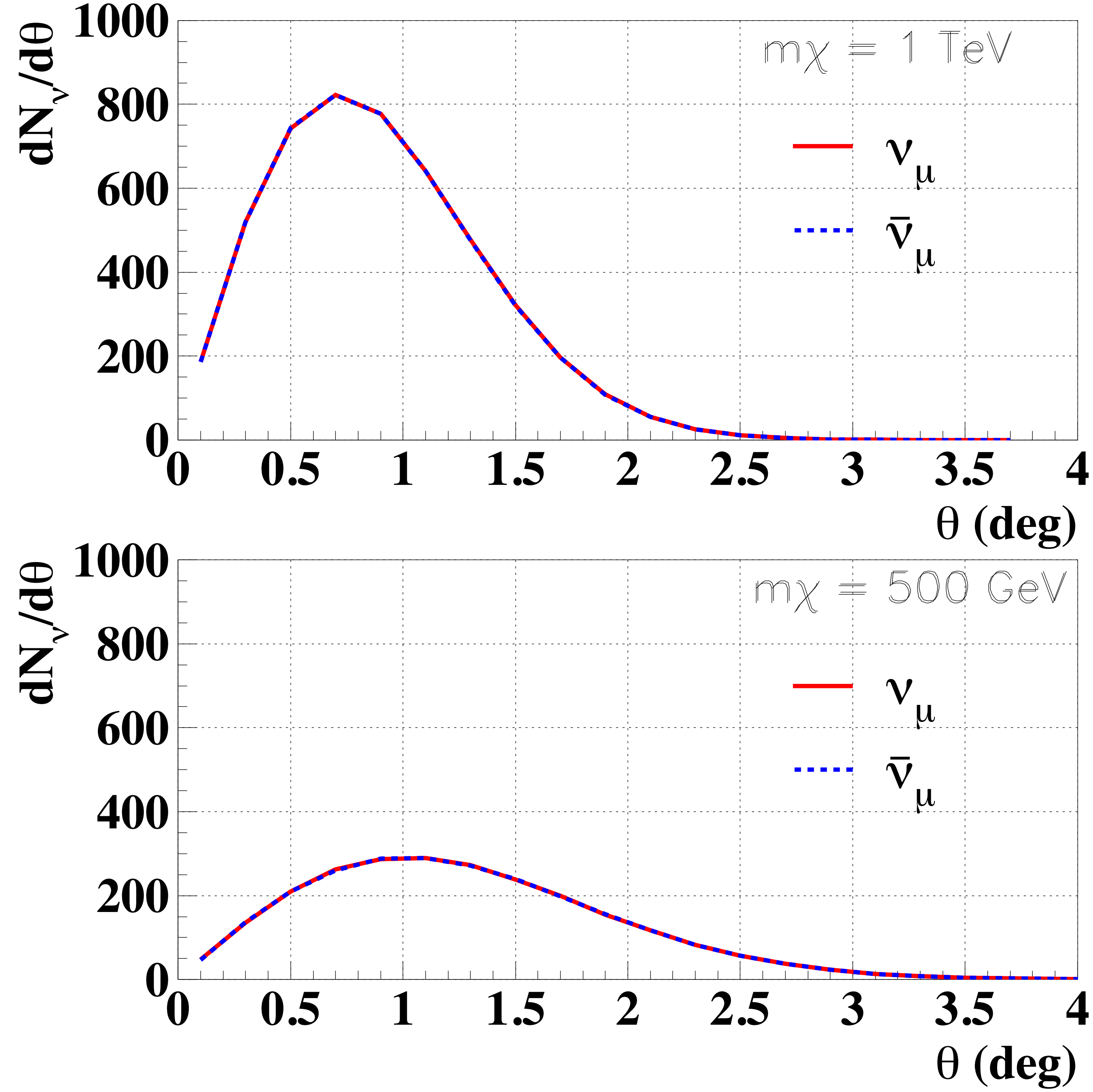

ν_s are collimated ~ 3°

ν_s from DM at IC40

- taking IC angular experimental resolution into account:

(2° for up-going vertical events)

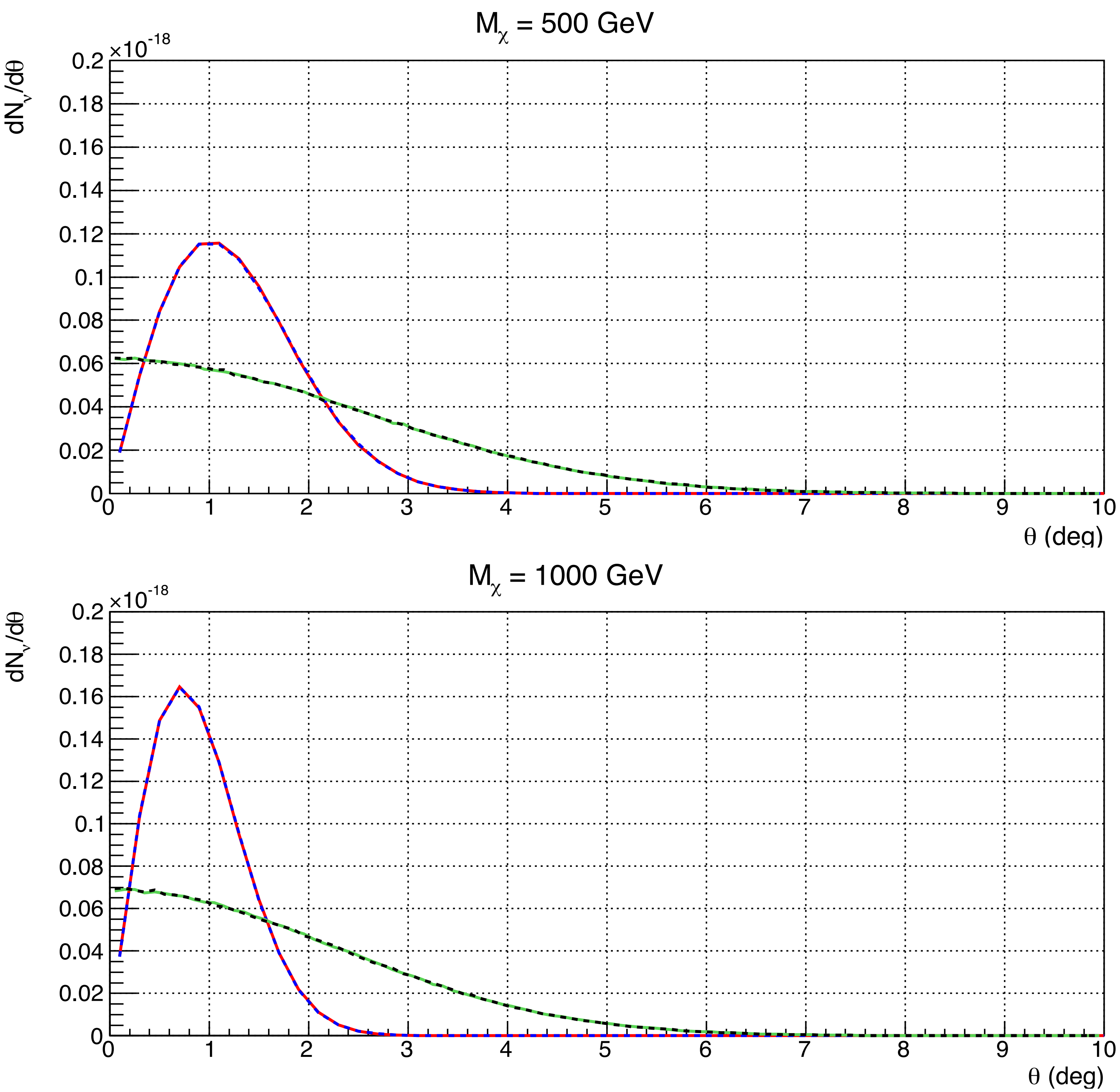

- angular window that contains 90% of expected signal:

4.1 (3.7)° for 500 (1000) GeV DM

ν_s from DM at IC40

- taking IC angular experimental resolution into account:

(2° for up-going vertical events)

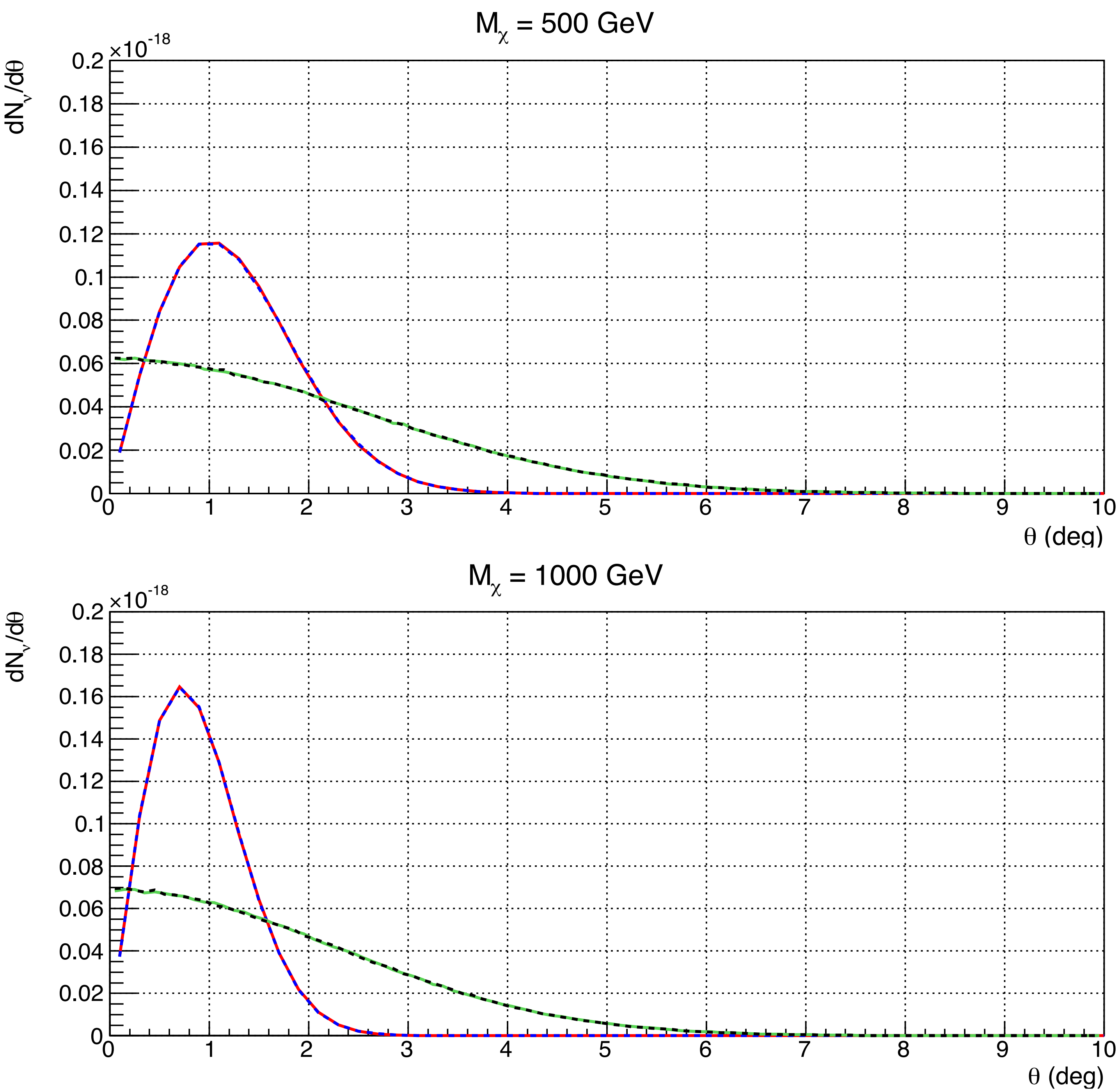

- angular window that contains 90% of expected signal:

4.1 (3.7)° for 500 (1000) GeV DM

main reduction of background contamination

IC-40 Effective Area

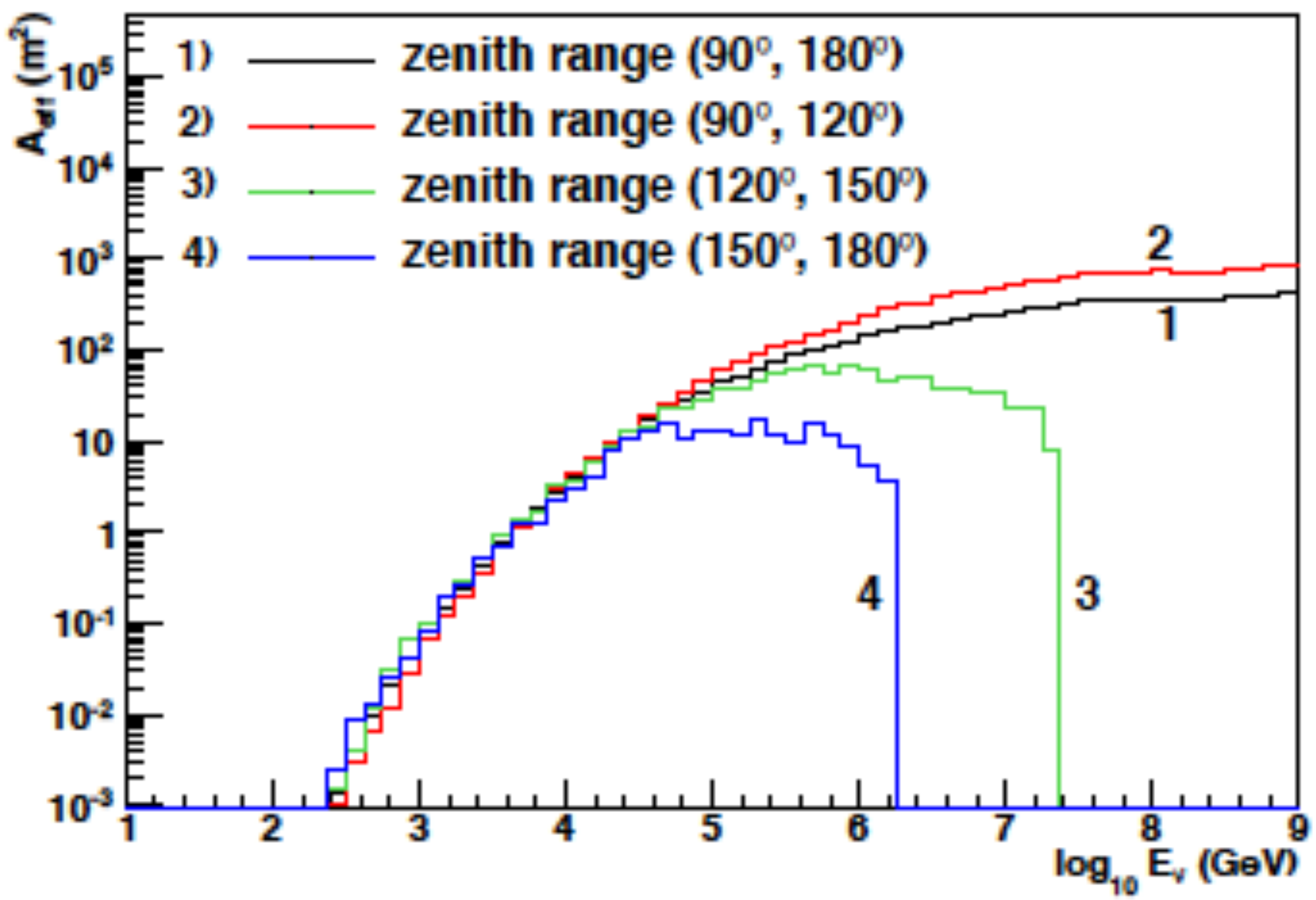

FIG. 5. Effective area for $\nu_\mu + \bar{\nu}_\mu$ as a function of the true neutrino energy in intervals of the true zenith angle of the neutrino. The angle averaged area is represented by the solid black line.

Expected ν_s from DM at IC40

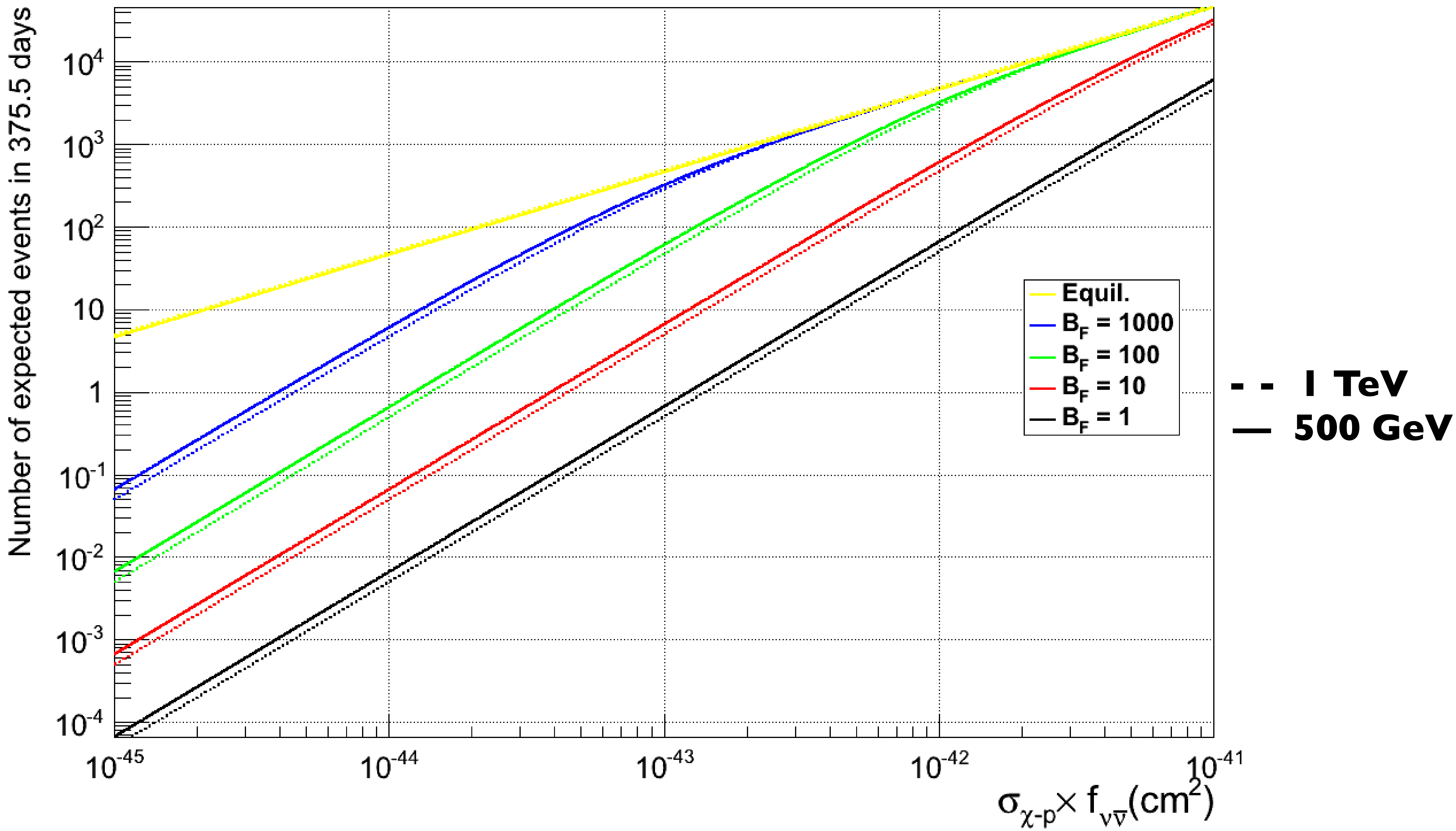

IC40 Results

IceCube 40 string configuration

- Measurement of atmospheric neutrino energy spectrum (0.1 => 400 TeV) (R.~Abbasi et al., PRD**83**, 2011)

- A Search for a Diffuse Flux of Astrophysical ν_μ (R.~Abbasi et al., PRD**83**, 2011)

=> search for diffuse E^{-2} flux of cosmic origin

IC40 Results

IceCube 40 string configuration

- Measurement of atmospheric neutrino energy spectrum (0.1 => 400 TeV) (R.~Abbasi et al., PRD**83**, 2011)

- A Search for a Diffuse Flux of Astrophysical ν_μ (R.~Abbasi et al., PRD**83**, 2011)

=> search for diffuse E^{-2} flux of cosmic origin

Both consistent with expected atmospheric flux

IC40 Data

- Public data from diffuse analysis:

  => www.icecube.wisc.edu/science/data

  - events from near or below the horizon
  - background contamination (atm μ from above) < 1%
  - final sample of 13 K events

- angular cut (4.1, 3.7°) corresponding to 500 (1000) GeV DM

IC40 Data

- Public data from diffuse analysis:
  => www.icecube.wisc.edu/science/data
  - events from near or below the horizon
  - background contamination (atm μ from above) < 1%
  - final sample of 13 K events
- angular cut (4.1, 3.7°) corresponding to 500 (1000) GeV DM

data reduced to 14 (9) events

Results

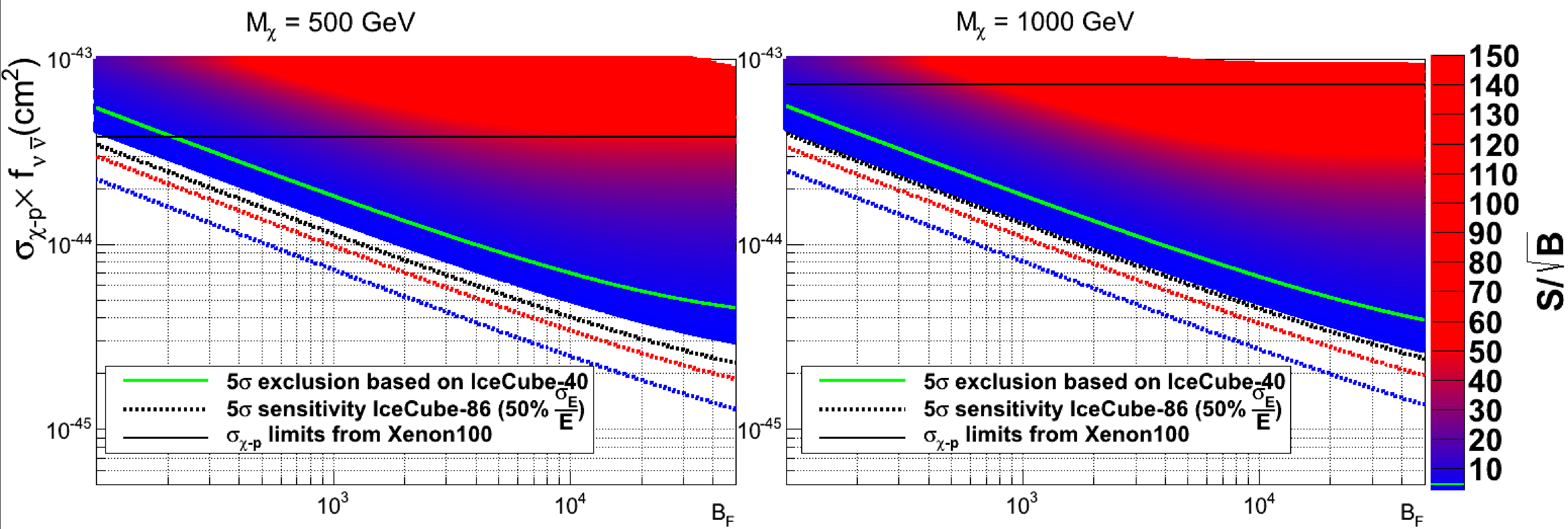

S ≡ predicted number of events

B ≡ measured IC40 events after angular cuts

Xe100 limits: $\sigma_{\chi p} \sim 4\ (8) \times 10^{-44}\ cm^2$ for m_χ = 500 (1000) GeV

At these limits: $B_F > 215\ (58)$ are excluded for $f_{\nu\nu} = 1$ at a 5σ level

Results

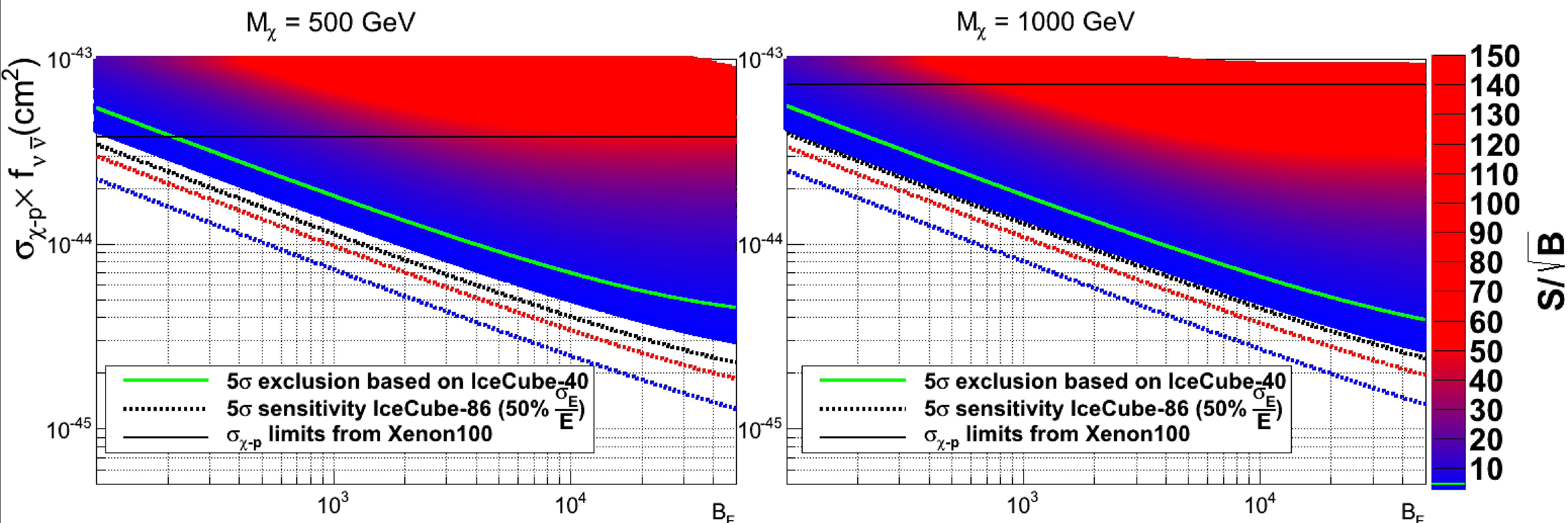

I.A, L. Beraldo Silva, Carlos de Los Heros, PRD **85,** 2012

S ≡ predicted number of events

B ≡ measured IC40 events after angular cuts

Xe100 limits: $\sigma_{\chi p} \sim 4\ (8) \times 10^{-44}\ \mathrm{cm}^2$ for $m_\chi = 500\ (1000)$ GeV

At these limits: $B_F > 215\ (58)$ are excluded for $f_{\nu\nu} = 1$ at a 5σ level

Comparison with other bounds

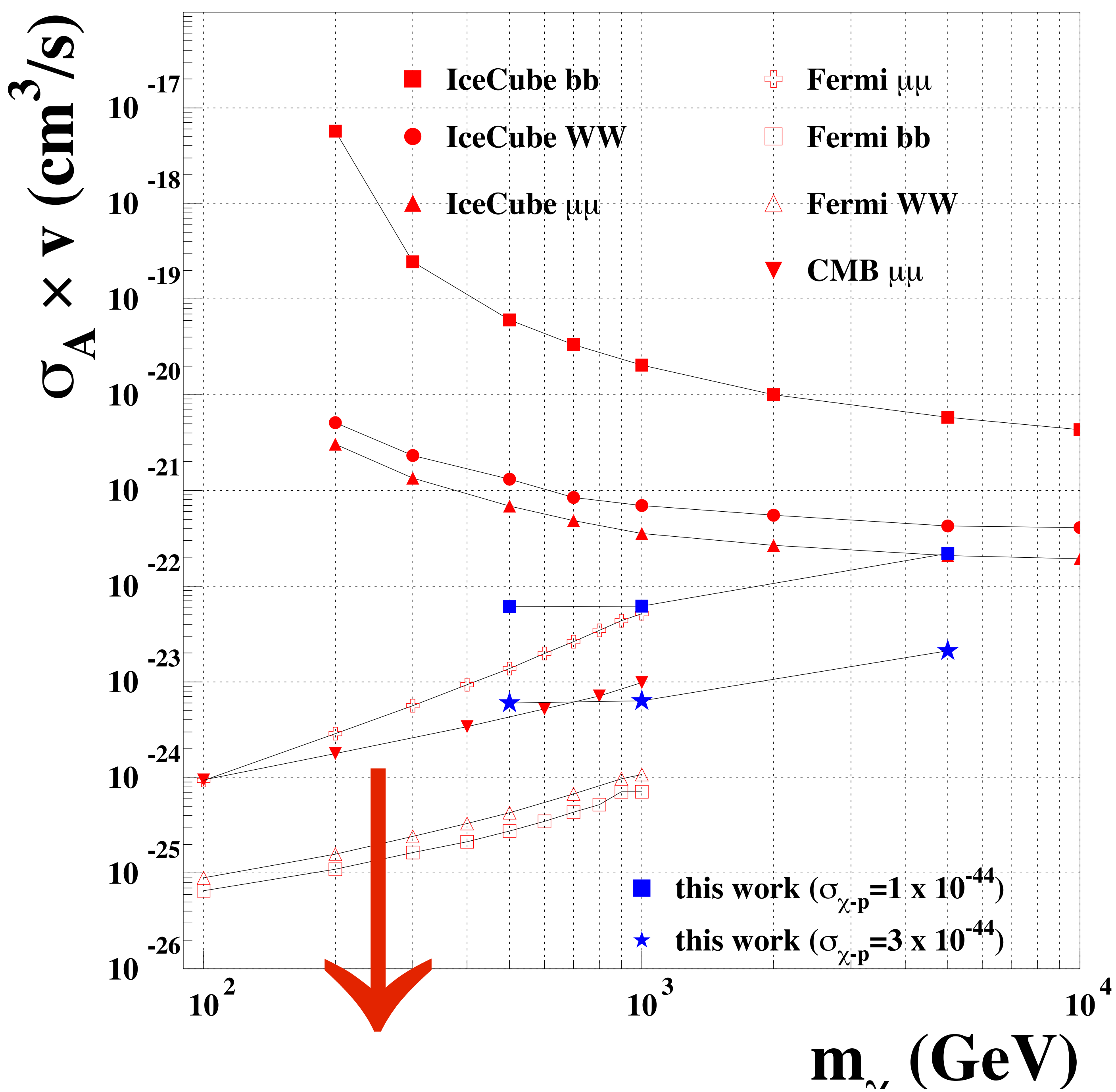

Comparison with other bounds

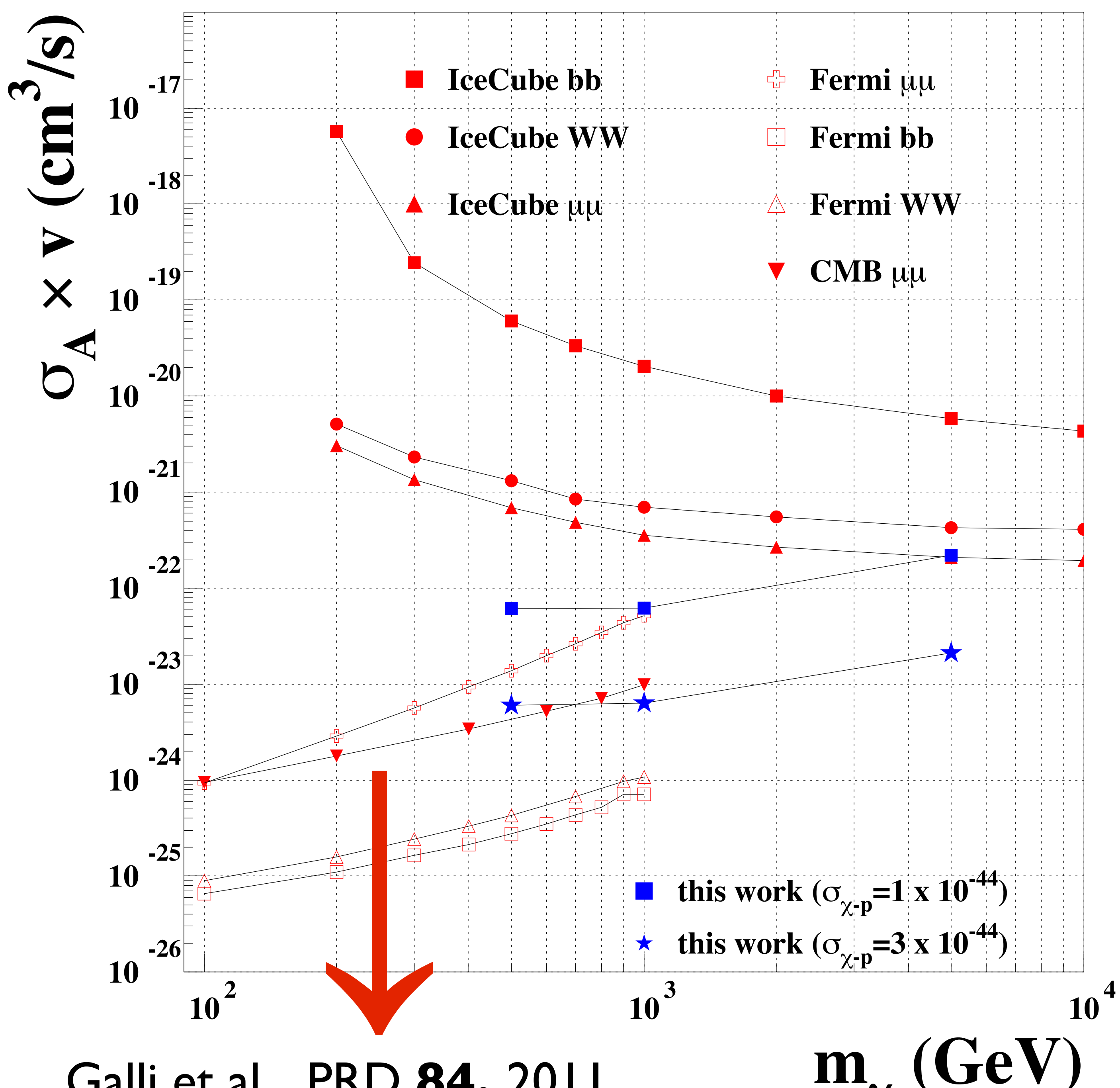

Galli et al., PRD **84,** 2011
DM annihilations (or decay) at recombination time => CMB power spectrum to constrain σ_A

Comparison with other bounds

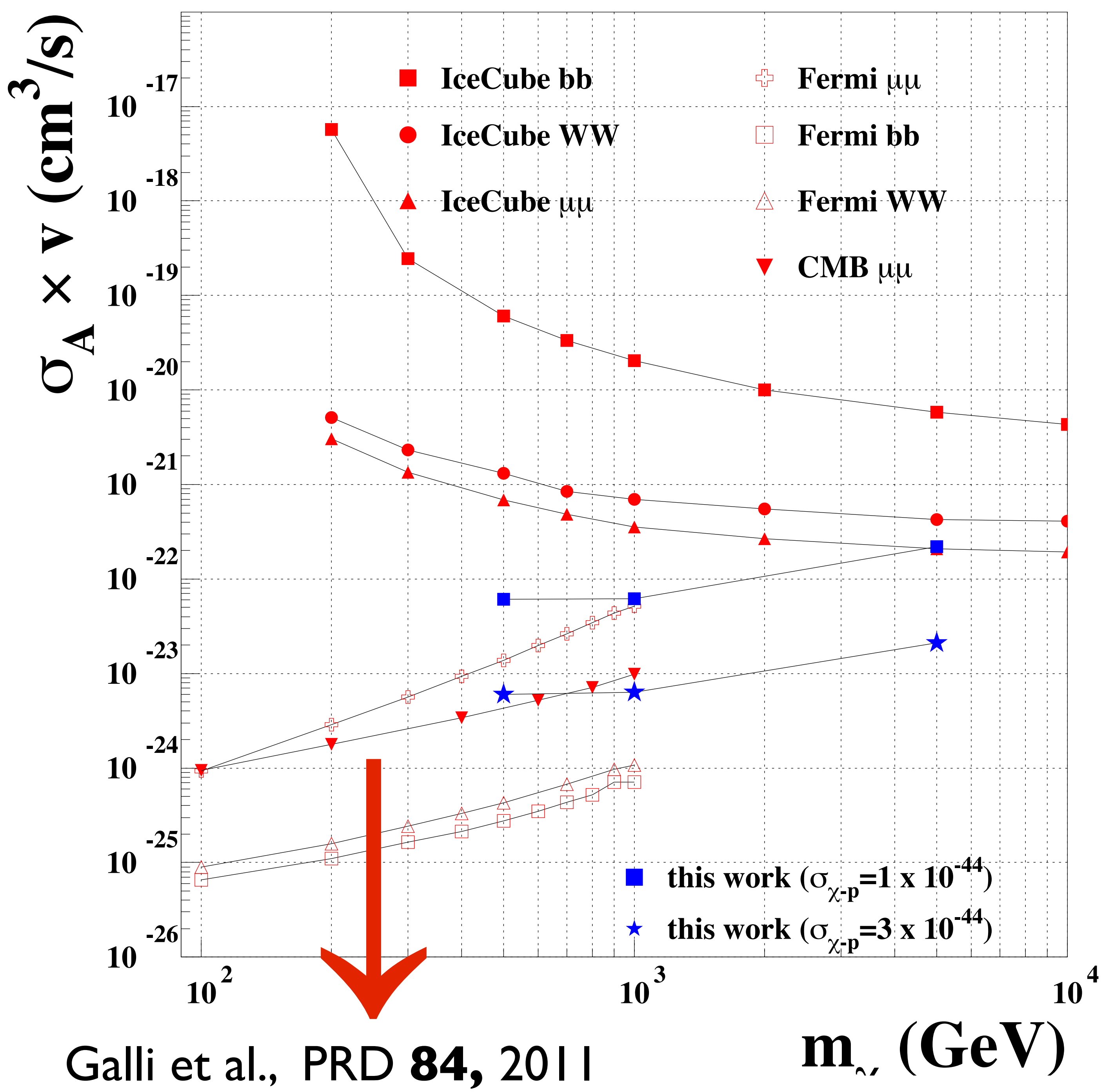

Galli et al., PRD **84,** 2011
DM annihilations (or decay) at recombination time => CMB power spectrum to constrain σ_A

Abbasi et al. (IceCube Coll.), arXiv:1210.3577v3, 2013

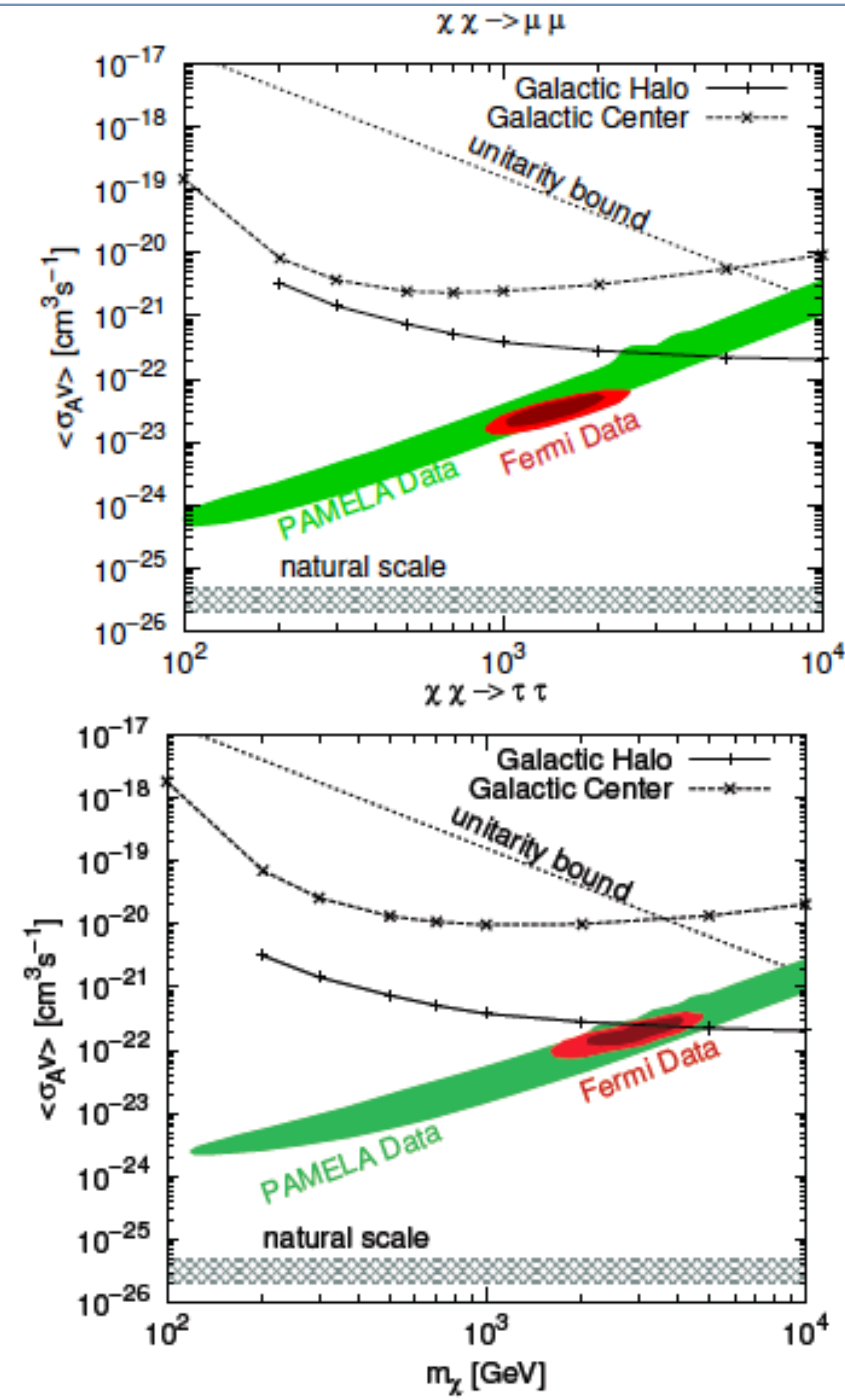

Comparison with other bounds

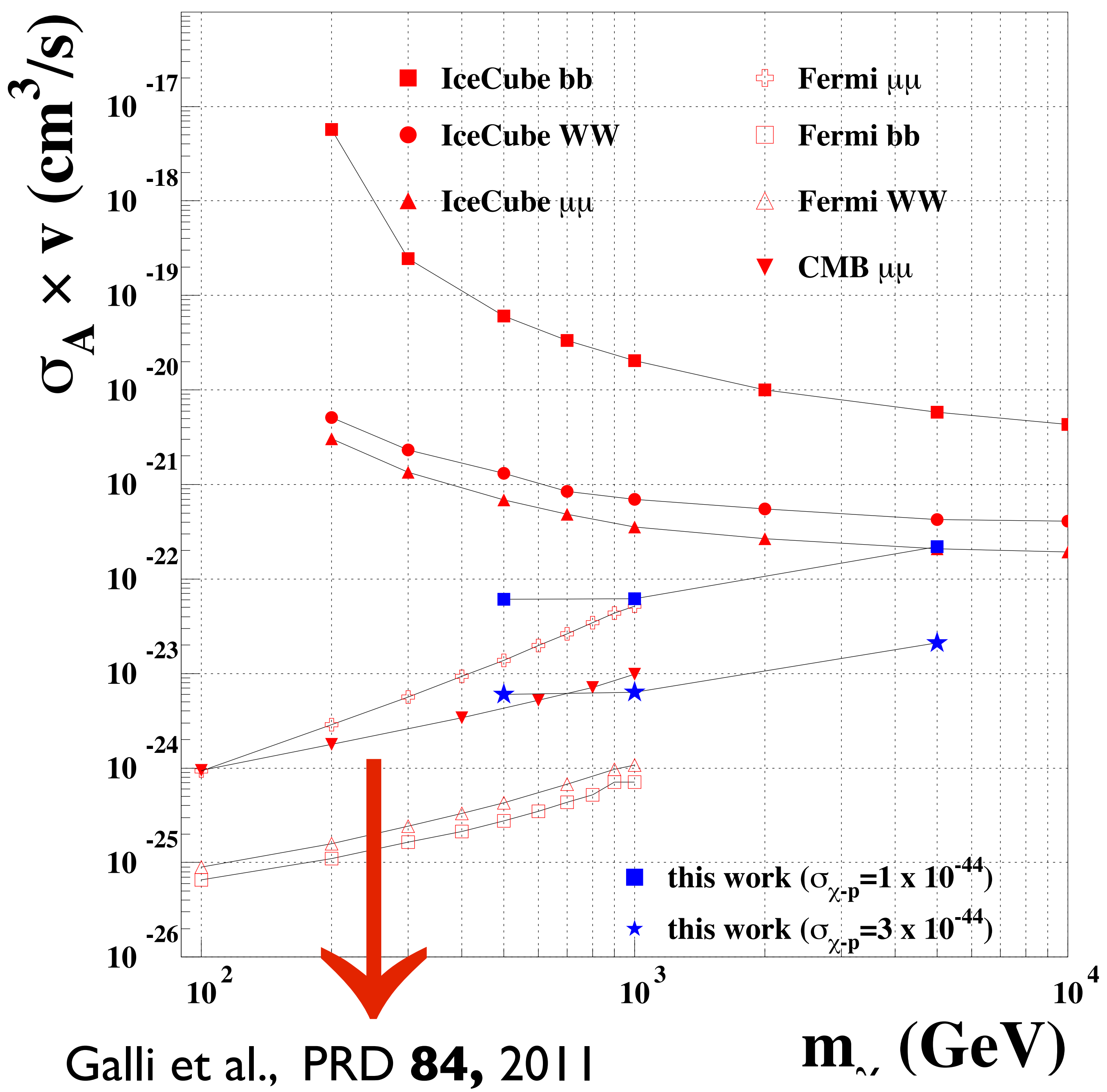

Galli et al., PRD **84,** 2011
DM annihilations (or decay) at recombination time => CMB power spectrum to constrain σ_A

Abbasi et al. (IceCube Coll.), arXiv:1210.3577v3, 2013

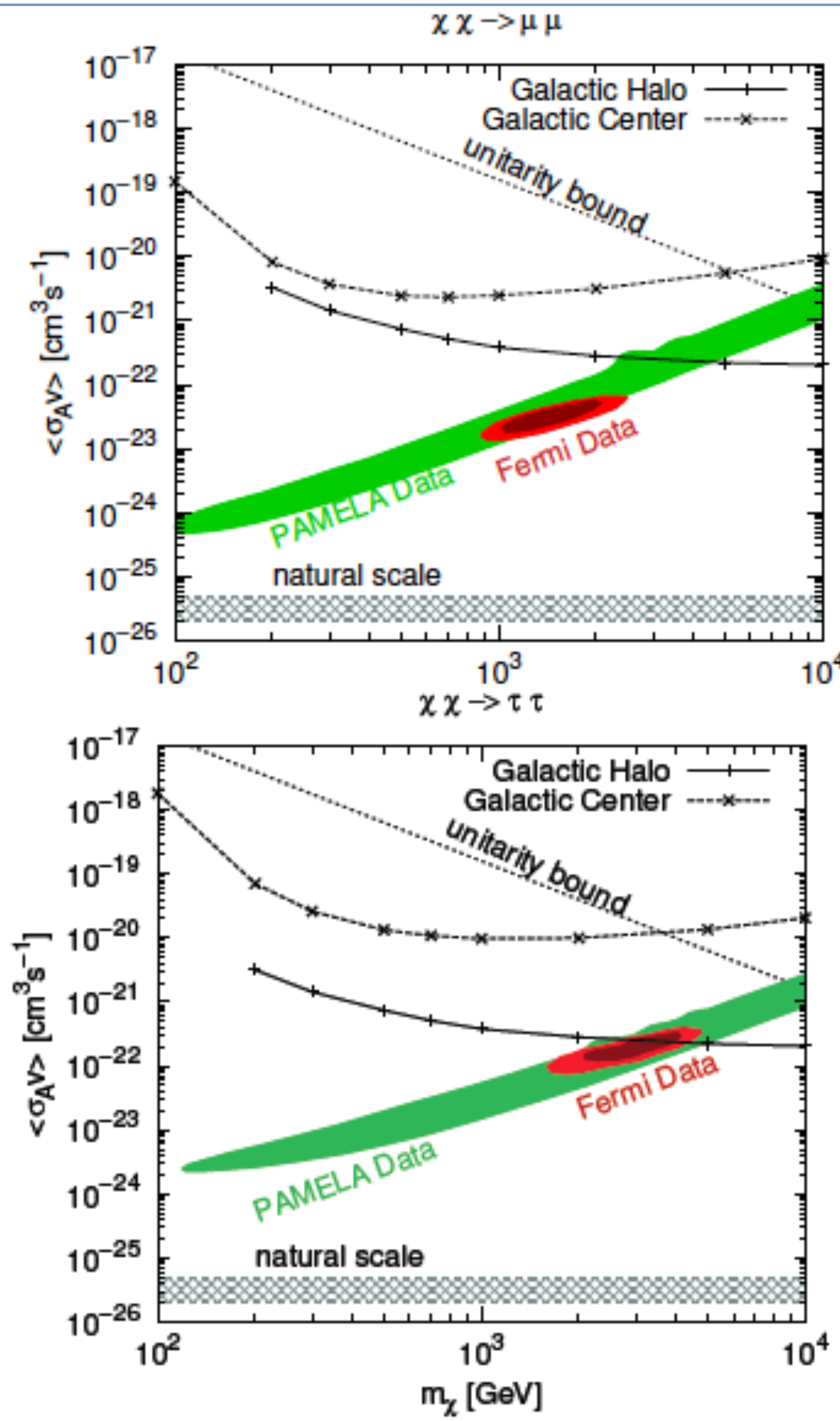

Strong constraints on leptophilic models

γ-ray lines

$$\chi\,\overline{\chi} \rightarrow \mathbf{X}\,\gamma$$

In DM rest frame: $$\mathbf{E}_\gamma = \mathbf{m}_\chi \left(1 - \frac{\mathbf{m}_\mathbf{X}^2}{4\,\mathbf{m}_\chi^2}\right)$$

γ-ray lines

$$\chi\,\bar{\chi} \rightarrow \mathbf{X}\,\gamma$$

In DM rest frame: $$\mathbf{E}_\gamma = \mathbf{m}_\chi \left(1 - \frac{\mathbf{m}_\mathbf{X}^2}{4\,\mathbf{m}_\chi^2}\right)$$

Monochromatic photons!

γ-ray lines

$$\chi\,\bar{\chi} \rightarrow \mathbf{X}\,\gamma$$

In DM rest frame: $\mathbf{E}_\gamma = \mathbf{m}_\chi \left(\mathbf{1} - \frac{\mathbf{m}_\mathbf{X}^\mathbf{2}}{\mathbf{4\,m}_\chi^\mathbf{2}}\right)$

Monochromatic photons!

If X => second γ => $\mathbf{E}_\gamma = \mathbf{m}_\chi$

γ-ray lines

$$\chi\,\overline{\chi} \rightarrow \mathbf{X}\,\gamma$$

In DM rest frame: $$\mathbf{E}_{\gamma} = \mathbf{m}_{\chi}\left(\mathbf{1} - \frac{\mathbf{m_X^2}}{\mathbf{4\,m_\chi^2}}\right)$$

Monochromatic photons!

If X => second γ => $\mathbf{E}_{\gamma} = \mathbf{m}_{\chi}$

DM is non relativistic in the halo:
monochromatic in lab frame as well

Exercise 1: In many models DM particles annihilate into a γ and another particle (X). Show that the produced γs are monochromatic with energy in its rest frame given by the equation shown in the previous slide.

Fermi-LAT search for γ-ray lines

Search for monochromatic γs from DM annihilation or decay

Gamma sky: 20 MeV to 300 GeV

Gamma lines: 5 to 300 GeV

	Annihilation		Decay	
Profile	ROI	J-factor (10^{22} GeV^2 cm^{-5})	ROI	J-factor (10^{23} GeV cm^{-2})
NFW Contracted	R3	13.9	R180	2.42
Einasto	R16	8.48	R180	2.49
NFW	R41	8.53	R180	2.46
Isothermal	R90	6.94	R180	2.80

3.7 years of data

(arXiv:1305.5597)

Fermi-LAT search for γ-ray lines

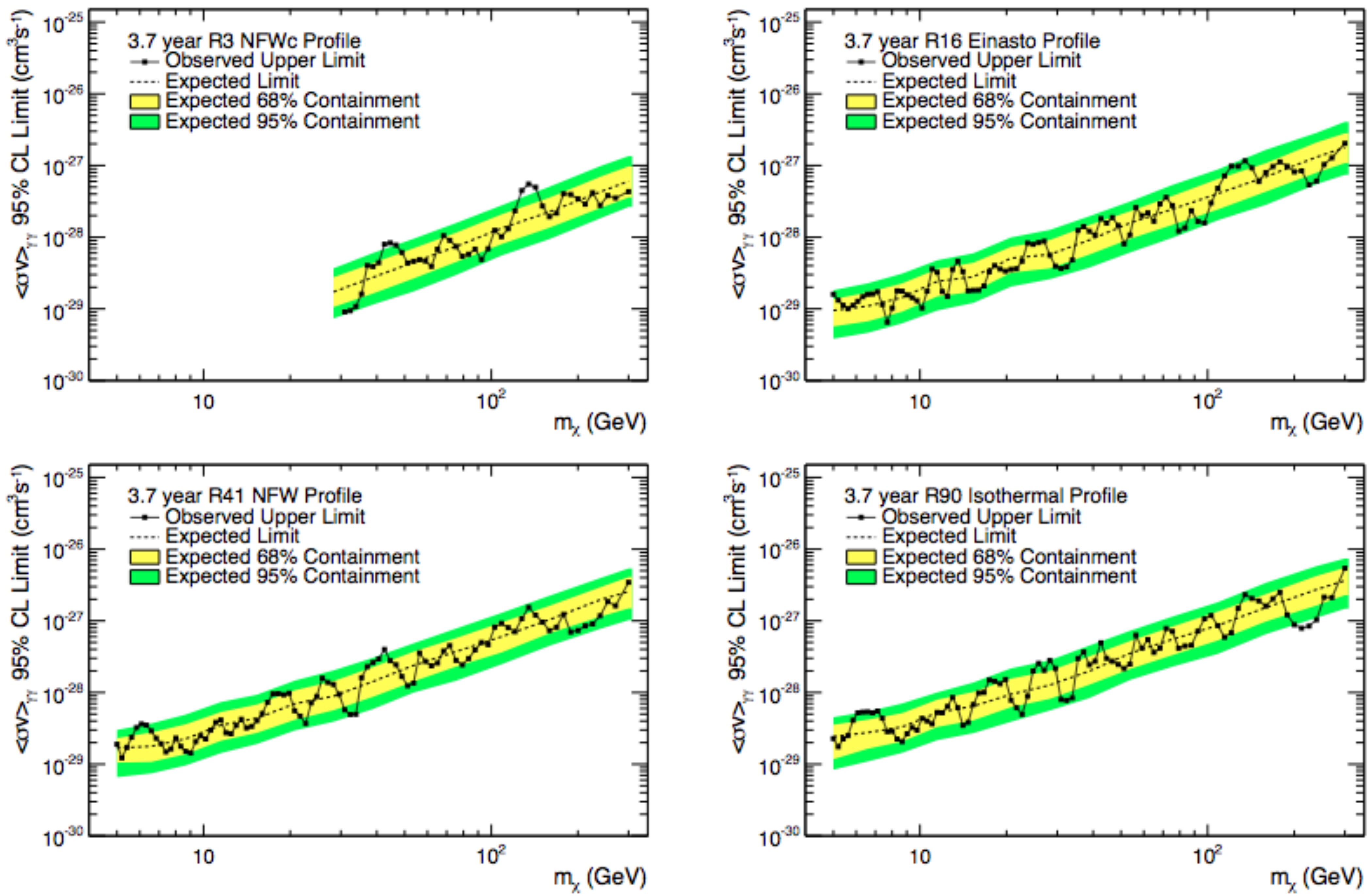

Fermi-LAT search for γ-ray lines

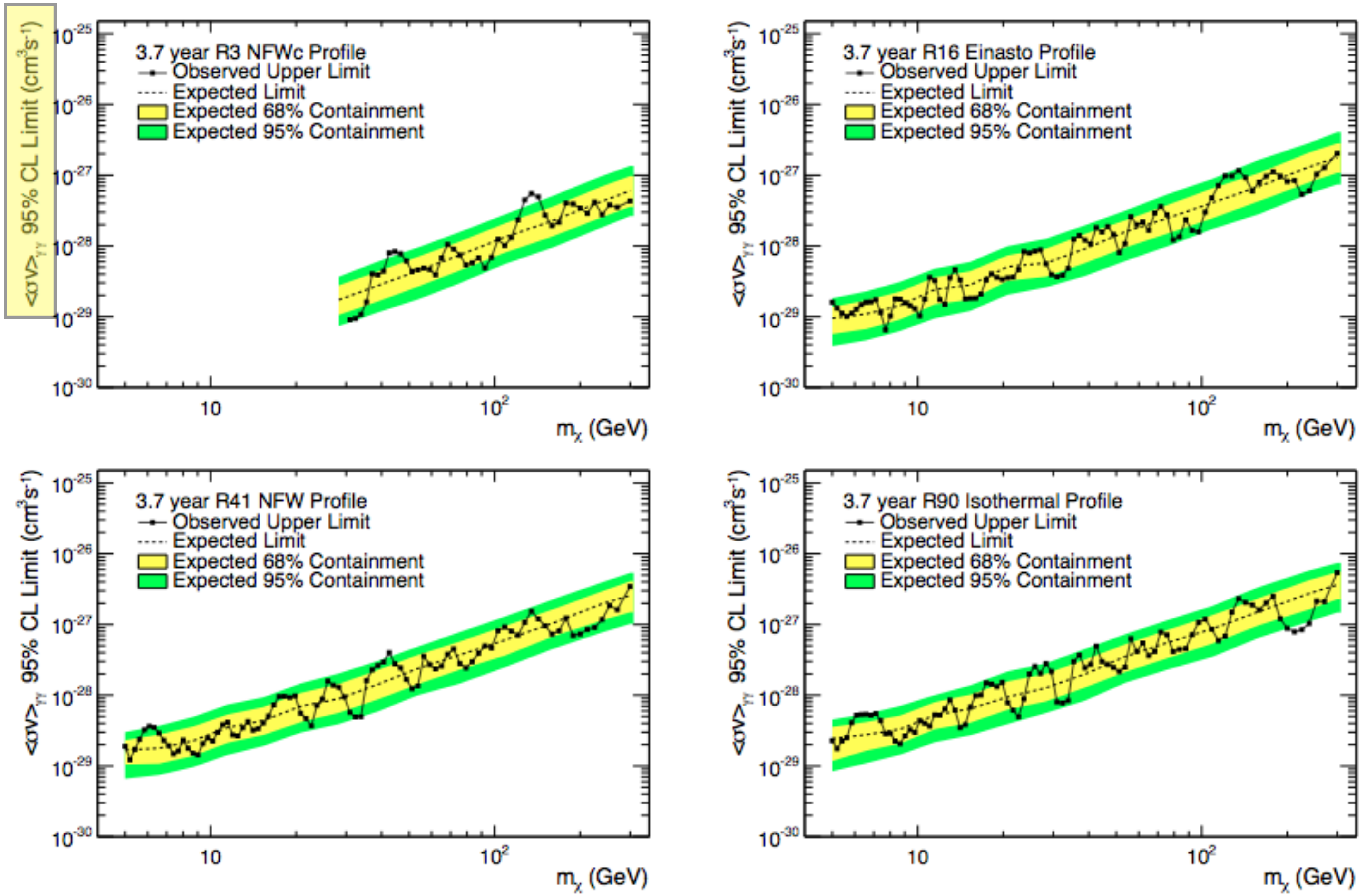

Fermi-LAT results on γ-ray lines

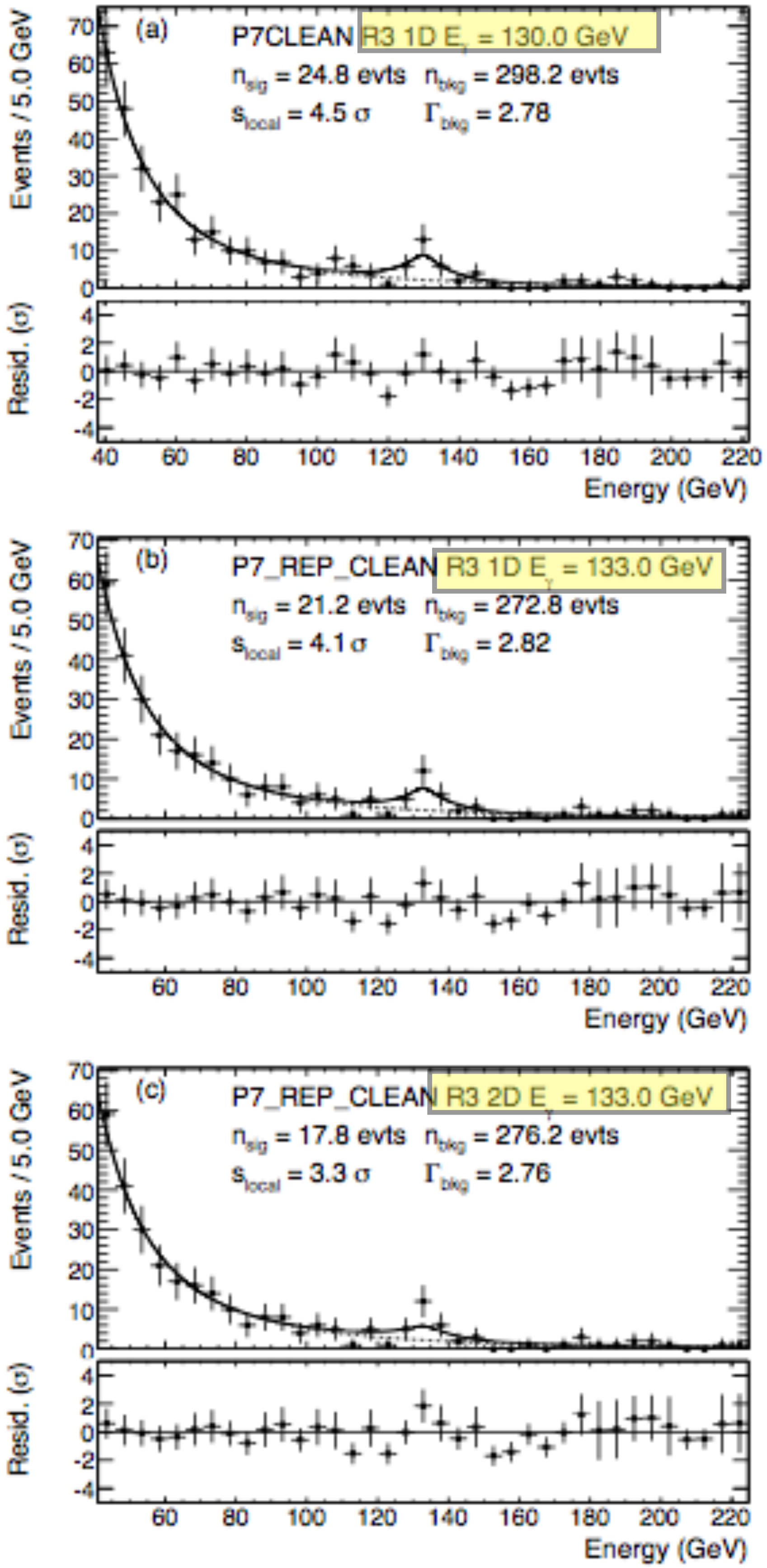

γ line feature at 133 GeV

(s_local = 3.3σ and s_global = 1.6σ)

(arXiv:1305.5597)

Fermi-LAT results on γ-ray lines

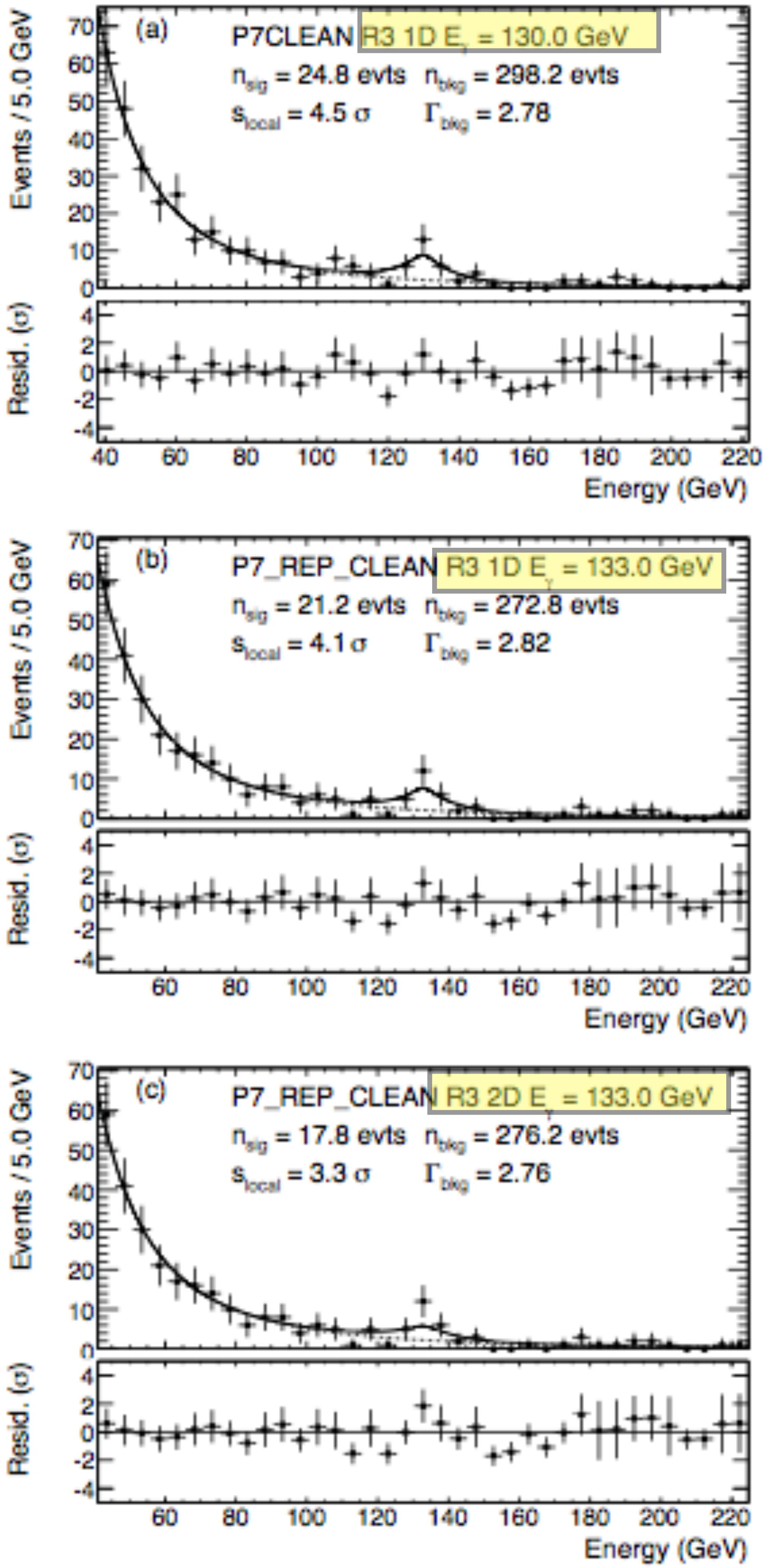

γ line feature at 133 GeV

(s_local = 3.3σ and s_global = 1.6σ)

"Found no globally significant spectral line signals"

(arXiv:1305.5597)

Fermi-LAT results on γ-ray lines

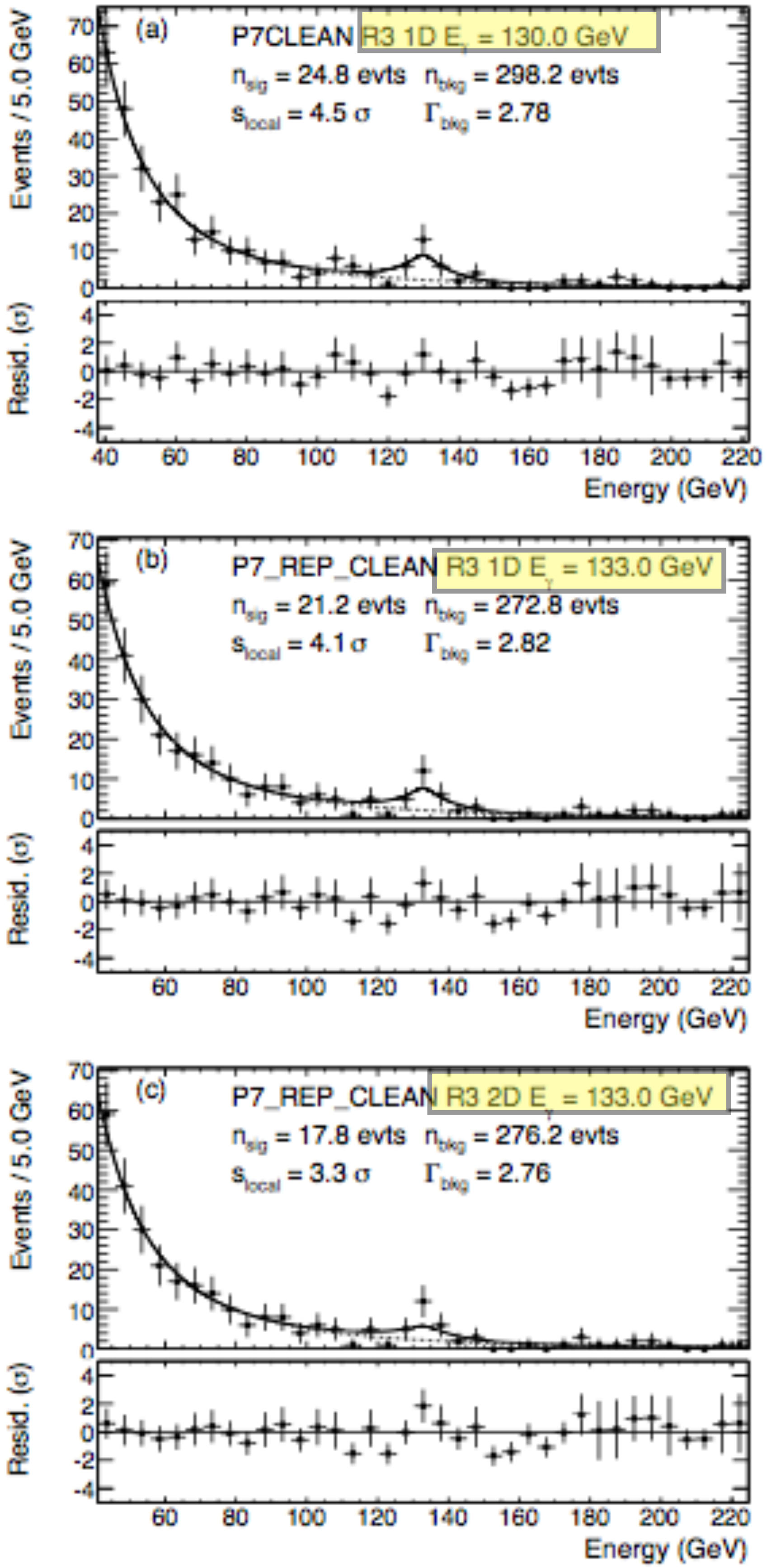

γ line feature at 133 GeV

(s_local = 3.3σ and s_global = 1.6σ)

"Found no globally significant spectral line signals"

velocity average limits ~ 10^{-29} - 10^{-27} much lower than thermal relic value

(arXiv:1305.5597)

Fermi-LAT results on γ-ray lines

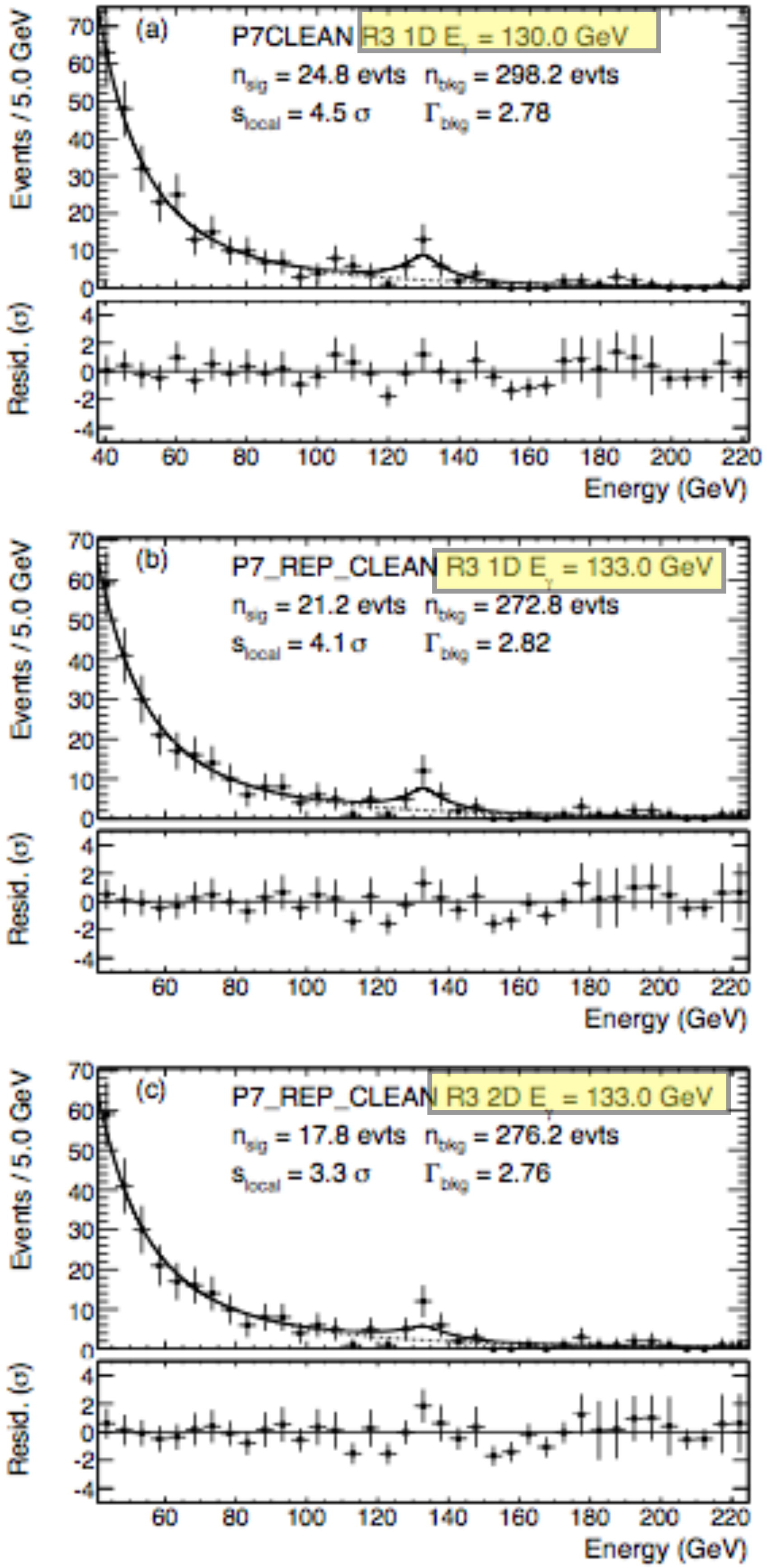

γ line feature at 133 GeV

(s_local = 3.3σ and s_global = 1.6σ)

"Found no globally significant spectral line signals"

velocity average limits ~ 10^{-29} - 10^{-27} much lower than thermal relic value

limits are on annihilation to γs

(arXiv:1305.5597)

FermiLAT "Bubbles"

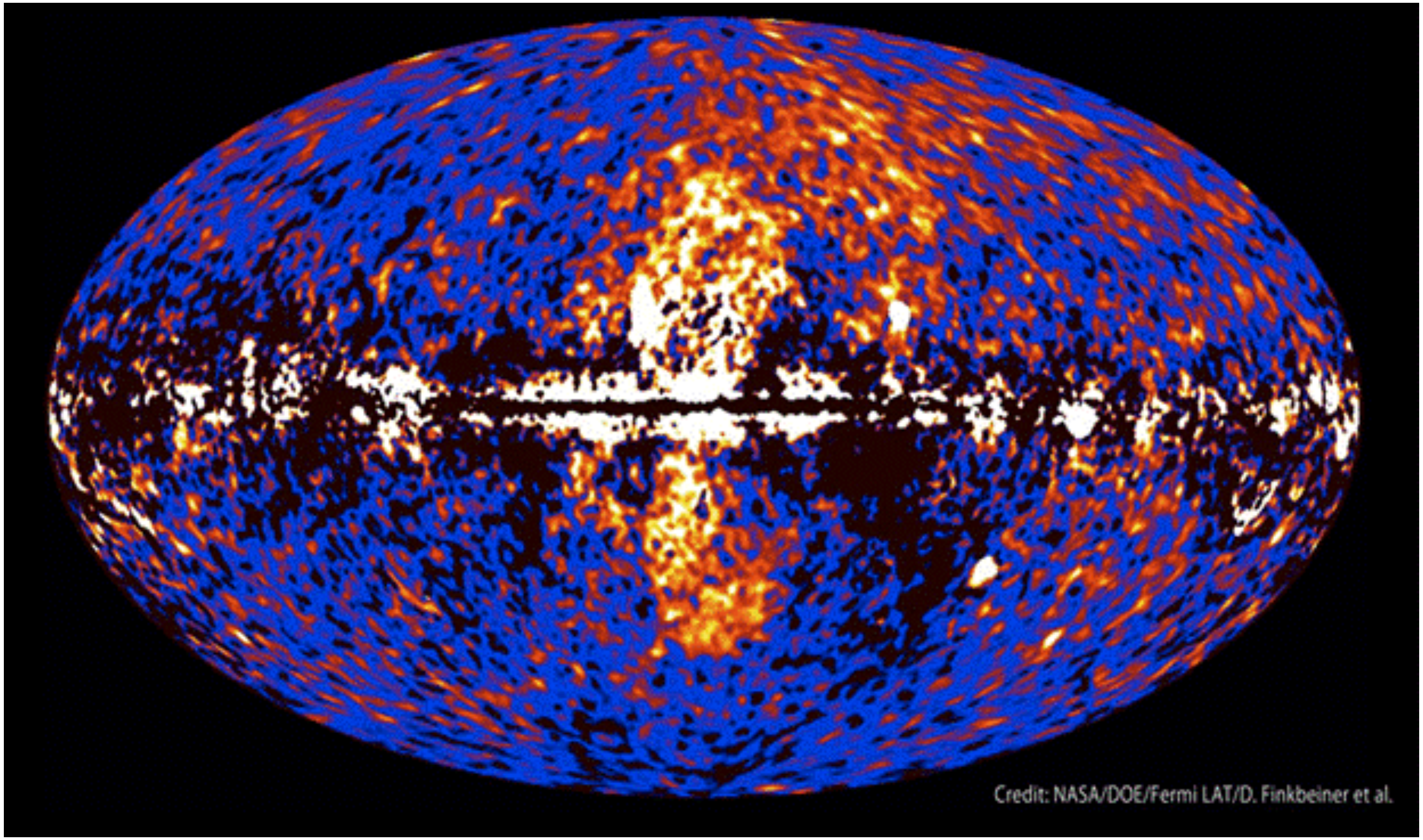

2 large γ ray structures above and below GC related to microwave haze in same region (found by WMAP and confirmed by Planck)

“Bubbles” and Haze

Many possible explanations

Problems when analyzing foreground?

Haze

synchrotron radiation from dark matter annihilations?

synchrotron radiation from astro sources?

production by 10 GeV electrons

Bubbles

TeV electrons scattering off CMB?
(same electrons that produce haze might scatter photons to higher energies => gamma rays)

DM?

“Bubbles” and Haze

(google cosmic invariance blog finkbeiner)

“Bubbles” and Haze

Finkbeiner, astro-ph/0409027 (2004)

(google cosmic invariance blog finkbeiner)

Planck results: compelling evidence that bubbles produce haze

Many explanations other than DM
Little room for DM as main source

Hooper, Finkbeiner and Dobler, PRD **76** (2007)

Finkbeiner and Dobler, Astrophys. J. **680** (2008)

Cholis, Goodenough and Weiner, PRD **79** (2009)